

DOT/FAA/AR-00/46

Office of Aviation Research
Washington, D.C. 20591

Repair of Composite Laminates

December 2000

Final Report

20010405 117

This document is available to the U.S. public
through the National Technical Information
Service (NTIS), Springfield, Virginia 22161.



U.S. Department of Transportation
Federal Aviation Administration

DISTRIBUTION STATEMENT A
Approved for Public Release
Distribution Unlimited

NOTICE

This document is disseminated under the sponsorship of the U.S. Department of Transportation in the interest of information exchange. The United States Government assumes no liability for the contents or use thereof. The United States Government does not endorse products or manufacturers. Trade or manufacturer's names appear herein solely because they are considered essential to the objective of this report. This document does not constitute FAA certification policy. Consult your local FAA aircraft certification office as to its use.

This report is available at the Federal Aviation Administration William J. Hughes Technical Center's Full-Text Technical Reports page: actlibrary.tc.faa.gov in Adobe Acrobat portable document format (PDF).

Technical Report Documentation Page

1. Report No. DOT/FAA/AR-00/46	2. Government Accession No.	3. Recipient's Catalog No.	
4. Title and Subtitle REPAIR OF COMPOSITE LAMINATES		5. Report Date December 2000	
		6. Performing Organization Code	
7. Author(s) Sung-Hoon Ahn and George S. Springer		8. Performing Organization Report No.	
9. Performing Organization Name and Address Department of Aeronautics and Astronautics Stanford University Stanford, CA 94305		10. Work Unit No. (TRAIS)	
		11. Contract or Grant No.	
12. Sponsoring Agency Name and Address U.S. Department of Transportation Federal Aviation Administration Office of Aviation Research Washington, DC 20591		13. Type of Report and Period Covered Final Report	
		14. Sponsoring Agency Code ACE-110	
15. Supplementary Notes The FAA William J. Hughes Technical Center COTR was Mr. Peter Shyprykevich.			
16. Abstract <p>The effectiveness of repair of damaged fiber reinforced composite laminates was investigated; the effectiveness of repair being assessed by the tensile failure load of the repaired laminate.</p> <p>First, tests were conducted measuring the failure loads of laminates repaired either by the scarf, the uniform lap, or the stepped lap technique. Data were generated with the following parameters having been varied: type of material of the damaged laminate, type of repair material, scarf angle and number of external plies in scarf repair, length and number of repair plies in uniform and stepped lap repair, moisture content of the laminate prior to repair, moisture content of the laminate after repair, test temperature, roughness of grinding tool used in preparing the repair surface, and the temperature applied during the cure of the repair patch. The aforementioned parameters were varied over wide ranges, and provided systematic sets of data which shed light on the influence of each of these parameters on the effectiveness of the repair.</p> <p>Second, models were developed for calculating the failure loads of composite laminates repaired by scarf and uniform lap techniques. The models take into account anisotropy of each ply in the laminate and in the repair ply and nonelastic behavior of the adhesive or resin interlayer between the laminate and the repair patch. On the basis of the models, two computer codes were written for generating numerical values of the failure loads. The first code is for calculating the failure loads of laminates repaired by the uniform lap technique, the second for calculating the failure loads of laminates repaired by the scarf technique. Failure loads calculated by the models and the corresponding computer codes were compared with data and good agreement was found between the results of the analysis and the tests.</p>			
17. Key Words Bonded repairs, Composites, Analysis methods, Parameter studies		18. Distribution Statement This document is available to the public through the National Technical Information Service (NTIS) Springfield, Virginia 22161.	
19. Security Classif. (of this report) Unclassified	20. Security Classif. (of this page) Unclassified	21. No. of Pages 85	22. Price

TABLE OF CONTENTS

	Page
EXECUTIVE SUMMARY	xi
1. INTRODUCTION	1
2. THE PROBLEM	1
PART I. EXPERIMENTAL RESULTS	3
3. EXPERIMENTAL	3
4. TEST RESULTS	10
4.1 Type of Repair Material	11
4.2 Geometry Effects	16
4.3 Effects of Specimen Moisture Content and Test Temperature	22
4.3.1 Base Laminates Premoisturized	22
4.3.2 Specimen Moisture Content and Test Temperature	24
4.4 Effect of Sanding	25
4.5 Effect of Cure Cycle	26
4.6 Summary	29
PART II. ANALYTICAL MODELS	30
5. INTRODUCTION	30
6. THE PROBLEM	30
7. MODEL OF UNIFORM LAP REPAIR	32
7.1 Tensile Failure of the Laminate or Repair Patch	34
7.2 Shear Failure	35
7.2.1 Boundary and Continuity Conditions	39
7.2.2 Calculation of the Shear Failure Load	43
8. MODEL OF SCARF REPAIR	43
8.1 Interlayer Shear Strain	45
8.1.1 Boundary and Continuity Conditions	49

8.1.2	Calculation of the Interlayer Shear Strain	55
8.2	Failure Load	55
9.	RESULTS	57
10.	CONCLUDING REMARKS	62
11.	REFERENCES	63

APPENDICES

- A—Moisture Loss of Specimen During Test
- B—Failure Loads of Specimens Exposed to Humid Air
- C—Test Results
- D—Failure Loads of Specimens Under Moisture and Temperature

LIST OF FIGURES

Figure		Page
1	Illustrations of the Scarf and Lap Repair Techniques	1
2	The Base Laminates Prior to Repair	2
3	Illustration of the Repair Techniques Used in This Study	2
4	The Temperature Cycle Used for Curing the Base Laminate and in Making the Repair	4
5	Geometries of the Test Specimens	5
6	Application of the Adhesive Layer When Repairing With Prepreg	5
7	Test Specimens Cut Out of the Repaired Base Laminate	6
8	Specimen Conditions and Test Temperatures	6
9	Failure Loads of Different Base Laminates Repaired With Different Repair Materials (Scarf Repair at 70°F)	12
10	Failure Loads of Different Base Laminates Repaired With Different Repair Materials (Scarf Repair at 180°F)	12
11	Failure Loads of Different Base Laminates Repaired With Different Repair Materials (Stepped Lap Repair at 70°F)	13
12	Failure Loads of Different Base Laminates Repaired With Different Repair Materials (Stepped Lap Repair at 180°F)	14
13	Typical Failure Modes of Specimens Repaired by Scarf and Stepped Lap Techniques	16
14	Definition of the Geometric Factors Investigated	17
15	The Variation of Failure Load With Scarf Angle	19
16	The Effect of the Number of External Plies on the Failure Load in Scarf Repair	19
17	The Effect of Lap Length on the Failure Load in Stepped Lap Repair	20
18	The Effect of Lap Length on the Failure Load in Uniform Lap Repair	20
19	Typical Failure Modes of Specimens Repaired by Stepped Lap and Uniform Lap Techniques With Various Lap Lengths	21

20	The Effect of the Number of Repair Plies on the Failure Load	21
21	Comparisons of the Failure Loads of Specimens Repaired by the Stepped Lap and Uniform Lap Repair Techniques	22
22	Failure Loads of Repaired Specimens When the Base Laminates Were Moisturized Prior to Repair	24
23	The Effects of Specimen Moisture Content and Test Temperature on the Failure Load	25
24	The Failure Loads of Specimens Sanded With Different Grit Diamond Sanders	26
25	Illustration of the Test Setup Used in Studying the Effects of Cure Cycle on the Repair	27
26	The Cure Time Required to Reach Full Cure at Different Cure Temperatures	27
27	A Typical Output of the Microdielectrometer	28
28	Failure Loads of Specimens Repaired at Different Cure Temperatures	29
29	Models of the Uniform Lap and the Scarf Repairs	31
30	The Interlayer Between the Laminate and the Repair Patch When the Repair is Performed With Wet Lay-Up (Lower Left) or Prepreg (Lower Right)	31
31	Illustration of the Shear Stress-Shear Strain Relationship of an Elastic-Perfectly Plastic Interlayer	32
32	Double-Sided Uniform Lap Repair Model	32
33	Double-Sided Uniform Lap Repair Treated in the Model	33
34	Illustration of the Types of Failure Which May Occur in a Laminate Repaired by the Double-Sided Uniform Lap Technique	33
35	The On-Axis (x, y) and Off-Axis (1, 2) Coordinate Systems	34
36	Loads on a Section dx in Length of the Laminate Repaired by the Double-Sided Uniform Lap Technique	36
37	Deformations of the Repair Patch, the Interlayer, and the Laminate	37
38	Possible Regions of the Interlayer Under an Applied Load P	38
39	The Boundary Conditions for the In-Plane Loads in the Laminate and in the Repair Patch and the Continuity Conditions for the Shear Strain in the Interlayer	40

40	The Equations and Boundary Conditions for Calculating the Shear Strain in the Interlayer When the Entire Interlayer Behaves in a Linearly Elastic Manner	41
41	The Equations and Boundary and Continuity Conditions for Calculating the Shear Strain in the Interlayer When the Interlayer is Perfectly Plastic Near the $x = 0$ End	41
42	The Equations and Boundary and Continuity Conditions for Calculating the Shear Strain in the Interlayer When the Interlayer is Perfectly Plastic Near the $x = d_l$ End	42
43	The Equations and Boundary and Continuity Conditions for Calculating the Shear Strain in the Interlayer When the Interlayer is Perfectly Plastic Near the $x = 0$ and $x = d_l$ Ends	42
44	Scarf Repairs Treated in the Model	44
45	The Types of Failure Which May Occur in a Laminate Repaired by the Scarf Technique	44
46	The Scarf Repair Treated in the Model	45
47	Loads on a Section dx in Length of the k -th Segment of the Laminate Repaired by the Scarf Technique	46
48	Deformations of the Repair Patch, the Interlayer, and the Laminate in the k -th Segment of a Laminate Repaired by the Scarf Technique	47
49	The Compliance Matrices in the Laminate and the Repair Patch	48
50	Possible Regions of the Interlayer Under an Applied Load P	48
51	Model of the Boundary at the Outer Edge ($x = x_K$) of the Repair Patch	51
52	The Boundary Conditions for the In-Plane Loads in the Laminate and in the Repair Patch	51
53	The Continuity Conditions at the Edge of the k -th Segment	52
54	The Continuity Conditions at the Interlayer Between the Elastic and Perfectly Plastic Regions	52
55	The Equations and Boundary Conditions for Calculating the Shear Strain in the Interlayer When the Entire Interlayer Behaves in a Linearly Elastic Manner	53
56	The Equations and Boundary and Continuity Conditions for Calculating the Shear Strain in the Interlayer When the Interlayer is Perfectly Plastic Near the $x = 0$ End	53
57	The Equations and Boundary and Continuity Conditions for Calculating the Shear Strain in the Interlayer When the Interlayer is Perfectly Plastic Near the $x = x_K$ End	54

58	The Equations and Boundary and Continuity Conditions for Calculating the Shear Strain in the Interlayer When the Interlayer is Perfectly Plastic Near the $x = 0$ and $x = x_K$ Ends	54
59	Comparisons of the Calculated (Model) and the Measured (Data) Failure Loads as a Function of Lap Length for 8-Ply Laminate	60
60	Comparison of the Calculated (Model) and the Measured (Data) Failure Loads as a Function of Lap Length for 32-Ply Laminate	61
61	Comparisons of the Calculated (Model) and the Measured (Data) Failure Loads as a Function of Scarf Angle	61
62	Comparison of the Calculated (Model) and the Measured (Data) Failure Loads as a Function of Extra Plies	62

LIST OF TABLES

Table		Page
1	The Base Materials, Repair Materials, and Cure Cycles Used for Fabricating the Base Laminate and for Making the Repair	3
2	Average Tensile Properties of Specimens Made of Materials Used for Fabricating the Base Laminates	7
3	Average Tensile Properties of Specimens Made of Materials Used for Repair	8
4	Normalized (63% Fiber Volume) Tensile Properties of Specimens Made of Materials Used for Fabricating the Base Laminates	9
5	Normalized (63% Fiber Volume) Tensile Properties of Specimens Made of Materials Used for Repair	10
6	The Test Matrix Used for Evaluating the Effectiveness of Different Repair Materials	11
7	The Failure Loads of Specimens Repaired by the Scarf Technique	13
8	The Failure Loads of Specimens Repaired by the Stepped Lap Technique	14
9	Test Matrix Used for Evaluating the Effects of Different Geometries of the Scarf and Lap Repairs	17
10	The Test Matrix Used for Evaluating the Effects of the Moisture Content of the Base Laminate Prior to Repair	23

11	The Test Matrix Used for Evaluating the Effects of Specimen Moisture Content and Test Temperature	24
12	Tests With Different Preparation of the Repair Surface	26
13	The Input Parameters Required by RepairL and the Numerical Values Used in the Present Calculations for 3k70 Plain Weave Fabric Impregnated With 9396 Resin	58
14	The Input Parameters Required by RepairS and the Numerical Values Used in the Present Calculations for 3k70 Plain Weave Fabric Impregnated With 9396 Resin	59

EXECUTIVE SUMMARY

As fiber reinforced organic matrix composites are gaining wide acceptance, it is becoming important to develop repair techniques for structures made of such composites. The present work studied the repair of composite laminates in a manner which shed light on significant factors influencing the effectiveness of a repair. Specifically, the objective was to obtain a systematic set of data which indicates how the type of repair material, the geometry of the repair, the moisture content of the repaired area, the preparation of the surface prior to repair, and the processing conditions used during repair affect the strength of the repaired part. In addition, analytic techniques were developed which can be used to estimate the strengths of composite laminates after they have been repaired.

Tests were conducted measuring the failure loads of laminates repaired either by the scarf, the uniform lap, or the stepped lap technique under tensile loading. Data were generated with the parameters having been varied. The aforementioned parameters were varied over wide ranges and provided systematic sets of data with the following findings.

- The type of wet lay-up repair material used in the repair or the type of parent laminate material on which the repair is made does not affect the quality (failure load) of the repaired part.
- For a scarf repair, there is a gradual decrease in the failure load with increasing scarf angle. In the present tests the highest failure load occurred at a scarf angle of about 1 degree.
- For a lap repair, there is a limiting lap length beyond which the failure load does not increase.
- If the parent laminate moisture content is low and the prior moisture history of the part is known, the repair area does not need to be dried prior to repair. However, if the laminate moisture content is high (above 1.1 percent), the repair area needs to be dried completely before repair.
- The failure loads of repaired specimens are reduced under hot/wet conditions, i.e., when both the moisture content and the test temperature are high.
- Preparing the repair surfaces by sanding them with diamond sander ranging from 60 to 400 grit number does not significantly affect failure load.
- Repair should be cured at the highest permissible temperature so as to achieve the shortest cure time.

In conjunction with experimental work, models were developed for calculating the failure loads of composite laminates repaired by scarf and uniform lap techniques. The models take into account anisotropy of each ply in the laminate and in the repair ply and nonelastic behavior of the adhesive or resin interlayer between the laminate and the repair patch. On the basis of the

models, two computer codes were written for generating numerical values of the failure loads. The first code is for calculating the failure loads of laminates repaired by the uniform lap technique, the second for calculating the failure loads of laminates repaired by the scarf technique. Failure loads calculated by the models and the corresponding computer codes were compared with data and good agreement was found between the results of the analysis and the tests.

1. INTRODUCTION.

As fiber reinforced organic matrix composites are gaining wide acceptance, it is becoming important to develop repair techniques for structures made of such composites. Owing to the importance of the problem, several techniques have been proposed for repairing composite laminates. Most of these techniques were developed for repairing specific parts with specific materials in the field [1-23], and can not readily be generalized to different repair applications.

It would be advantageous to develop repair techniques which can be employed in a wide range of applications. With this objective in mind, the Commercial Aircraft Composite Repair Committee (CACRC) was formed under the aegis of Air Transport Association (ATA), International Air Transport Association (IATA), and Society of Automotive Engineers (SAE) [24]. The major goal of the CACRC is to develop standard repair procedures for composite structures. To develop the procedures, several parameters relevant to the effectiveness of repair need to be thoroughly investigated.

Therefore, the objective of the present work was to study the repair of composite laminates to shed light on significant factors influencing the effectiveness of a repair. Specifically, the objective was to obtain a systematic set of data which indicates how the type of repair material, the geometry of the repair, the moisture content of the repaired area, the preparation of the surface prior to repair, and the processing conditions used during repair affect the strength of the repaired part. In addition, analytic techniques are presented which can be used to estimate the strengths of composite laminates after they have been repaired. The specific problems investigated are described in next section.

2. THE PROBLEM.

When composite laminates are damaged the damage frequently occurs only in a certain region of the laminate, as illustrated in figure 1. The damage is then repaired by removing some of the material around the damaged area and by applying a repair patch.

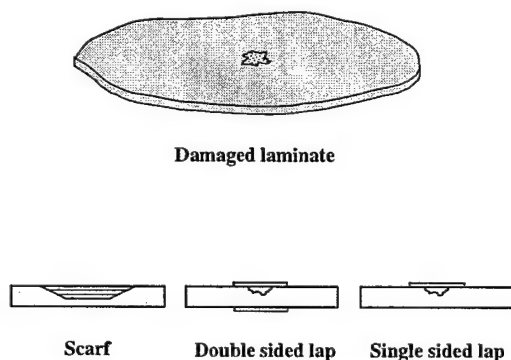


FIGURE 1. ILLUSTRATIONS OF THE SCARF AND LAP REPAIR TECHNIQUES

There are two main repair techniques, and these are referred to as scarf and lap (see figure 1). In the scarf technique the repair material is inserted into the laminate in place of the material removed due to the damage. In the lap technique the repair material is applied either on one or on both sides of the laminate over the damaged area.

In this investigation, a repair was simulated by joining two laminates (referred to as the base laminates, see figure 2) either by the scarf or by the lap technique (see figure 3).

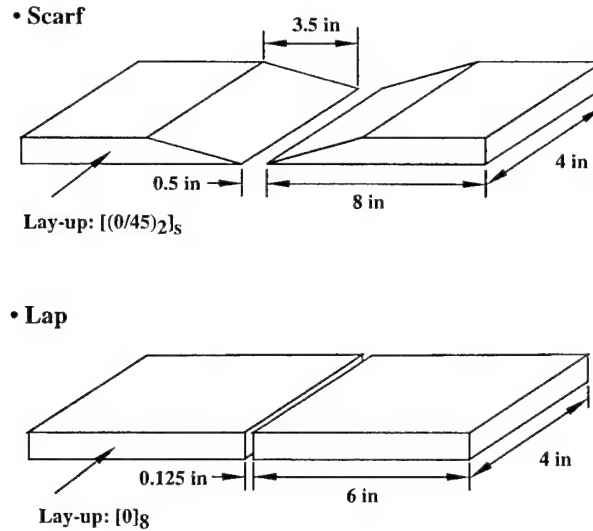


FIGURE 2. THE BASE LAMINATES PRIOR TO REPAIR
(Top: laminates used for scarf repair. Bottom: laminates used for lap repair.)

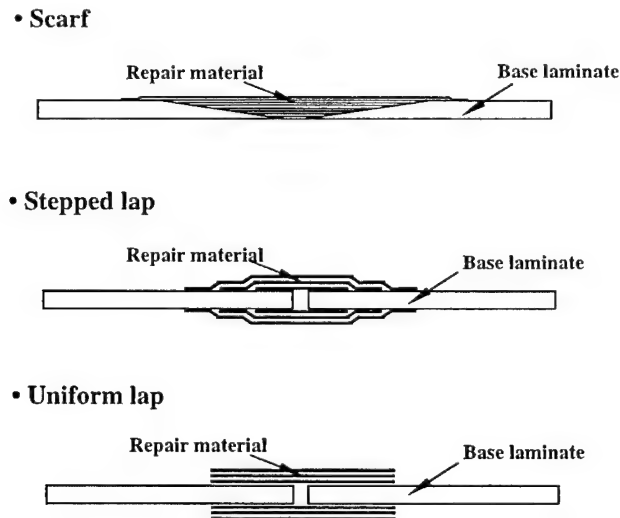


FIGURE 3. ILLUSTRATION OF THE REPAIR TECHNIQUES USED IN THIS STUDY

For lap repairs two types were considered. One is the double-sided uniform lap, where the lengths of the layers in the lap are the same. The other one is the double-sided stepped lap, where the lengths of the repair layers increase, the shortest layer being next to the surface and the longest on the outside.

The effectiveness of repair was evaluated by subjecting 1-in-wide test specimens, cut out of the base laminate, to longitudinal tensile loads. The effectiveness of the repair was taken to be the tensile load at which the specimen fails.

Five series of tests were performed to evaluate the effects of the following parameters on the failure load of the repaired laminate.

1. Type of repair material (i.e., the material used for the repair)
2. Geometry of the repair
3. Moisture content of the specimen and the test temperature
4. Preparation of the surface on which the repair is performed
5. Processing (cure) condition applied during the repair

In addition, analytic techniques are presented for estimating the failure loads of composite laminates repaired by scarf and by double-sided uniform lap techniques.

This report covers the experimental and analytical research performed for repairs evaluated under tensile loading. Sandwich test results under compression loads and fracture mechanics tests characterizing repair materials were reported previously in [25] and [26].

PART I. EXPERIMENTAL RESULTS.

3. EXPERIMENTAL.

Plain weave carbon fiber fabric prepreg plies (with either Hexcel F593, Ciba Geigy R922, or Ciba Geigy R6376 resin system) were used in the construction of the base laminates (table 1).

TABLE 1. THE BASE MATERIALS, REPAIR MATERIALS, AND CURE CYCLES USED FOR FABRICATING THE BASE LAMINATE AND FOR MAKING THE REPAIR

Base Material		Cure Temperature (°F)	Final Processing Temperature (°F)	Δt_1 (min)	Δt_2 (min)	Δt_3 (min)	Pressure (Psi)
Fabric	3k70 plain weave carbon fiber fabric						
Resin	Hexcel F593 Ciba Geigy R922 Ciba Geigy R6376	350	140	120	120	90	45 75 75
Repair Materials (Wet lay-up)							
Fabric	3k70 plain weave carbon fiber fabric						
Resin	Dexter Hysol EA9396/C2 Dexter Hysol EA9390 Ciba Geigy Epocast 52-A/B	200	70	20	60 220 120	30	14.7
Repair Materials (Prepreg)*							
Fabric	3k70 plain weave carbon fiber fabric						
Resin	Ciba Geigy M20	250	70	30	120	40	14.7

* Dexter Hysol EA 9628 is used as a film adhesive.

The base laminates were 8 in by 4 in for scarf repair and 6 in by 4 in for lap repair (see figure 2). The lay-up of the base laminate was $[(0/45)_2]_s$ for scarf repair and $[0]_8$ for lap repair. The 0°

refers to fabric which has fibers parallel and perpendicular to the longitudinal axis. The 45° designates plies in which the fibers are $\pm 45^\circ$ from the longitudinal axis. Each base laminate was laid up by hand, vacuum bagged, and cured in an autoclave by the manufacturer's cure cycle (figure 4 and table 1). Same cure cycle was used for the scarf and patch repairs, figure 4. The thicknesses of the cured base laminates ranged from 0.057 to 0.070 in. The autoclave pressure (during fabrication of base laminates) or the vacuum (during repair) were applied at time $t = 0$ and were kept constant during the cure.

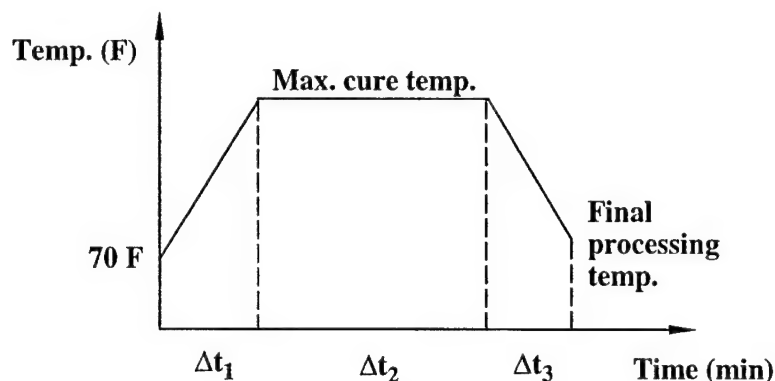


FIGURE 4. THE TEMPERATURE CYCLE USED FOR CURING THE BASE LAMINATE AND IN MAKING THE REPAIR

After curing, the surfaces of the base laminate, on which a scarf or a lap repair was to be applied, were sanded with a 120 grit diamond sander. The uniformity of the sanded surface was assessed by the water-break test, i.e., by spreading a thin layer of water on the surface, and by observing whether or not the entire surface was wetted [27]. The water was removed by drying the specimen in an oven. The surface was cleaned by acetone just prior to repair.

Two base laminates were joined (repaired) either by the scarf or by the lap technique, as follows. The two base laminates were placed side by side (see figure 2) with a 0.5-in gap between the laminates for scarf repair and a 0.125-in gap for lap repair. The repair was applied with carbon fiber fabric plies, cut into the desired shape, either in wet lay-up or in prepreg form. For a wet lay-up repair, the plies were impregnated with a two parts epoxy resin (Dexter Hysol EA9396/C2, Dexter Hysol EA9390, or Ciba Geigy Epocast 52-A/B, table 1). The prepreg plies were preimpregnated with Ciba Geigy M20 resin. Each ply (wet lay-up or prepreg) was placed either into the base laminate (scarf repair) or on the surface of the base laminate (lap repair) (see figure 5). The 0 degree direction is along the longitudinal axis of the specimen. Zero refers to plies with 0 and 90 degree fiber orientations. Forty-five refers to plies with +45 and -45 degree fiber orientations. For the repair with prepreg plies a layer of film adhesive was placed between the base laminate and the repair material to facilitate bonding between the base laminate and the repair material (see figure 6).

For the scarf repair, the orientation of each repair ply in the repaired zone was the same as the corresponding ply orientation of the base laminate. In addition, two 0° external plies were placed on the surface of the base laminate covering the repaired area (see figure 5). For the lap

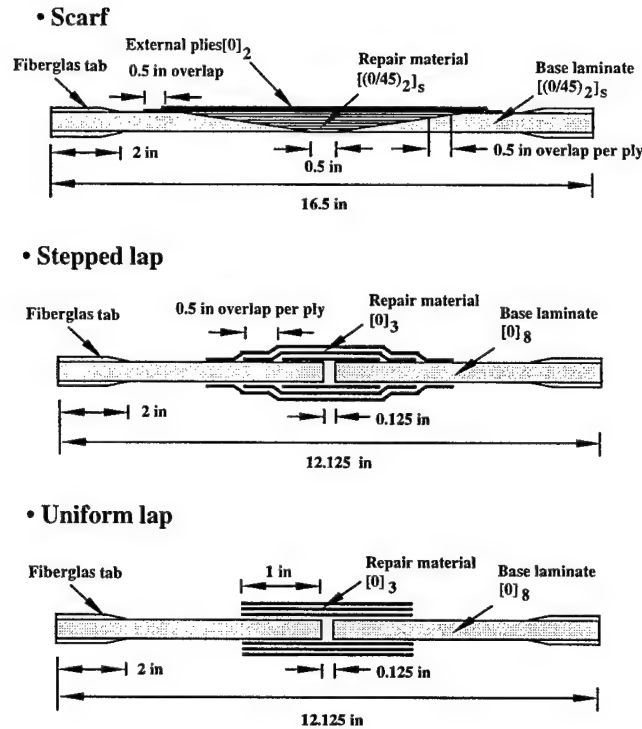


FIGURE 5. GEOMETRIES OF THE TEST SPECIMENS

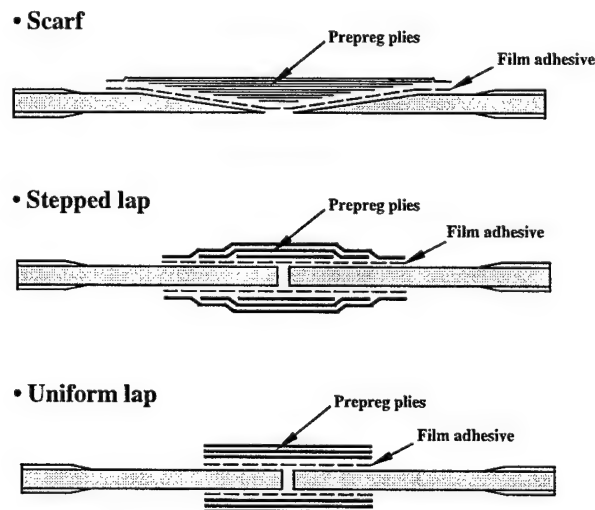


FIGURE 6. APPLICATION OF THE ADHESIVE LAYER WHEN REPAIRING WITH PREPREG

repair, the repair plies (with the same 0° orientations as the base laminate) were placed on both sides of the base laminate, as illustrated in figure 5.

After the repair material was applied, the repair area was vacuum bagged and cured in an oven under atmospheric pressure (see table 1). After curing, 2-in-long and 0.125-in-thick fiberglass tabs were attached with room temperature cure Epoxy 907.

To make test specimens, the base laminate, repaired in the manner described above, was cut into 1-in-wide strips (see figure 7). The detailed geometries of the specimens are given in figure 5.

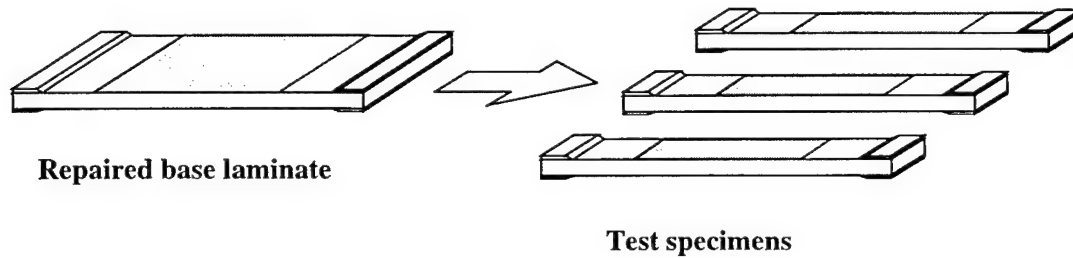


FIGURE 7. TEST SPECIMENS CUT OUT OF THE REPAIRED BASE LAMINATE

Each test specimen was subjected to uniaxial tensile loads at a constant displacement rate of 0.05 in./mm. The load at which the specimen failed (failure load) was recorded. The failed specimens were also inspected visually to establish the mode of failure.

Some of the specimens were tested dry (as prepared), while some were moisturized before testing either by immersing the specimen in 180°F water for 14 days or by exposing the specimen to 100 percent humid air at 180°F until 1.1 percent moisture content (weight gain) was reached (see figure 8). These conditions were adopted because the same conditions are frequently used in the aircraft industry in testing adhesively bonded joints.

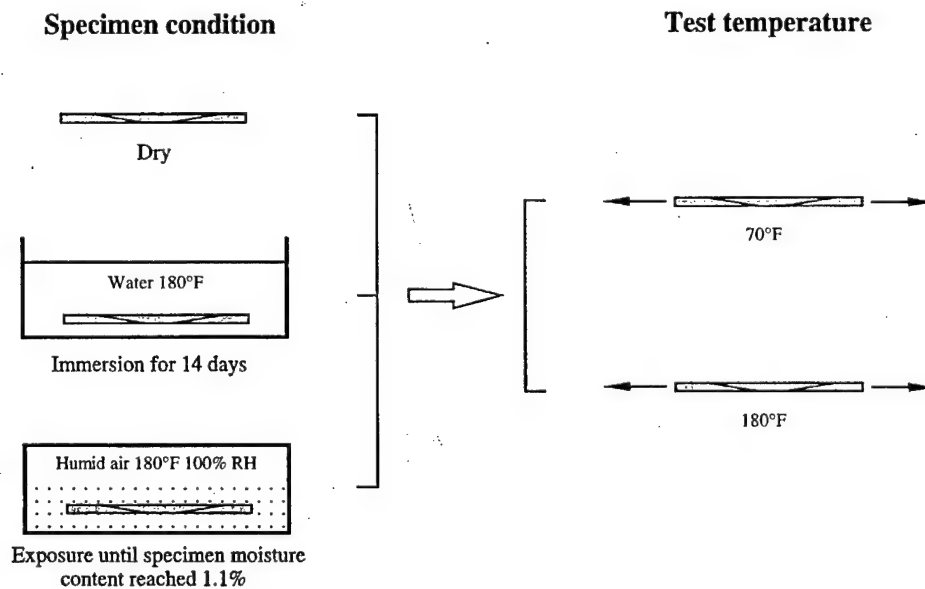


FIGURE 8. SPECIMEN CONDITIONS AND TEST TEMPERATURES

Each specimen was tested either at 70° or 180°F. The temperature was maintained by a chamber surrounding the specimen. In this chamber the relative humidity was not regulated. Thus, a small amount (less than 0.007 percent, appendix A) of drying occurred during the 180°F tests, which lasted about 10 minutes.

For reference purposes, the tensile properties of undamaged laminates made of the materials used in constructing the base laminates and in the repair were measured. To this end, 12- by 4-in ($[(0/45)_2]_s$ and $[0]_8$) plates were prepared in the same manner as the base laminates (see previous section). Fiberglass tabs were mounted on the plates, and 1-inch-wide, straight-sided tensile specimens were cut out of the plates. The specimens were subjected to uniaxial tensile loads at a constant displacement rate of 0.05 in/mm. The load versus strain and the failure load were recorded. The strain was measured by an extensometer. These tests were performed under the same conditions as were used for the repaired test specimens (see figure 8). The measured tensile strengths and longitudinal stiffnesses are given in tables 2 and 3. The values are the average values of three tests.

TABLE 2. AVERAGE TENSILE PROPERTIES OF SPECIMENS MADE OF MATERIALS USED FOR FABRICATING THE BASE LAMINATES

Lay-Up	Material*	Specimen Condition/ Test Temperature**	Failure Load (lbf)	Strength (ksi)	Stiffness (Msi)
$[0]_8$	F593	Dry/70°F	6600	101	8.1
		Moist-H ₂ O/180°F	6110	93	8.5
		Moist-humid air /180°F	6180	95	8.4
	R922	Dry/70°F	5890	105	10.8
		Moist-H ₂ O/180°F	4580	96	10.8
		Moist-humid air/180°F	5560	102	10.4
	R6376	Dry/70°F	6550	107	9.2
		Moist-H ₂ O/180°F	6720	107	10.2
		Moist-humid air/180°F	6330	101	9.8
$[(0/45)_2]_s$	F593	Dry/70°F	4780	72	5.9
		Moist-H ₂ O/180°F	4100	59	5.8
		Moist-humid air/180°F	4190	64	6.0
	R922	Dry/70°F	4850	90	7.4
		Moist-H ₂ O/180°F	4010	69	7.4
		Moist-humid air/180°F	4490	83	7.4
	R6376	Dry/70°F	5850	90	6.5
		Moist-H ₂ O/180°F	4730	76	6.9
		Moist-humid air/180°F	5070	80	7.3

* The material was plain weave carbon fiber fabric impregnated with the type of resin indicated in this column (see table 1).

** Specimens were either dry, immersed in 180°F water for 14 days (moist-H₂O), or exposed to 180°F air at 100% relative humidity until 1.1% moisture content was reached (moist-humid air). Test temperature was either 70° or 180°F (figure 8).

From the data in tables 2 and 3, the properties of unidirectional plies made from the base and repair materials were deduced. These values, though of not direct concern in this study, are listed in tables 4 and 5. The data in tables 4 and 5 were normalized to apply to a 0.011-in-thick ply with a nominal fiber volume content of 63 percent.

TABLE 3. AVERAGE TENSILE PROPERTIES OF SPECIMENS MADE OF MATERIALS USED FOR REPAIR

Lay-Up	Material*	Specimen Condition/ Test Temperature**	Failure Load (lbf)	Strength (ksi)	Stiffness (Msi)
[0] ₈	EA9396	Dry/70°F	5608	75	7.2
		Moist-H ₂ O/180°F	5581	68	7.7
	EA9390	Dry/70°F	6458	91	7.9
		Moist-H ₂ O/180°F	6039	83	8.7
	Epocast	Dry/70°F	5934	73	7.0
		Moist-H ₂ O/180°F	5635	73	9.7
	M20	Dry/70°F	7253	118	9.2
		Moist-H ₂ O/180°F	7252	106	8.5
[(0/45) ₂] _s	EA9396	Dry/70°F	4623	58	5.0
		Moist-H ₂ O/180°F	3722	47	5.2
	EA9390	Dry/70°F	4150	58	5.5
		Moist-H ₂ O/180°F	4049	56	6.2
	Epocast	Dry/70°F	4428	51	5.0
		Moist-H ₂ O/180°F	4277	58	5.6
	M20	Dry/70°F	6035	95	6.7
		Moist-H ₂ O/180°F	5101	77	5.9

* The material was plain weave carbon fiber fabric impregnated with the type of resin indicated in this column (see table 1).

** Specimens were either dry, or immersed in 180°F water for 14 days (moist-H₂O). Test temperature was either 70° or 180°F (figure 8).

TABLE 4. NORMALIZED (63% FIBER VOLUME) TENSILE PROPERTIES OF SPECIMENS MADE OF MATERIALS USED FOR FABRICATING THE BASE LAMINATES

Lay-Up	Material*	Specimen Condition/ Test Temperature**	Strength (ksi)	Stiffness (Msi)
[0] ₈	F593	Dry/70°F	137	11.0
		Moist-H ₂ O/180°F	118	10.8
		Moist-humid air /180°F	125	11.0
	R922	Dry/70°F	175	17.9
		Moist-H ₂ O/180°F	156	17.6
		Moist-humid Air/180°F	166	16.9
	R6376	Dry/70°F	157	13.5
		Moist-H ₂ O/180°F	150	14.2
		Moist-humid air/180°F	138	13.5
[(0/45) ₂] _s	F593	Dry/70°F	96	7.8
		Moist-H ₂ O/180°F	74	7.3
		Moist-humid air/180°F	84	7.8
	R922	Dry/70°F	117	12.1
		Moist-H ₂ O/180°F	108	12.5
		Moist-humid air/180°F	110	12.3
	R6376	Dry/70°F	126	9.1
		Moist-H ₂ O/180°F	104	9.4
		Moist-humid air/180°F	110	10.0

* The material was plain weave carbon fiber fabric impregnated with the type of resin indicated in this column (see table 1).

** Specimens were either dry, immersed in 180°F water for 14 days (moist-H₂O), or exposed to 180°F air at 100% relative humidity until 1.1% moisture content was reached (moist-humid air). Test temperature was either 70° or 180°F (figure 8).

TABLE 5. NORMALIZED (63% FIBER VOLUME) TENSILE PROPERTIES OF SPECIMENS MADE OF MATERIALS USED FOR REPAIR

Lay-Up	Material*	Specimen Condition/ Test Temperature**	Strength (ksi)	Stiffness (Msi)
[0] ₈	EA9396	Dry/70°F	88	8.5
		Moist-H ₂ O/180°F	75	8.2
	EA9390	Dry/70°F	108	9.4
		Moist-H ₂ O/180°F	98	10.4
	Epocast	Dry/70°F	76	7.3
		Moist-H ₂ O/180°F	80	10.7
	M20	Dry/70°F	162	12.6
		Moist-H ₂ O/180°F	139	11.2
[(0/45) ₂] _s	EA9396	Dry/70°F	64	5.5
		Moist-H ₂ O/180°F	51	5.7
	EA9390	Dry/70°F	71	6.7
		Moist-H ₂ O/180°F	67	7.5
	Epocast	Dry/70°F	61	6.3
		Moist-H ₂ O/180°F	69	6.7
	M20	Dry/70°F	103	9.2
		Moist-H ₂ O/180°F	101	7.8

* The material was plain weave carbon fiber fabric impregnated with the type of resin indicated in this column (see table 1).

** Specimens were either dry, or immersed in 180°F water for 14 days (moist-H₂O). Test temperature was either 70° or 180°F (figure 8).

4. TEST RESULTS.

The failure loads of repaired specimens under different conditions are presented in this section. The failure loads are normalized with respect to failure loads appropriate to the given test. The actual values of the measured failure loads are included in appendix B. Each data shown in this section is the average of three to six tests. The spread in the data is indicated by bars.

The materials used for fabricating the base laminates and the repair were given in table 1. The materials were chosen for this study because they are currently used or being considered for use in several different commercial aircraft. In the following, for simplicity, both the base laminates and the repair materials are identified by their resin system. The base laminates are referred to as

F593, R922, and R6376, while the repair materials as 9396, 9390, Epocast, and M20 (see table 1). Note again, that the repair materials using 9396, 9390, and Epocast resins were prepared by wet lay-up, while the repair material designated as M20 was in prepreg form.

Five series of tests were performed. The results of each five test series are given below.

4.1 TYPE OF REPAIR MATERIAL.

To evaluate the effectiveness of different repair materials, four types of material were used to repair the base laminates which were made of three different materials. Repairs were made both by the scarf and the stepped lap techniques. The complete test matrix used in this test series is given in table 6. Each test was performed with specimens repaired by the scarf and the stepped lap technique.

TABLE 6. THE TEST MATRIX USED FOR EVALUATING THE EFFECTIVENESS OF DIFFERENT REPAIR MATERIALS

Base Laminate*	Repair Material*	Specimen Condition/Test Temperature**		
		Dry/70°F	Moist-H ₂ O/180°F	Moist-Humid Air/180°F
F593	9396	X	X	X
	9390	X	X	X
	Epocast	X	X	X
	M20	X	X	X
R922	9396	X	X	X
	9390	X	X	X
	Epocast	X	X	X
	M20	X	X	X
R6376	9396	X	X	X
	9390	X	X	X
	Epocast	X	X	X
	M20	X	X	X

* The material was plain weave carbon fiber fabric impregnated with the type of resin indicated in this column (see table 1).

** Specimens were either dry, immersed in 180°F water for 14 days (moist-H₂O), or exposed to 180°F air at 100% relative humidity until 1.1% moisture content was reached (moist-humid air). Test temperature was either 70° or 180°F (figure 8).

The failure loads of different base laminates repaired with different repair materials (normalized with respect to the failure load of undamaged laminates) are shown in figures 9 and 10 and table 7 for scarf repair and in figures 11 and 12 and table 8 for stepped lap repair. The results in these figures are for dry specimens and for specimens moisturized by immersion in water for 14 days.

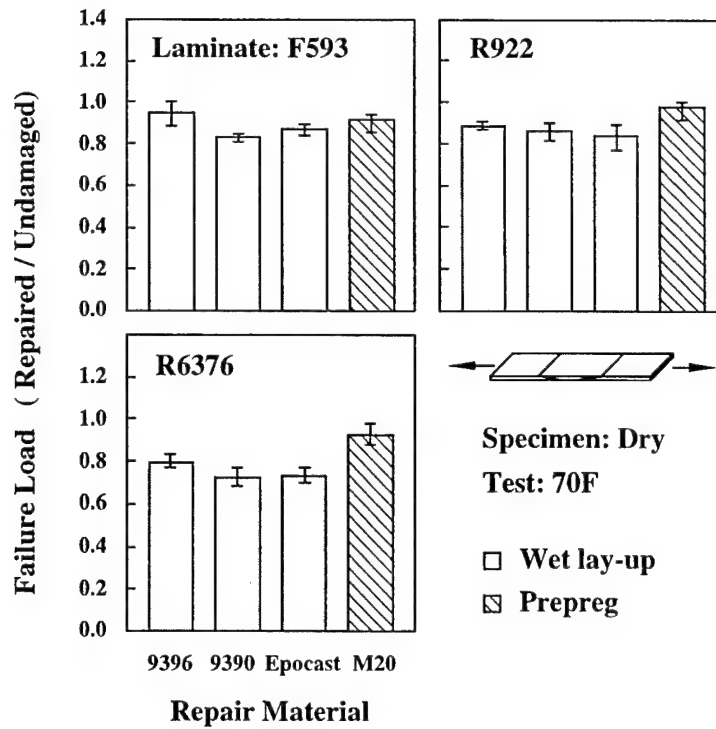


FIGURE 9. FAILURE LOADS OF DIFFERENT BASE LAMINATES REPAIRED WITH DIFFERENT REPAIR MATERIALS (SCARF REPAIR 70°F)

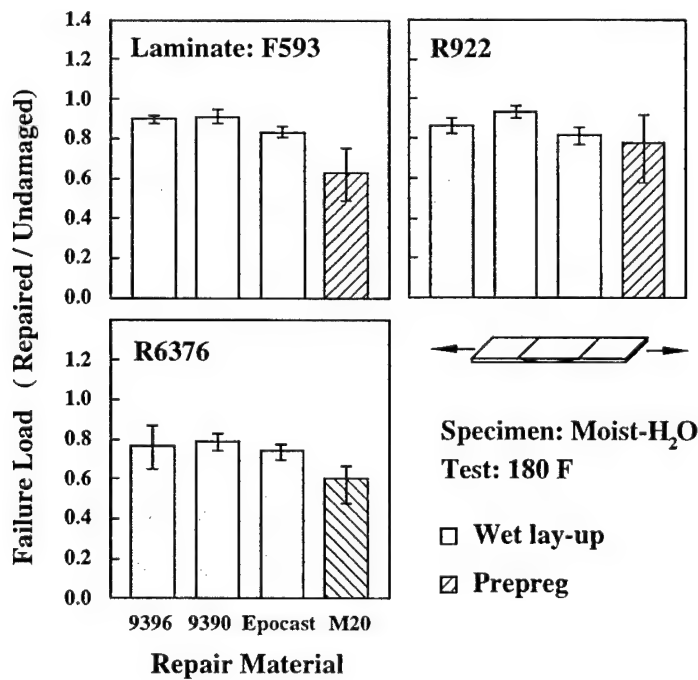


FIGURE 10. FAILURE LOADS OF DIFFERENT BASE LAMINATES REPAIRED WITH DIFFERENT REPAIR MATERIALS (SCARF REPAIR AT 180°F)

TABLE 7. THE FAILURE LOADS OF SPECIMENS REPAIRED BY THE SCARF TECHNIQUE

Base Laminate*	Repair Material*	Specimen Condition/Test Temperature**		
		Dry/70°F	Moist-H ₂ O/180°F	Moist-Humid Air/180°F
9396	F593	4526	3693	3558
	R922	4282	3468	3400
	R6376	4658	3621	3294
9390	F593	3695	3705	3404
	R922	4168	3746	3293
	R6376	4222	3735	3124
Epocast	F593	4175	3408	4178
	R922	4064	3279	3388
	R6376	4281	3514	3580
M20	F593	4386	2585	3176
	R922	4745	3123	3735
	R6376	5558	2862	2855

* The material was plain weave carbon fiber fabric impregnated with the type of resin indicated in this column (see table 1).

**Specimens were either dry, immersed in 180°F water for 14 days (moist-H₂O), or exposed to 180°F air at 100% relative humidity until 1.1% moisture content was reached (moist-humid air). Test temperature was either 70° or 180°F (figure 8).

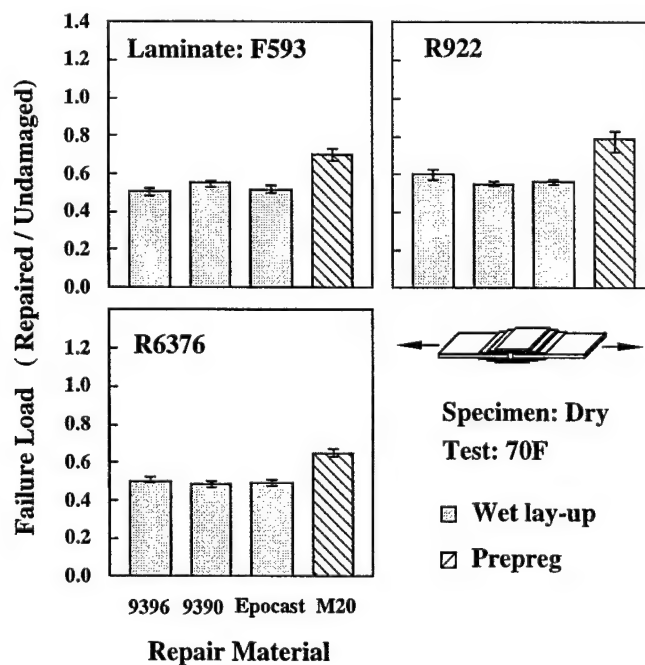


FIGURE 11. FAILURE LOADS OF DIFFERENT BASE LAMINATES REPAIRED WITH DIFFERENT REPAIR MATERIALS (STEPPED LAP REPAIR AT 70°F)

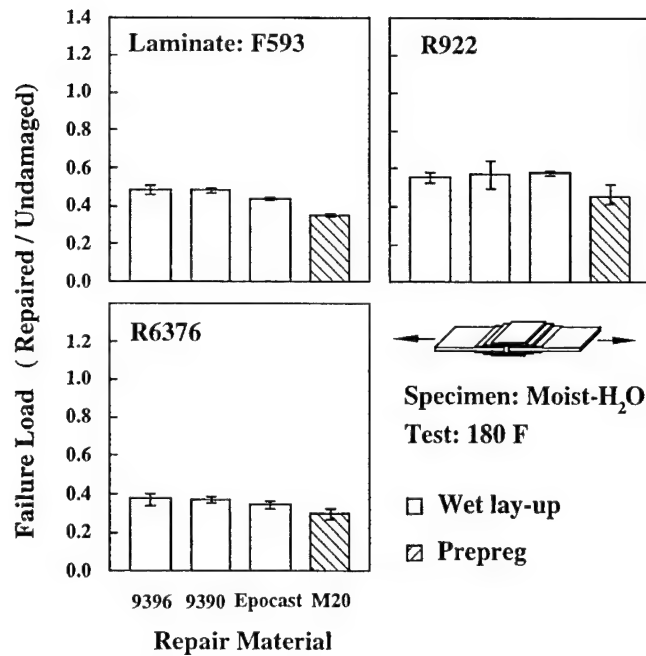


FIGURE 12. FAILURE LOADS OF DIFFERENT BASE LAMINATES REPAIRED WITH DIFFERENT REPAIR MATERIALS (STEPPED LAP REPAIR AT 180°F)

TABLE 8. THE FAILURE LOADS OF SPECIMENS REPAIRED BY THE STEPPED LAP TECHNIQUE

Base Laminate*	Repair Material*	Specimen Condition/Test Temperature**		
		Dry/70°F	Moist-H ₂ O/180°F	Moist-Humid Air/180°F
9396	F593	3360	2958	2624
	R922	3547	2533	2311
	R6376	3302	2520	2096
9390	F593	3638	2945	2351
	R922	3238	2612	2821
	R6376	3195	2497	2003
Epocast	F593	3420	2674	2570
	R922	3298	2642	2777
	R6376	3223	2307	2284
M20	F593	4516	2148	3150
	R922	4646	2097	3995
	R6376	4249	2033	3189

* The material was plain weave carbon fiber fabric impregnated with the type of resin indicated in this column (see table 1).

** Specimens were either dry, or immersed in 180°F water for 14 days (moist-H₂O), or exposed to 180°F air at 100% relative humidity until 1.1% moisture content was reached (moist-humid air). Test temperature was either 70° or 180°F (figure 8).

Data were also obtained with specimens with 1.1 percent moisture content achieved by exposure to 100 percent humid air at 180°F. Both the repaired specimens and the undamaged base laminates were tested dry at 70°F. Both the repaired specimens and the undamaged base laminates were immersed in 180°F water for 14 days and were tested at 180°F. Specimen geometry is given in figure 5. Failure loads of undamaged specimens are given in table 2. The failure loads of specimens moisturized by water and by humid air showed similar trends. Therefore, the data for specimens moisturized by humid air are not given here, but are included in appendix C. The following trends are indicated by the data:

- For the wet lay-up repair (scarf and stepped lap) the type of repair material did not significantly affect the failure load.
 - Failure of these specimens generally occurred due to shear along the base laminate-repair interface (see figure 13). Apparently, the interfacial shear strengths were similar for the three wet lay-up repair materials, resulting in similar failure loads, irrespective on which base material the repair was made.
 - The failure loads of specimens repaired by wet lay-up were nearly the same, irrespective of the base material that was repaired (tables 7 and 8).
- The failure loads were higher with the prepreg repair (scarf and stepped lap) than with the wet lay-up repair for specimens dry and tested at 70°F.
 - For the scarf repair with wet lay-up, failure occurred along the base laminate-repair interface. (With the prepreg repair, the failure was due to tensile failure of the base laminate (see figure 13).) This indicates that the failure load (in shear) of the adhesive film used in the prepreg repair was higher than either the failure load (in shear) of the wet lay-up interface or the failure load (in tension) of the base laminate. Thus specimens repaired with prepreg had higher failure loads than specimens repaired by wet lay-up.
 - For stepped lap repair, both with wet lay-up and with prepreg repair, failure occurred along the base laminate-repair interface (see figure 13). The shear strength of the adhesive film used in the prepreg repair was higher than the shear strength of the wet lay-up interface, resulting in the prepreg repair having higher failure loads than the wet lay-up repair.
- With the prepreg repair (scarf and stepped lap), the failure loads were lower than with wet lay-up when the specimens were moisturized and tested at 180°F.
 - For moisturized specimens tested at 180°F, failure always occurred along the base laminate-repair interface (see figure 13). Under these conditions the shear strength of the adhesive film used in the prepreg repair was lower than the shear strength of the wet lay-up interface. For this reason, specimens repaired by prepreg had lower failure loads than specimens repaired by wet lay-up.

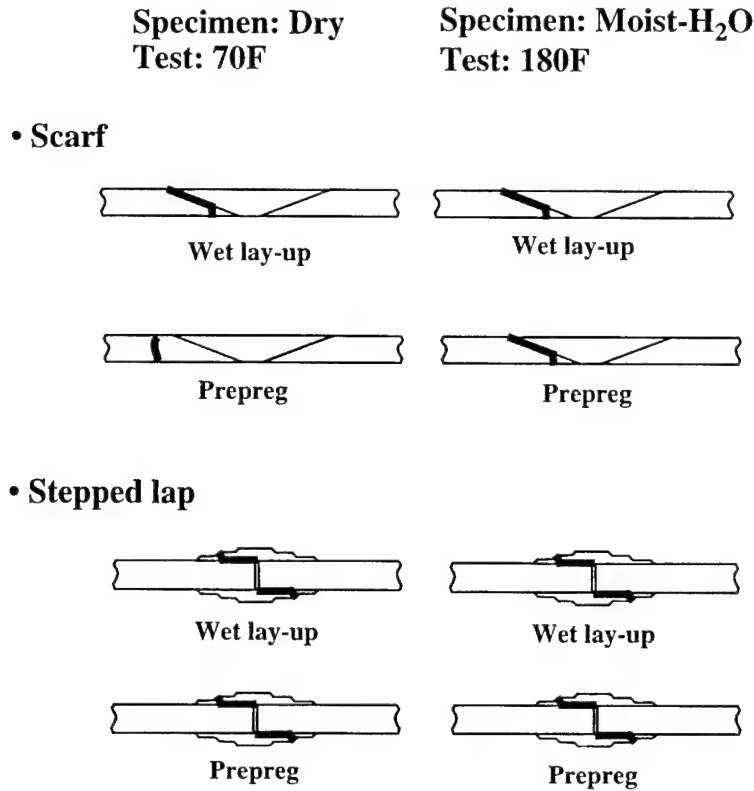


**FIGURE 13. TYPICAL FAILURE MODES OF SPECIMENS REPAIRED BY
SCARF AND STEPPED LAP TECHNIQUES**

(Solid lines indicate failure. Left: dry specimens tested at 70°F, right: moisturized specimens immersed in 180°F water for 14 days and tested at 180°F.)

The results shown in figures 10, 12, B-1, and B-2 also indicate the effects of specimen moisture content and test temperature on the failure load. These effects are discussed in section 4.3.

Since the results were similar and consistent for the three wet lay-up repair materials (9396, 9390, and Epocast), the tests presented in the following sections were conducted only with the 9396 repair material.

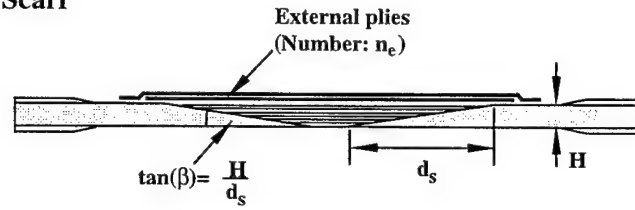
4.2 GEOMETRY EFFECTS.

The effects of the following geometric factors on the failure load were evaluated (see figure 14):

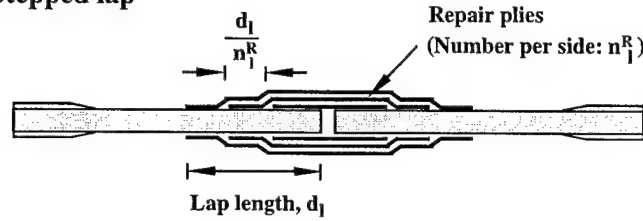
- For the scarf repair: the scarf angle β and the number of external plies n_e
- For the lap repair: the shape of the repair plies (stepped or uniform), the length of the repair plies (lap length, d_l), and the number of repair plies per side n_l^R .

The effects of these factors on the failure load were evaluated by testing dry as well as moisturized specimens at 70° and 180°F. The complete test matrix is shown in table 9.

• Scarf



• Stepped lap



• Uniform lap

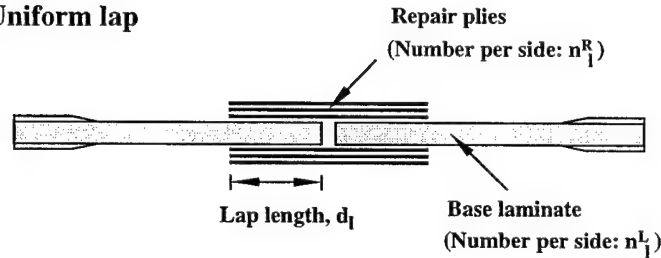


FIGURE 14. DEFINITION OF THE GEOMETRIC FACTORS INVESTIGATED

TABLE 9. TEST MATRIX USED FOR EVALUATING THE EFFECTS OF DIFFERENT GEOMETRIES OF THE SCARF AND LAP REPAIRS
(Base Laminate: F593, Repair Material: 9396)

Repair Type	Parameter	Specimen Condition/ Test Temperature	
		Dry/70°F	Moist-H ₂ O/180°F
Scarf	Scarf angle, β (degree)	0.72, 1.07, 2.15	0.72, 1.07, 2.15
	Number of external plies, n_e	0, 1, 2	0, 1, 2
Stepped lap	Lap length, d_l (in)	0.5, 1, 1.5, 2, 3	0.5, 1, 1.5, 2, 3
	number of repair plies per side, n_l^R	1, 2, 3	1, 2, 3
Uniform lap	Lap length, d_l (in)	0.25, 0.5, 1, 2, 3	0.25, 0.5, 1, 2, 3
	Number of plies in the base laminate, n_l^L	8, 32	8, 32
	Number of repair plies per side, n_l^R	1, 2, 3, 4	1, 2, 3, 4

* Specimens were either dry or immersed in 180°F water for 14 days (Moist-H₂O). Test temperature was either 70° or 180°F (figure 8).

The results are presented in figures 15 and 16 for the scarf repair and in figures 17 to 21 for the lap repair. The following general observations can be made on the basis of the data given in these figures.

- For the scarf repair
 - The failure load decreased with increasing scarf angle (see figure 15). Similar observations were made by Kim, Lee, and Lee [28].
 - The addition of external plies on the surface of the specimen resulted in an increased failure loads (see figure 16). These results are in agreement with those found by Myhre and Beck [29].
- For the lap repair
 - The failure load increased with increasing lap length but only up to a certain “limiting lap length” d_{limit} (see figures 17 to 18). This limiting lap length was generally between 2 and 3 inches for the specimens used in this investigation. Beyond the limiting lap length an increase in lap length did not affect the failure load. Thus, there is no benefit to be gained by making the lap length longer than the limiting lap length. Similar results were reported by Chan and Sun [30], and John, Kinloch, and Matthews [31].
 - The mode of failure changed with lap length (see figure 19). At short ($d_l \leq 0.3d_{limit}$) and intermediate lap length ($0.3d_{limit} \leq d_l \leq d_{limit}$), failure occurred mostly along the interface, with some of the repair plies also failing by tension at the intermediate lap length. At and beyond the limiting lap length ($d_l \geq d_{limit}$) failure was due to tensile failure of the repair plies. These conclusions seemed to hold even when the total number of repair plies ($2n_l^R$) was the same as the number of plies in the base laminate (n_l^L). (Note, that for the specimens in section 4.1, the lap length was 1.5 in, and this corresponds to an intermediate lap length.)
 - The failure load increased linearly with the number of plies used in the repair (see figure 20). This result was valid even when the total number of repair plies ($2n_l^L$) was equal to the number of plies in the base laminate (n_l^R) (see figure 20 middle).
 - When the lap length was greater than limiting lap length ($d_l \geq d_{limit}$), the shape of the repair plies did not markedly affect the failure load (see figure 21). The failure loads were nearly the same for specimens repaired by stepped and by uniform repair, provided the following two conditions were simultaneously satisfied: (a) the number of repair plies were the same and (b) the lap length of the uniform lap repair was the same as the length of the outside lap of the stepped repair.

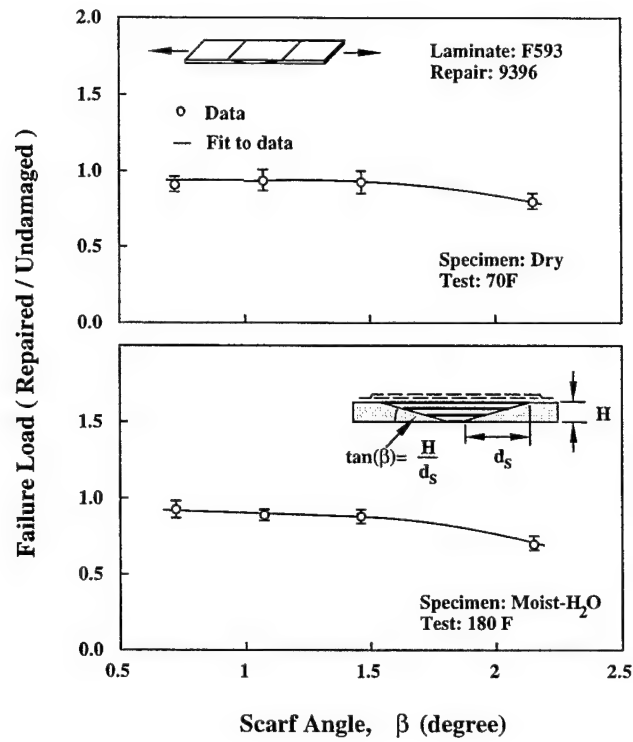


FIGURE 15. THE VARIATION OF FAILURE LOAD WITH SCARF ANGLE

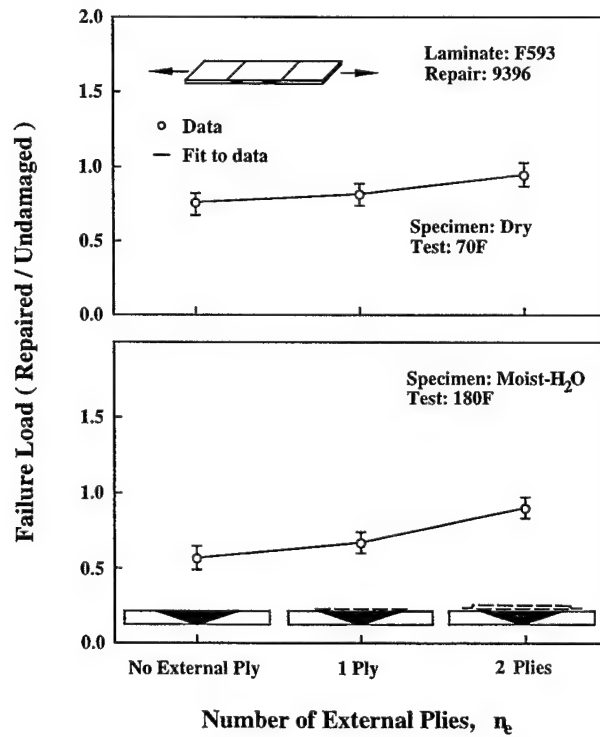


FIGURE 16. THE EFFECT OF THE NUMBER OF EXTERNAL PLYS ON THE FAILURE LOAD IN SCARF REPAIR

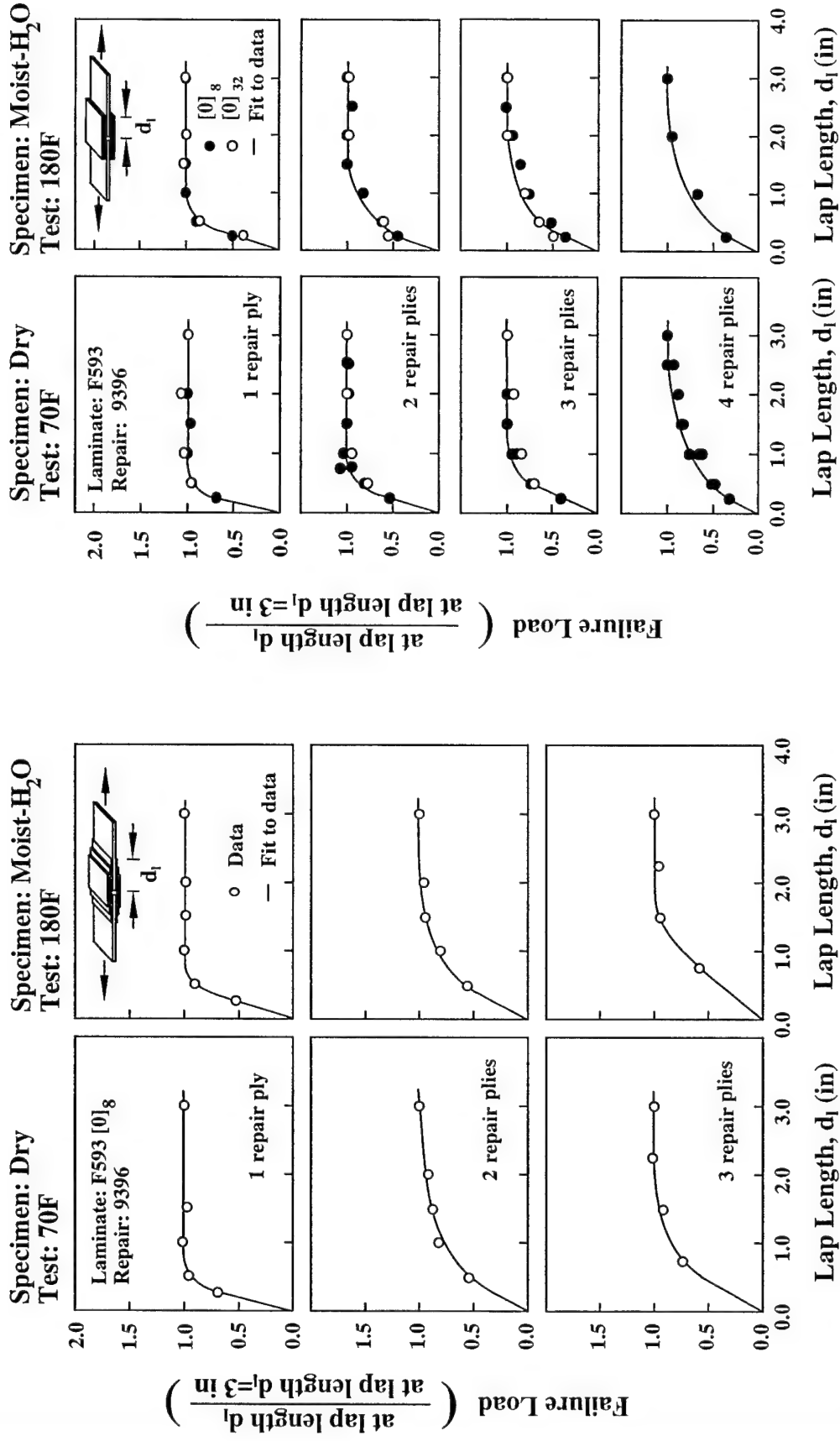


FIGURE 17. THE EFFECT OF LAP LENGTH ON THE FAILURE LOAD IN STEPPED LAP REPAIR

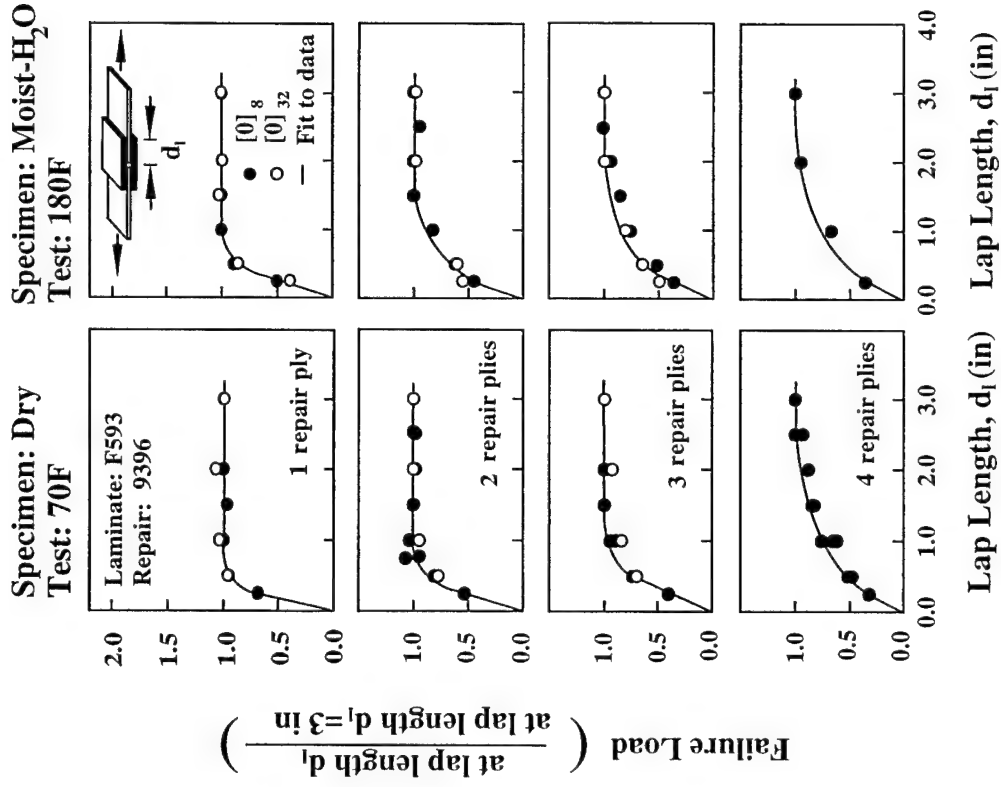


FIGURE 18. THE EFFECT OF LAP LENGTH ON THE FAILURE LOAD IN UNIFORM LAP REPAIR

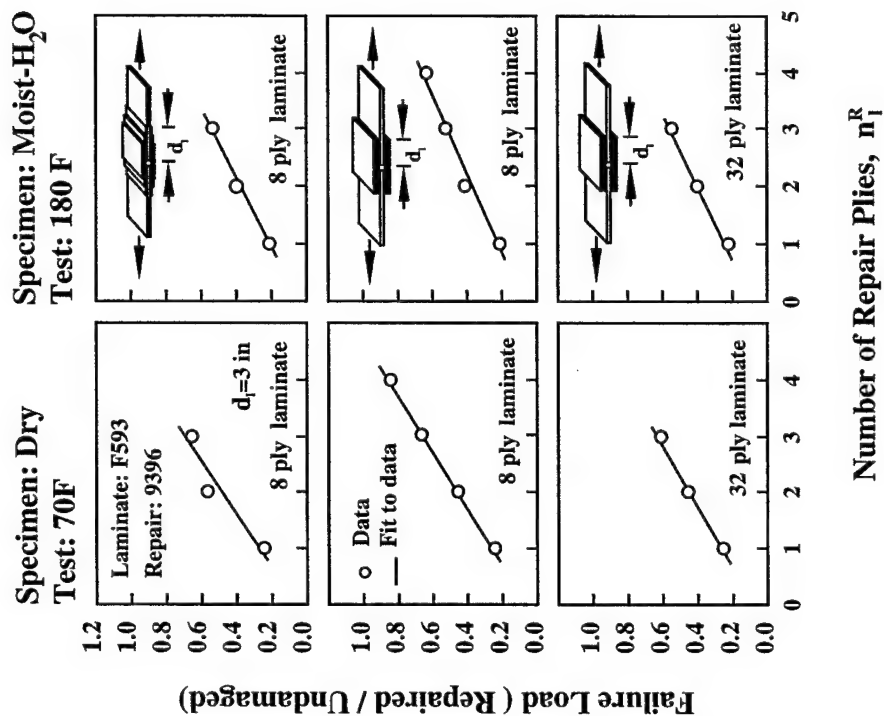


FIGURE 20. THE EFFECT OF THE NUMBER OF REPAIR PLIES ON THE FAILURE LOAD

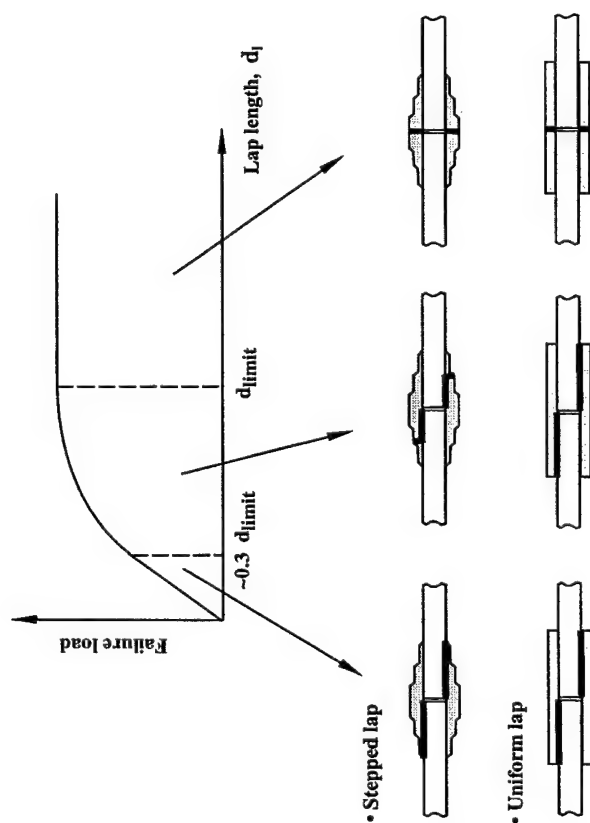


FIGURE 19. TYPICAL FAILURE MODES OF SPECIMENS REPAIRED BY STEPPED LAP AND UNIFORM LAP TECHNIQUES WITH VARIOUS LAP LENGTHS (Specimen geometries are given in figures 5 and 14)

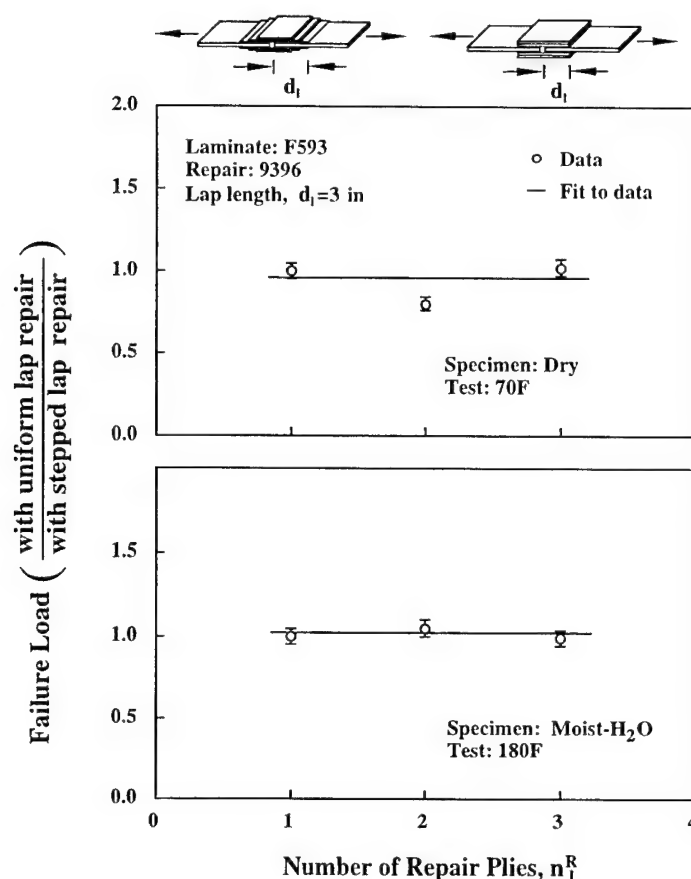


FIGURE 21. COMPARISONS OF THE FAILURE LOADS OF SPECIMENS REPAIRED BY THE STEPPED LAP AND UNIFORM LAP REPAIR TECHNIQUES

4.3 EFFECTS OF SPECIMEN MOISTURE CONTENT AND TEST TEMPERATURE.

Two series of tests were performed to evaluate the effects of specimen moisture content and test temperature on the failure loads of repaired specimens. In one series of tests, the base laminates were moisturized prior to repair. In the second series, the base laminates were dried prior to repair, and the repaired specimens were moisturized before being tested.

4.3.1 Base Laminates Premoisturized.

There were two types of premoisturized specimens. The first type of specimen consisted of the base laminate moisturized prior to repair by exposing the unrepaired base laminate to 100 percent humid air at 180°F. The base laminates were kept in the environmental chamber until the desired moisture content was reached. The base laminates were then removed from the environmental chamber, repaired, and tested at 70°F.

The second type of specimen consisted of the base laminate whose moisture content was established by moisturization followed by drying. In this case the base laminate was moisturized to either 1.1 percent or 1.5 percent moisture content. When the desired moisture content was

reached, the base laminate was removed from the environmental chamber and was dried in an oven at 180°F. Once the desired moisture content was reached during the drying process, the base laminate was taken out of the oven, repaired, and tested at 70°F.

With above procedures, the moisture content of the base laminate was established either by moisturization of the base laminate or by moisturization followed by drying. The test matrix is given in table 10.

TABLE 10. THE TEST MATRIX USED FOR EVALUATING THE EFFECTS OF THE MOISTURE CONTENT OF THE BASE LAMINATE PRIOR TO REPAIR
(Base Laminate: F593, Repair Material: 9396)

Repair Type	Parameter	Specimen Condition/Test Temperature	
		Moist-Humid Air/70°F*	180°F Dry Air/70°F**
Scarf	Moisture content (% weight)	0.0 to 1.1	1.1 to 0.0
		0.0 to 1.5	1.5 to 0.0
Stepped lap	Moisture content (% weight)	0.0 to 1.1	1.1 to 0.0
		0.0 to 1.5	1.5 to 0.0

* Specimens were exposed to 180°F air at 100% relative humidity until either 1.1% or 1.5% moisture content was reached (moist-humid air). Test temperature was either 70° or 180°F (figure 8).

** Specimens were dried at 180°F after having been moisturized to either 1.1% or 1.5% moisture content.

The failure loads of specimens repaired with premoisturized base laminates are given in figure 22. In this figure, the failure loads are normalized with respect to the failure load of the dry specimen. The following major observations can be made on the basis of the data in figure 22.

- The failure loads of repaired specimens decreased only slightly when the base laminates were moisturized prior to the repair, provided that the moisture content did not exceed 1.1 percent (see figure 22, top). This conclusion was valid when the base laminate moisture content was established either by moisturization (solid circle) or by moisturization followed by drying (open circle).
- The behavior was quite different when the moisture content of the base laminates exceeded about 1.1 percent (see figure 22, bottom). The same phenomenon was observed by Robson, et al. [32] in their tests with scarf joints. The failure loads of repaired specimens made with base laminates which have first been moisturized to 1.5 percent moisture content then dried (dotted line in figure 22 bottom) were lower than the failure loads of repaired specimens made with base laminates in which the moisture was introduced during moisturization (solid line). In fact, the base laminates had to be dried almost completely to recover the failure loads of specimens made with premoisturized (but not dried) base laminates. Similar observations were made by Parker [33] on adhesively bonded single lap joints.

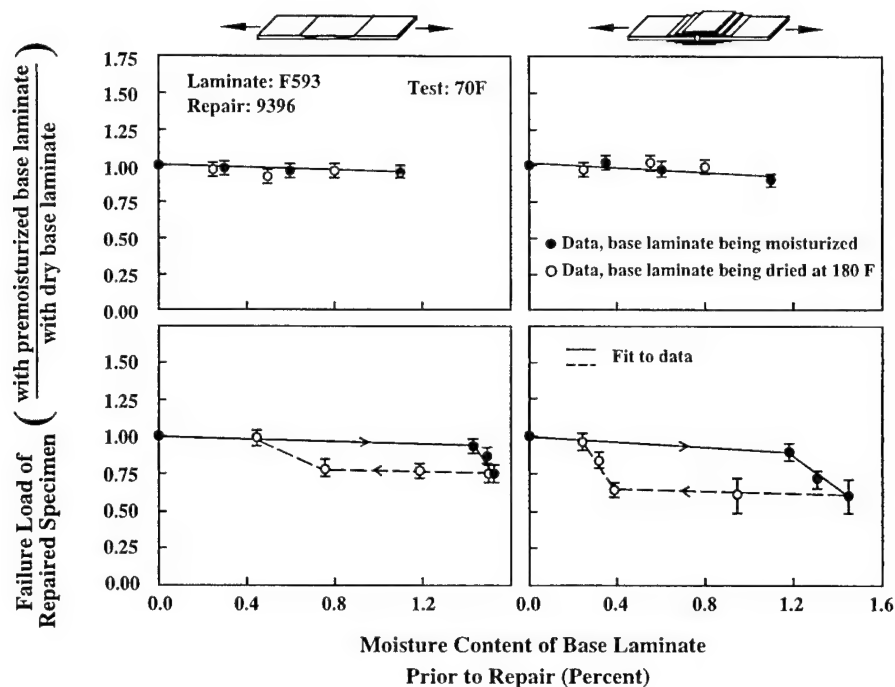


FIGURE 22. FAILURE LOADS OF REPAIRED SPECIMENS WHEN THE BASE LAMINATES WERE MOISTURIZED PRIOR TO REPAIR

The above mentioned results have two significant ramifications. First, it is not necessary to dry the repair area prior to repair as long as the moisture content of the laminates is low (less than 1.0 percent). Second, the repair area should be dried completely (not just partially) when the laminate moisture content is high (above 1.0 percent).

4.3.2 Specimen Moisture Content and Test Temperature.

Specimens were repaired by scarf and stepped lap techniques using dry base laminates. Each specimen was then either immersed in 180°F water for 14 days or exposed to 100 percent humid air at 180°F until 1.1 percent moisture content was reached. The failure loads of the dry and the moisturized specimens were measured at 70° and 180°F. The complete test matrix is shown in table 11.

TABLE 11. THE TEST MATRIX USED FOR EVALUATING THE EFFECTS OF SPECIMEN MOISTURE CONTENT AND TEST TEMPERATURE
(Base Laminate: F593, Repair Material: 9396)

Repair Type	Dry 70°F	Dry 180°F	Moist-H ₂ O 70°F	Moist-H ₂ O 180°F	Specimen Condition/Test Temperature	
					Moist-Humid Air/ 70°F	Moist-Humid Air/ 180°F
Scarf	x	x	x	x	x	x
Stepped lap	x	x	x	x	x	x

The trend in the data was similar for the specimens moisturized in water and in humid air. Therefore, here data presented is only for specimens moisturized by exposure to humid air (see figure 23). The data obtained during moisturization in water are included in appendix D. The data in figure 23 indicate the following trends.

- The moisture content did not significantly reduce the failure load when the specimens were tested at 70°F.
- Testing at the elevated temperature (180°F) did not significantly reduce the failure load when the specimens were tested at dry condition.
- The failure load of the specimen was reduced under hot/wet conditions i.e., when the specimen was both wet and tested at 180°F. Similar observations were made by Stone [16] with single lap shear specimens, Mylire, Labor, and Aker [34] with modified single lap specimens, and John, Kinloch, and Matthews [31] with double lap joints.

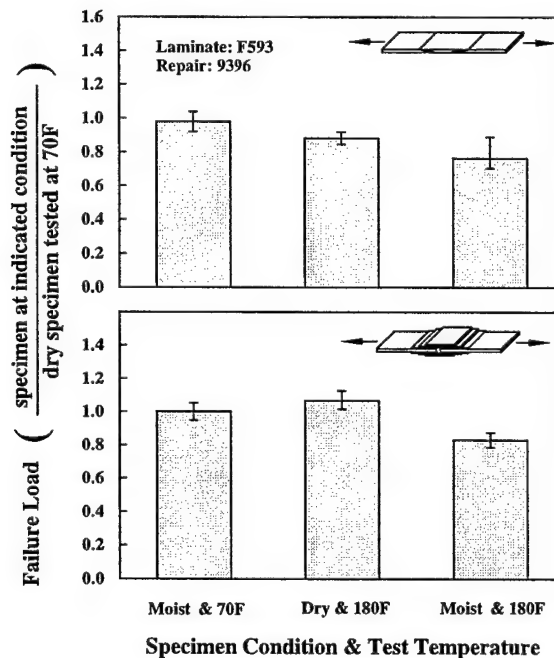


FIGURE 23. THE EFFECTS OF SPECIMEN MOISTURE CONTENT AND TEST TEMPERATURE ON THE FAILURE LOAD

4.4 EFFECT OF SANDING.

Prior to repair the repair surface of the base laminate is usually sanded. To evaluate the influence of sanding on the failure load of repaired specimens, the repair surfaces were sanded with different grit diamond sanders (see table 12). The failure loads of specimens repaired using different grit sanders are shown in figure 24. The data indicate that the grit number of the sander did not have a major effect on the failure load. For the material and type of repair used in this study, a sander with grit number about 100 seems appropriate.

TABLE 12. TESTS WITH DIFFERENT PREPARATION OF THE REPAIR SURFACE
(Base Laminate: F593, Repair Material: 9396)

Repair Type	Parameter	Specimen Condition/Test Temperature*	
		Dry/70°F	Moist-H ₂ O/180°F
Scarf	Grit number of diamond sander, g	60, 120, 400	60, 120, 400
Stepped lap	Grit number of diamond sander, g	60, 120, 400	60, 120, 400

* Specimens were either dry, or immersed in 180°F water for 14 days (Moist-H₂O). Test temperature was either 70° or 180°F (figure 8).

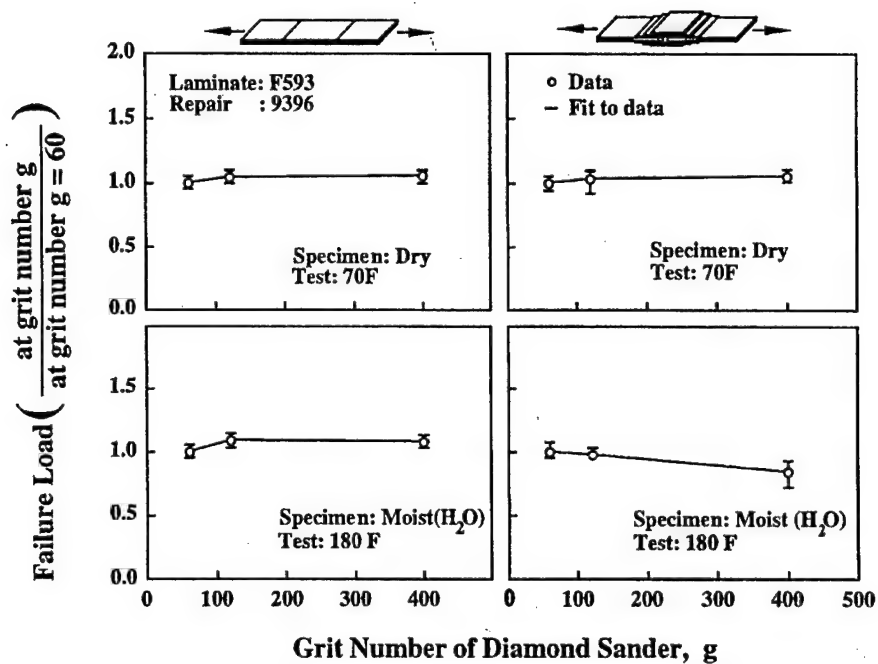


FIGURE 24. THE FAILURE LOADS OF SPECIMENS SANDED WITH DIFFERENT GRIT DIAMOND SANDERS

4.5 EFFECT OF CURE CYCLE.

Composite material is generally repaired at an elevated temperature to expedite the chemical reactions and to cure the resin used in the repair. In addition to the temperature, time is factor in the cure. For economical reasons, it is desirable to have a low cure temperature and a short cure time.

The effects of the temperature-time history (referred to as cure cycle) on the effectiveness of the repair were studied on specimens repaired by scarf and stepped lap techniques. Each specimen was repaired by surrounding it with a heating blanket. This assembly was enclosed in a vacuum bag and was kept under vacuum during the repair (see figure 25). The specimen was heated at a constant rate of 6.5°F/min until the desired cure temperature T_c was reached (see figure 26 insert). This cure temperature was maintained until the repair material was fully cured.

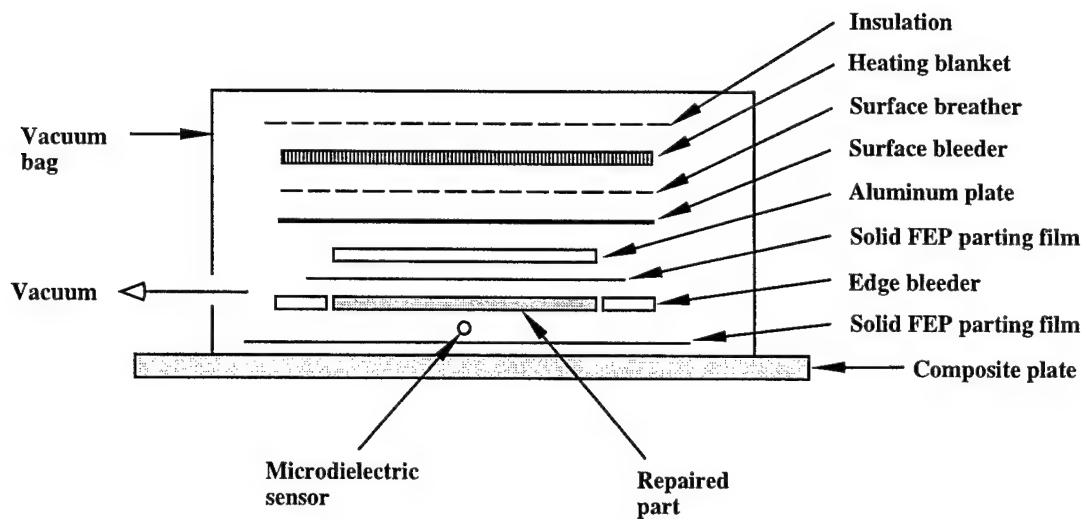


FIGURE 25. ILLUSTRATION OF THE TEST SETUP USED IN STUDYING THE EFFECTS OF CURE CYCLE ON THE REPAIR

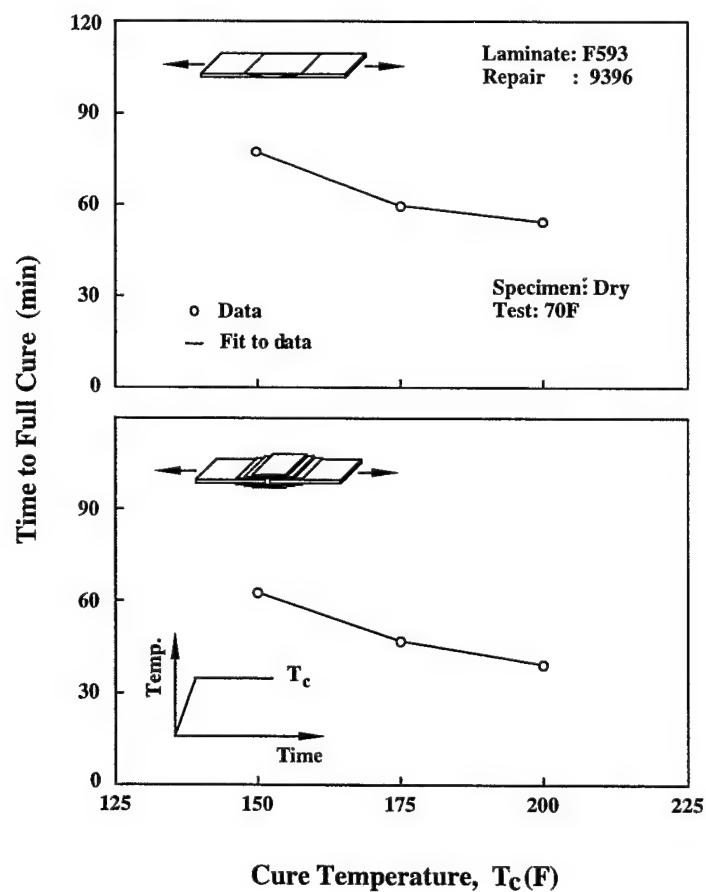


FIGURE 26. THE CURE TIME REQUIRED TO REACH FULL CURE AT DIFFERENT CURE TEMPERATURES (Specimen geometries are given in figures 5 and 14)

The progress of the cure and the specimen temperature were monitored by a Eumetric System II Microdielectrometer (Micromet Instruments, Inc.). This instrument provided the temperature and the ion viscosity of the repair resin, the latter being an indicator of the degree of cure. A typical output of the instrument is shown in figure 27. Each specimen was cured at a preset cure temperature T_c (150°, 175°, or 200°F) until the instrument indicated that full cure was reached.

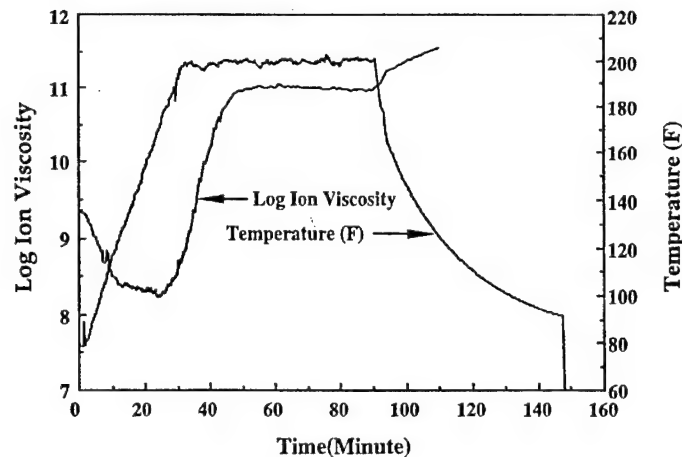


FIGURE 27. A TYPICAL OUTPUT OF THE MICRODIELECTROMETER

The time required to reach full cure is shown in figure 26. As the heating rate was constant at 6.5°F/min, the time required to reach full cure decreased with increasing cure temperature.

The failure loads of specimens cured at different temperatures are shown in figure 28. The cure temperature did not seem to affect significantly the failure load for the dry specimens tested at 70°F. It is unknown what would happen if the specimens were tested at 180°F. This limited testing suggests that it is advantageous to use the highest cure temperature (permissible for the resin system used in the repair) since this results in shortest cure (and repair) time.

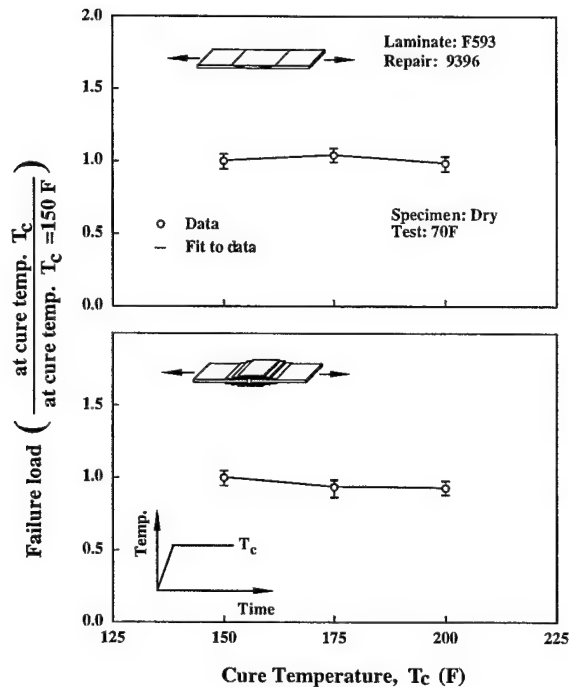


FIGURE 28. FAILURE LOADS OF SPECIMENS REPAIRED AT DIFFERENT CURE TEMPERATURES
(Specimen geometries are given in figures 5 and 14. Failure loads of the specimens at cure temperature 150°F are given in appendix C.)

4.6 SUMMARY.

The major findings of the tests are summarized below.

- The type of wet lay-up repair material used in the repair, or the type of parent laminate material on which the repair is made, does not affect the quality (failure load) of the repaired part.
- For a scarf repair, there is a gradual decrease in the failure load with increasing scarf angle. In the present tests the highest failure load occurred at a scarf angle of about 1 degree. Small variations in the scarf angle around this value did not have a significant effect on the failure load.
- For a lap repair, there is a limiting lap length beyond which the failure load does not increase.
- If the parent laminate moisture content is low and the prior moisture history of the part is known, the repair area does not need to be dried prior to repair. However, if the laminate moisture content is high (above 1.1 percent), the repair area needs to be dried completely before repair.

- The failure loads of repaired specimens are reduced under hot/wet conditions, i.e., when both the moisture content and the test temperature are high.
- Preparing the repair surfaces by sanding them with diamond sander ranging from 60 to 400 grit number does not significantly affect failure load.
- A repair should be cured at the highest permissible temperature so as to achieve the shortest cure time.

The aforementioned findings are strictly valid only for the specimens and test conditions used in this investigation. It is likely that the trends observed here are valid for specimens and test conditions not covered in the present tests.

PART II. ANALYTICAL MODELS.

5. INTRODUCTION.

Our objective is to develop analytical models which can be used to calculate the failure loads of laminates repaired by the scarf and lap techniques. In developing the models, previous models for adhesively bonded joints were consulted because repair patches and bonded joints have similar features.

Numerous models are available for isotropic materials bonded adhesively by single lap [30, 35-46], double lap [30, 43, 46-48], and scarf [49] joints.

Fewer models exist for adhesive bonds joining composite materials, and most of these are restricted to adhesives which may be treated as linearly elastic [28, 38, 40, 50-55]. However, in many practical situations, the adhesive does not behave in a linearly elastic manner. Nonelastic behavior of adhesives in bonding composite laminates has been considered for single lap [56], double lap [57-61], and scarf joints [59, 61, 62] by Hart-Smith and Adams, et al. Of these, the scarf and double lap joint models are relevant here because of our interest in scarf and double-sided uniform lap repair. Adams [61] performed stress analysis of scarf and double-lap joints using finite element methods, but as far as authors can ascertain, their codes are not in the public domain. Hart-Smith [57-59, 62] did not treat each composite layer separately, but smeared the properties of the composite laminates which were adhesively bonded.

In this investigation, the Hart-Smith models were adapted to model the scarf and double-sided lap repair by accounting for each individual layer separately.

6. THE PROBLEM.

Symmetric composite laminates can be repaired either by the uniform lap or by the scarf technique (see figure 29). Both the laminate and the repair patch consist of fiber reinforced plies which behave in a linearly elastic manner. The repair may be made by wet lay-up or by prepreg. For wet lay-up repair there is a thin resin layer, while for prepreg repair there is an adhesive between the laminate and the repair patch (see figure 30). Both the resin layer and the adhesive

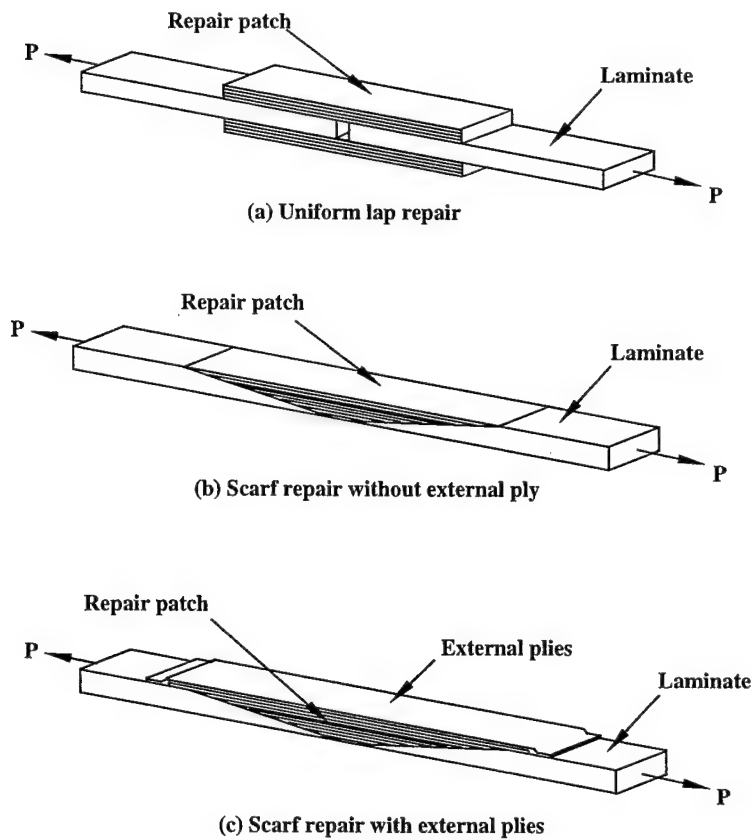


FIGURE 29. MODELS OF THE UNIFORM LAP AND THE SCARF REPAIRS

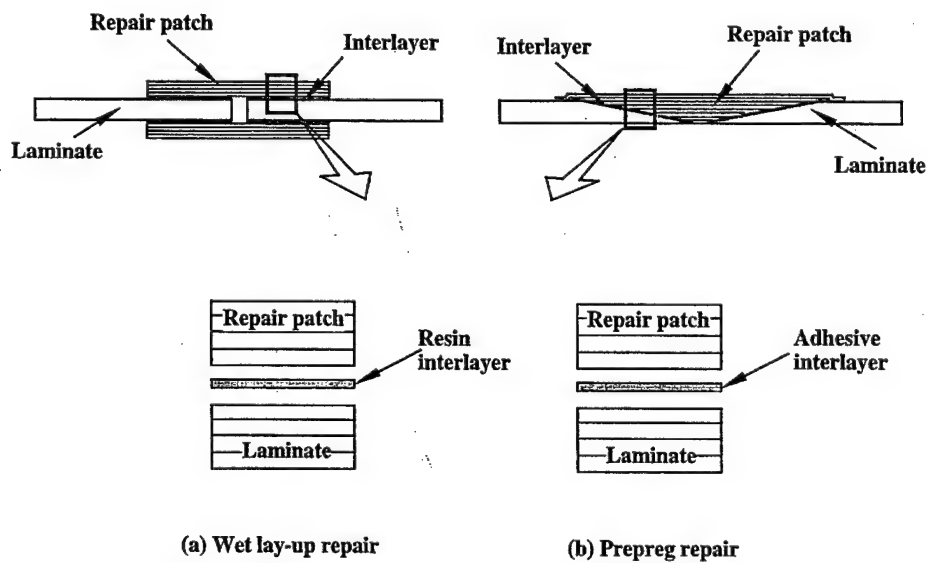


FIGURE 30. THE INTERLAYER BETWEEN THE LAMINATE AND THE REPAIR PATCH WHEN THE REPAIR IS PERFORMED WITH WET LAY-UP (LOWER LEFT) OR PREPREG (LOWER RIGHT)

are treated as an “interlayer” which exhibits elastic-perfectly plastic behavior (see figure 31). The shear strains at the elastic limit and at plastic failure are γ_{ef} and γ_{pf} , respectively.

The laminate is subjected to an in-plane tensile load P . The objective is to find the value of this load (failure load, $P = F$) which fails the repaired laminate.

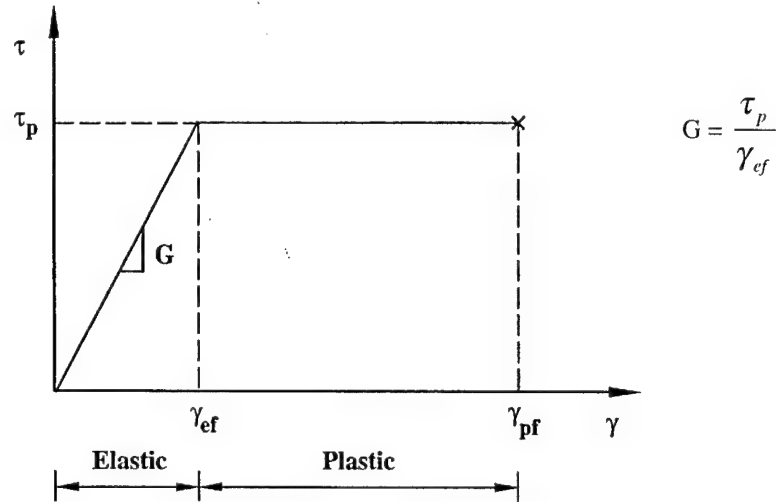


FIGURE 31. ILLUSTRATION OF THE SHEAR STRESS-SHEAR STRAIN RELATIONSHIP OF AN ELASTIC-PERFECTLY PLASTIC INTERLAYER

7. MODEL OF UNIFORM LAP REPAIR.

A model for the double-sided uniform lap repair is illustrated in figure 32. The model for the stepped lap repair is not given separately because, as was shown in section 4.2, the failure loads of laminates repaired by uniform and stepped lap techniques are similar. Thus, the model of the uniform lap repair can be applied to a stepped lap repair.

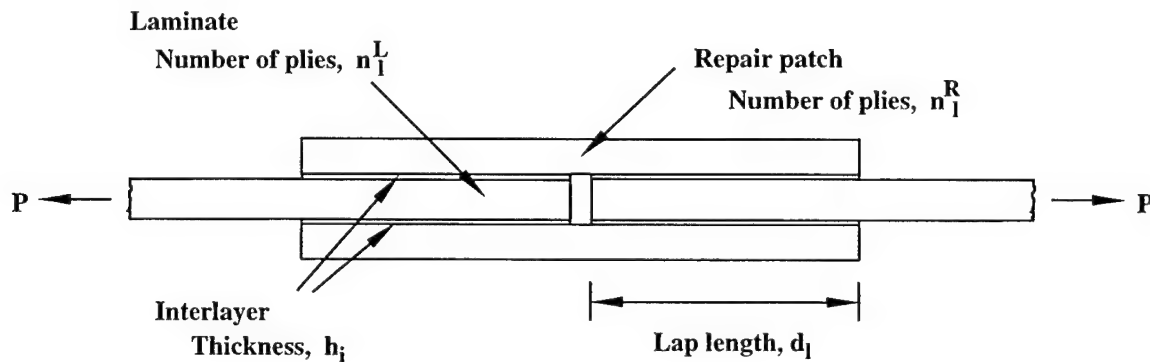


FIGURE 32. DOUBLE-SIDED UNIFORM LAP REPAIR MODEL

The lay-up of the laminate/repair patch assembly is symmetric. For modeling such a repair it is sufficient to consider only one half the repaired laminate, as shown in figure 33.

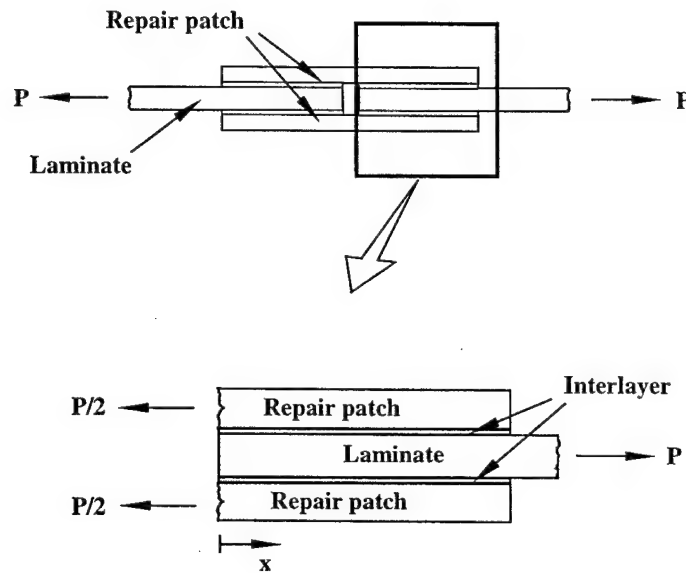
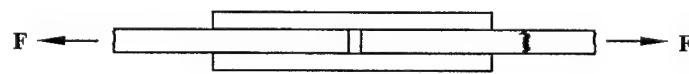
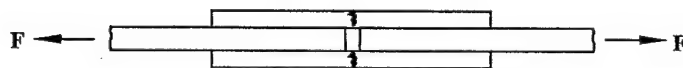


FIGURE 33. DOUBLE-SIDED UNIFORM LAP REPAIR TREATED IN THE MODEL

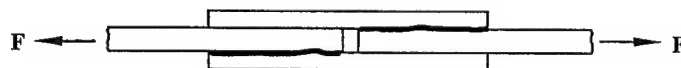
When the repaired laminate is subjected to a tensile load, the laminate may fail in tension, the repair patch may fail in tension, or the interlayer may fail in shear (see figure 34). In the following, models are presented which provide the failure loads when failure is due to any of the three scenarios.



(a) Laminate failure in tension



(b) Repair patch failure in tension



(c) Interlayer failure in shear

FIGURE 34. ILLUSTRATION OF THE TYPES OF FAILURE WHICH MAY OCCUR IN A LAMINATE REPAIRED BY THE DOUBLE-SIDED UNIFORM LAP TECHNIQUE

7.1 TENSILE FAILURE OF THE LAMINATE OR REPAIR PATCH.

When the laminate or the repair patch fails in tension (see figure 34), the failure load is calculated as follows. At tensile failure (of either the laminate or the repair patch) the applied in-plane tensile load (per unit width) is denoted by F ($P = F$). At the middle of the repair zone ($x = 0$, figure 33) the in-plane failure load (per unit width) in the repair plies is $F/2$ ($P/2 = F/2$). Since the model is symmetric, the in-plane strains at failure are [63]

Laminate	Repair Patch	
$(\epsilon_x^L)_F = \alpha_{11}^L F$	$(\epsilon_x^R)_F = \alpha_{11}^R F / 2$	
$(\epsilon_y^L)_F = \alpha_{21}^L F$	$(\epsilon_y^R)_F = \alpha_{21}^R F / 2$	
$(\epsilon_s^L)_F = \alpha_{61}^L F$	$(\epsilon_s^R)_F = \alpha_{61}^R F / 2$	(1)

where ϵ_x , ϵ_y , and ϵ_s are the off-axis in-plane strains (see figure 35). The α_{ij} 's are the components of the compliance matrix. The superscripts L and R refer to the laminate and the repair patches, respectively.

The on-axis (1, 2, and 6 in figure 35) components of the strains are

$$\begin{Bmatrix} \epsilon_1^{L,R} \\ \epsilon_2^{L,R} \\ \epsilon_6^{L,R} \end{Bmatrix} = \begin{pmatrix} \cos^2 \theta^{L,R} & \sin^2 \theta^{L,R} & \cos \theta^{L,R} \sin \theta^{L,R} \\ \sin^2 \theta^{L,R} & \cos^2 \theta^{L,R} & -\cos \theta^{L,R} \sin \theta^{L,R} \\ -2 \cos \theta^{L,R} \sin \theta^{L,R} & 2 \cos \theta^{L,R} \sin \theta^{L,R} & \cos^2 \theta^{L,R} - \sin^2 \theta^{L,R} \end{pmatrix} \begin{Bmatrix} \epsilon_x^{L,R} \\ \epsilon_y^{L,R} \\ \epsilon_s^{L,R} \end{Bmatrix}_F \quad (2)$$

where θ is the fiber orientation measured with respect to the direction of the applied load.

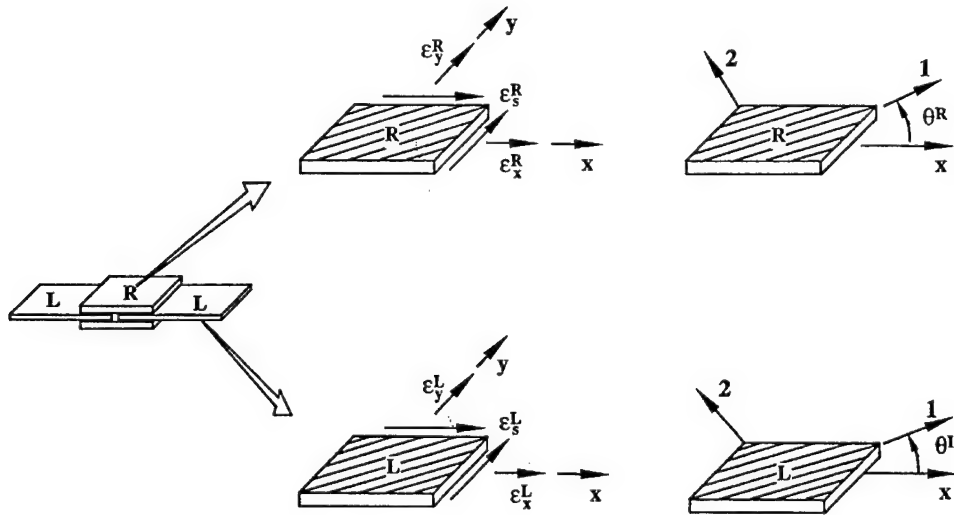


FIGURE 35. THE ON-AXIS (x, y) AND OFF-AXIS (1, 2) COORDINATE SYSTEMS

Failure occurs when, in any of the laminate or repair plies, one of the following maximum strain failure criteria is met

$$\begin{aligned}
 \frac{X^L}{E_1^L(\epsilon_1^L)_F} &= 1 & \frac{X^R}{E_1^R(\epsilon_1^R)_F} &= 1 \\
 \frac{X^L}{E_2^L(\epsilon_2^L)_F} &= 1 & \frac{Y^R}{E_2^R(\epsilon_2^R)_F} &= 1 \\
 \frac{S^L}{E_6^L(\epsilon_6^L)_F} &= 1 & \frac{S^R}{E_6^R(\epsilon_6^R)_F} &= 1
 \end{aligned} \tag{3}$$

X , Y , and S are the on-axis longitudinal, transverse, and shear strengths of the ply, respectively. E_1 , E_2 , and E_6 are the on-axis longitudinal, transverse, and shear moduli of the ply, respectively. Six F values are calculated for each ply from equations 1-3. The lowest value of F resulting from these calculations is the failure load.

7.2 SHEAR FAILURE.

When the repaired laminate fails due to shear failure of the interlayer (see figure 34(c)), the failure load is calculated as follows.

At the start of the analysis the repaired laminate has an applied in-plane load P ($P \neq F$, figure 36). At $x = 0$, the loads on the repair patches (plies) are $P/2$. For a section dx in length (x being in the direction of the applied load), balancing the forces for the laminate and each of the repair patches gives:

$$\begin{aligned}
 \frac{dN^L}{dx} - 2\tau &= 0 & \text{Laminate} \\
 \frac{dN^R}{dx} + \tau &= 0 & \text{Repair Patch}
 \end{aligned} \tag{4}$$

$N^L(= N_x^L)$ and $N^R(= N_x^R)$ are the in-plane loads (per unit width) in the laminate and each repair patch, respectively. $\tau(= \tau_{zx})$ is the shear stress in the interlayer.

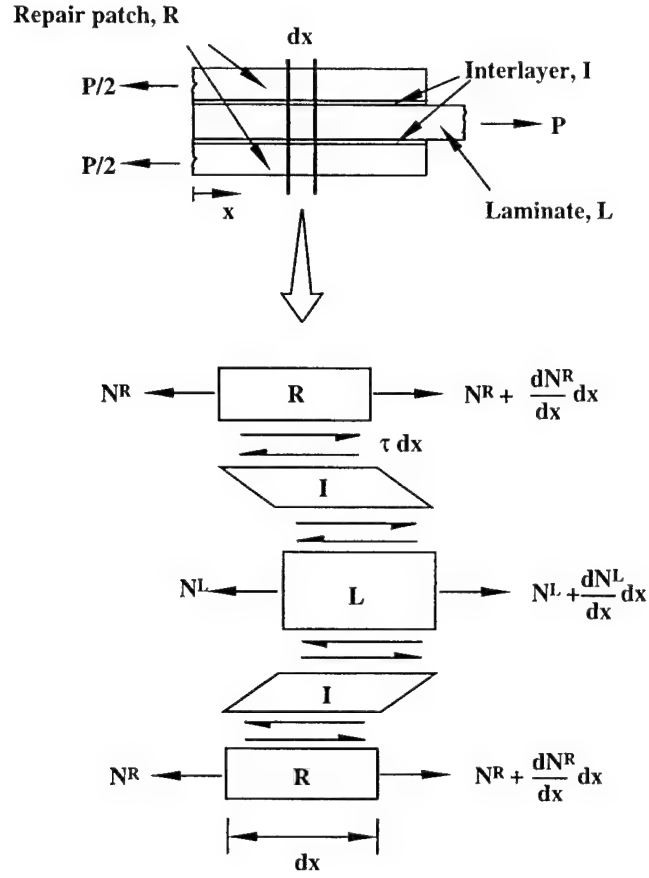


FIGURE 36. LOADS ON A SECTION dx IN LENGTH OF THE LAMINATE REPAIRED BY THE DOUBLE-SIDED UNIFORM LAP TECHNIQUE

By neglecting the shear deformations of the laminate and the repair patch, compatibility requires that the following condition be satisfied [64] (see figure 37)

$$(\varepsilon_x^L + I)dx + \gamma h_i = (\varepsilon_x^R + I)dx + \left(\gamma + \frac{d\gamma}{dx} dx\right)h_i \quad (5)$$

This can be simplified to give

$$\frac{d\gamma}{dx} = \frac{\varepsilon_x^L - \varepsilon_x^R}{h_i} \quad (6)$$

where ε_x^L and ε_x^R are the off-axis in-plane strains in the laminate and in the repair patch, respectively, h_i is the thickness of the interlayer, and $\gamma (= \gamma_{zx})$ is the interlayer shear strain.

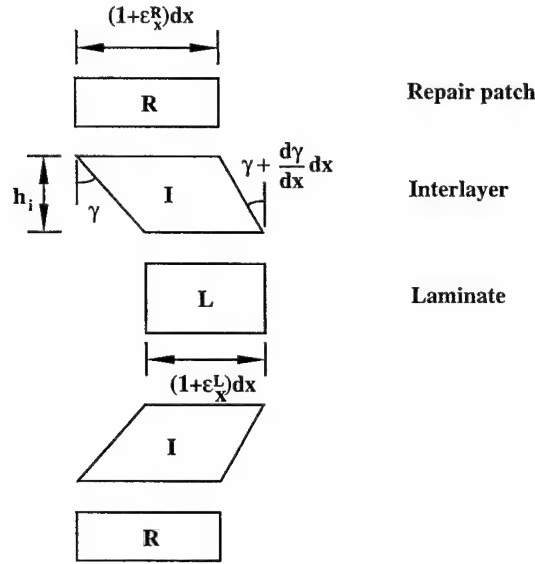


FIGURE 37. DEFORMATIONS OF THE REPAIR PATCH, THE INTERLAYER, AND THE LAMINATE
(Double-sided uniform lap technique.)

For the symmetric arrangement considered here, the x components of the strains in the laminate and in the repair patch are [63]

$$\begin{aligned}\epsilon_x^L &= \alpha_{11}^L N^L && \text{Laminate} \\ \epsilon_x^R &= \alpha_{11}^R N^R && \text{Repair Patch}\end{aligned}\tag{7}$$

where α_{11} is the 11 component of the α_{ij} compliance matrix. Equations 6 and 7 yield

$$\frac{d\gamma}{dx} = \frac{1}{h_i} (\alpha_{11}^L N^L - \alpha_{11}^R N^R)\tag{8}$$

By combining equations 4 and 8 obtains

$$\frac{d^2\gamma}{dx^2} = \frac{1}{h_i} (2\alpha_{11}^L + \alpha_{11}^R)\tag{9}$$

There are four possible scenarios for the behavior of the interlayer: (1) the entire interlayer behaves in a linearly elastic manner, (2) a perfectly plastic region near the $x = 0$, (3) a perfectly plastic region near the $x = d_i$ end of the interlayer, or (4) a perfectly plastic region near both the $x = 0$ and $x = d_i$ ends of the interlayer (figure 38).

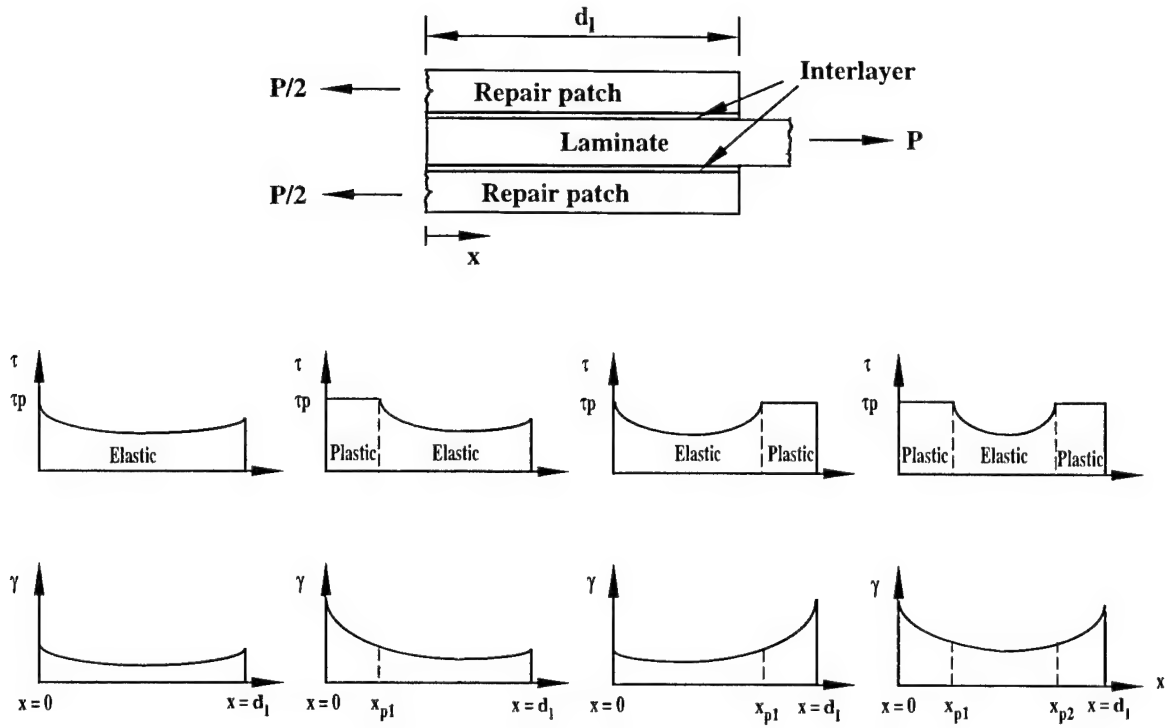


FIGURE 38. POSSIBLE REGIONS OF THE INTERLAYER UNDER AN APPLIED LOAD P

In the elastic region, the shear strain and shear stress are

$$\gamma = \gamma_e \quad \text{and} \quad \tau = G\gamma_e \quad (10)$$

where G is the shear modulus of the interlayer. From equations 9 and 10 the following expression for the shear strain can be obtained.

$$\gamma = p \sinh(\lambda x) + q \cosh(\lambda x) \quad \text{Elastic Region} \quad (11)$$

where λ is defined as

$$\lambda^2 = \frac{G}{h_i} (2\alpha_{II}^L N^L + \alpha_{II}^R) \quad (12)$$

In the plastic region the shear strain and the shear stress are (see figures 31 and 38)

$$\gamma = \gamma_p \quad \text{and} \quad \tau = \tau_p = G\gamma_{ef} \quad (13)$$

where, as shown in figure 31, γ_{ef} is constant. Equations 9 and 13 yield

$$\gamma_p = \frac{\lambda^2 \gamma_{ef}}{2} x^2 + rx + s \quad \text{Plastic Region} \quad (14)$$

In equations 11 and 14, p , q , r , and s are constants which must be determined from the boundary and continuity conditions.

7.2.1 Boundary and Continuity Conditions.

The following are the boundary and continuity conditions for to equations 11 and 14.

- At the free ends of the laminate and the repair patches, the axial load is zero (see figure 39)

$$\begin{aligned} N^L &= 0 & \text{at } x = 0 \\ N^R &= 0 & \text{at } x = d_l \end{aligned} \quad (15)$$

- At the ends of the laminate and the repair patches where loads are applied (see figure 39), the load per unit width N^L in the laminate is equal to the applied load per unit width P , and the load per unit width N^R in each repair patch is equal to $P/2$

$$\begin{aligned} N^R &= \frac{P}{2} & \text{at } x = 0 \\ N^L &= P & \text{at } x = d_l \end{aligned} \quad (16)$$

By combining equations 8, 15, and 16, these boundary conditions can be expressed as

$$\frac{d\gamma}{dx} = -\frac{P\alpha_{11}^R}{2h_i} \quad \text{at } x = 0 \quad (17)$$

and

$$\frac{d\gamma}{dx} = \frac{P\alpha_{11}^L}{h_i} \quad \text{at } x = d_l \quad (18)$$

In equations 17 and 18 $\frac{d\gamma}{dx}$ is either $\frac{d\gamma_e}{dx}$ or $\frac{d\gamma_p}{dx}$ depending on whether the interlayer is in the elastic or in the perfectly plastic region at the boundary (see figures 40 through 43).

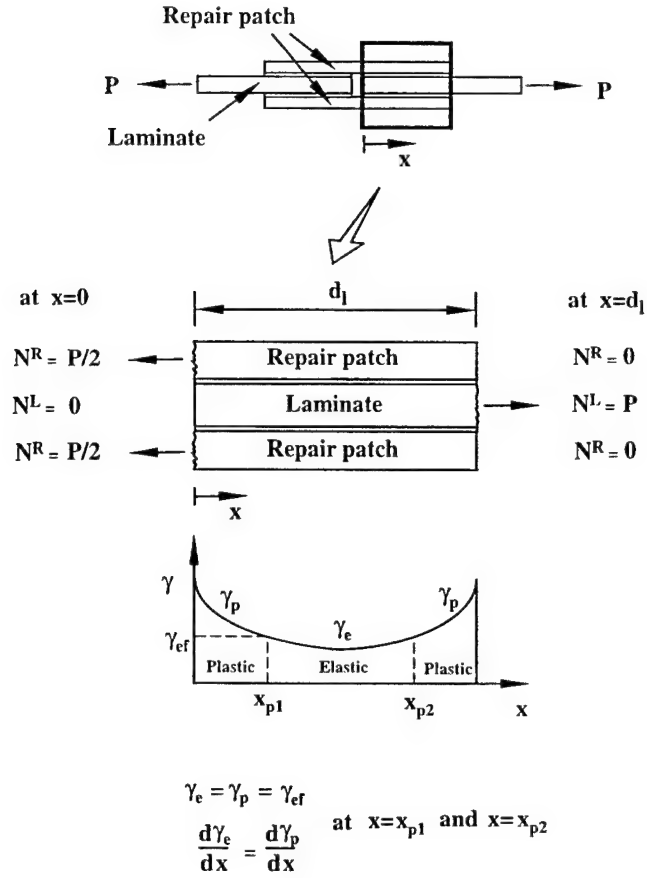


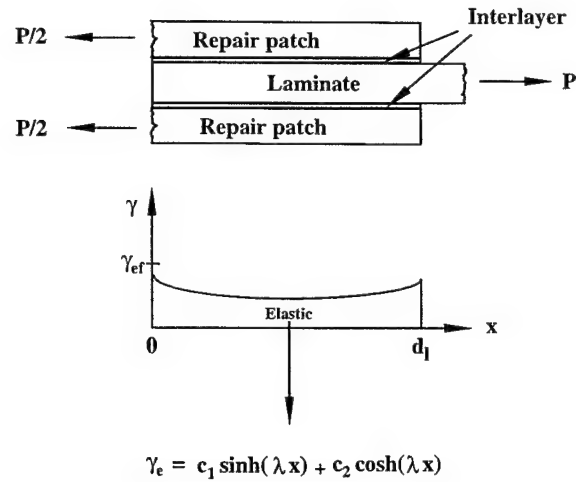
FIGURE 39. THE BOUNDARY CONDITIONS FOR THE IN-PLANE LOADS IN THE LAMINATE AND IN THE REPAIR PATCH AND THE CONTINUITY CONDITIONS FOR THE SHEAR STRAIN IN THE INTERLAYER

At the locations where the elastic and plastic regions meet ($x = x_{p1}$ and $x = x_{p2}$ in figure 38) the shear strains in the elastic and plastic regions are equal (with the value γ_{ef}) and are continuous (see figures 39, 41 through 43). Correspondingly,

$$\gamma_e = \gamma_p = (\gamma_{ef}) \quad \text{at } x = x_{p1}, x = x_{p2} \quad (19)$$

$$\frac{d\gamma_e}{dx} = \frac{d\gamma_p}{dx}$$

The locations x_{p1} and x_{p2} are unknown and must be determined from the solutions of the equations summarized in figures 41 through 43.



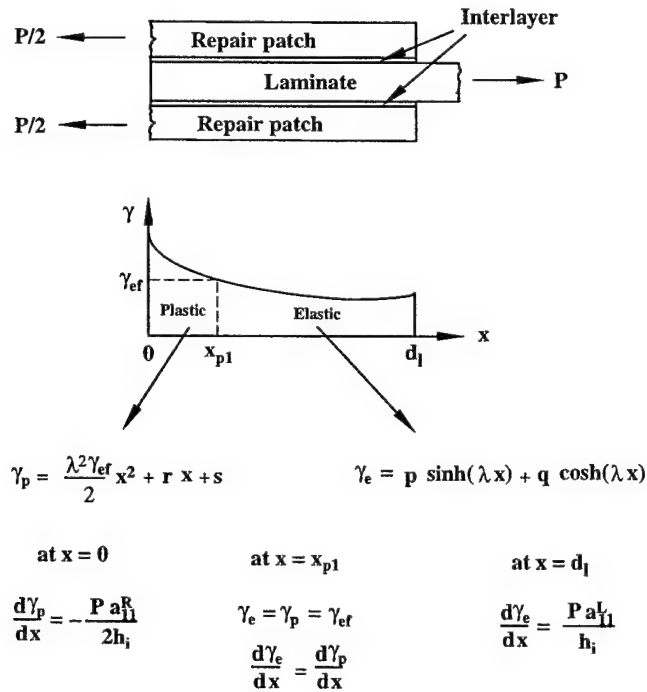
at $x = 0$

$$\frac{d\gamma_e}{dx} = -\frac{P a_{f1}^R}{2h_i}$$

at $x = d_l$

$$\frac{d\gamma_e}{dx} = \frac{P a_{f1}^L}{h_i}$$

FIGURE 40. THE EQUATIONS AND BOUNDARY CONDITIONS FOR CALCULATING THE SHEAR STRAIN IN THE INTERLAYER WHEN THE ENTIRE INTERLAYER BEHAVES IN A LINEARLY ELASTIC MANNER



at $x = 0$

$$\frac{d\gamma_p}{dx} = -\frac{P a_{f1}^R}{2h_i}$$

at $x = x_{p1}$

$$\gamma_e = \gamma_p = \gamma_{ef}$$

$$\frac{d\gamma_e}{dx} = \frac{d\gamma_p}{dx}$$

at $x = d_l$

$$\frac{d\gamma_e}{dx} = \frac{P a_{f1}^L}{h_i}$$

FIGURE 41. THE EQUATIONS AND BOUNDARY AND CONTINUITY CONDITIONS FOR CALCULATING THE SHEAR STRAIN IN THE INTERLAYER WHEN THE INTERLAYER IS PERFECTLY PLASTIC NEAR THE $x = 0$ END

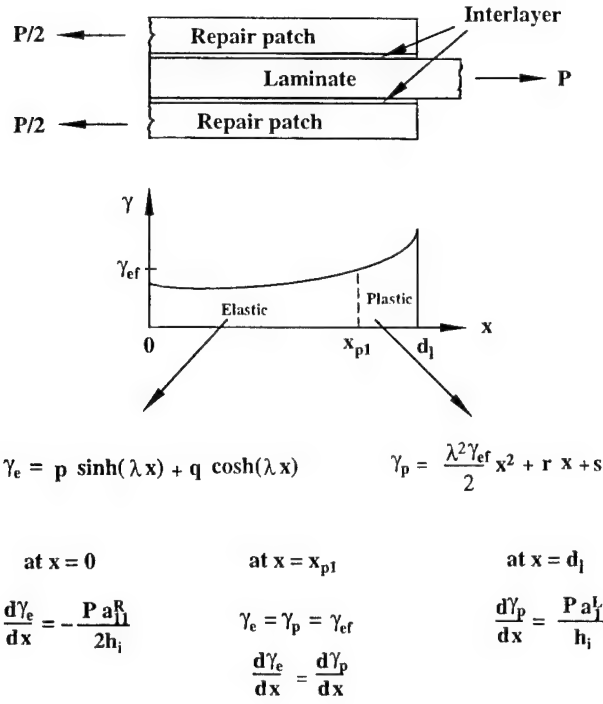


FIGURE 42. THE EQUATIONS AND BOUNDARY AND CONTINUITY CONDITIONS FOR CALCULATING THE SHEAR STRAIN IN THE INTERLAYER WHEN THE INTERLAYER IS PERFECTLY PLASTIC NEAR THE $x = d_l$ END

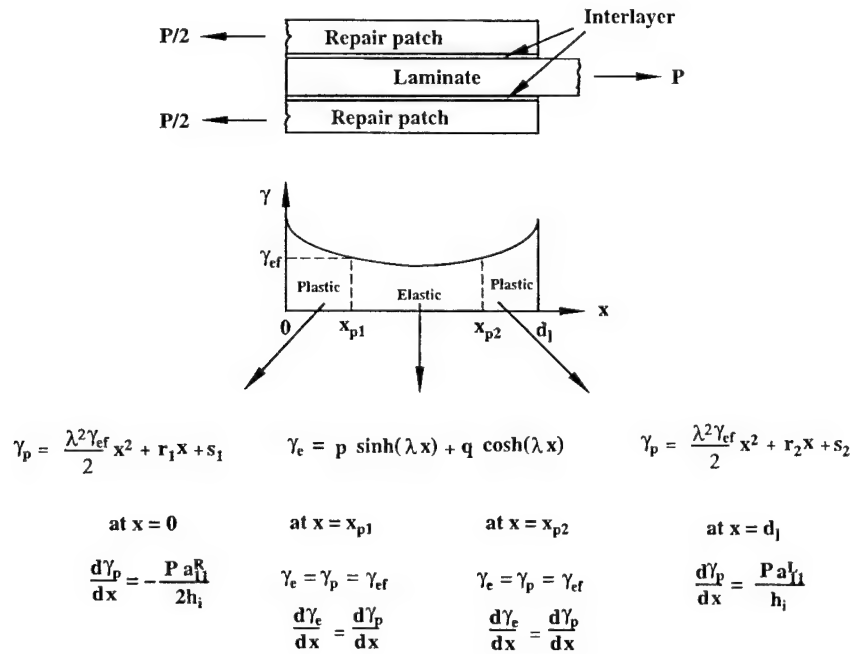


FIGURE 43. THE EQUATIONS AND BOUNDARY AND CONTINUITY CONDITIONS FOR CALCULATING THE SHEAR STRAIN IN THE INTERLAYER WHEN THE INTERLAYER IS PERFECTLY PLASTIC NEAR THE $x = 0$ AND $x = d_l$ ENDS

7.2.2 Calculation of the Shear Failure Load.

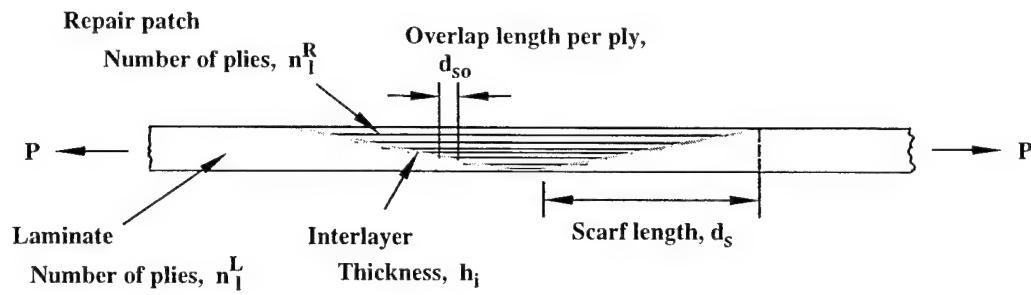
The applied tensile load F which fails the interlayer in shear is calculated by the following steps using the equations and boundary and continuity conditions summarized in figure 40 through figure 43.

- a. A load P is applied such that under this load the entire interlayer is in the elastic region (figure 38, left). The shear strain as a function of location x is calculated by the equation in figure 40. The load is gradually increased, and at each load the shear strain is calculated. The procedure is repeated until the shear strain reaches the elastic limit γ_{ef} either near the $x = 0$ or near $x = d_l$ end of the interlayer.
- b. The applied load is gradually increased, and at each load the shear strain as a function of x is calculated by the equation given either in figure 41 (when the plastic region is near $x = 0$) or in figure 42 (when the plastic region is near $x = d_l$). The procedure is repeated until the shear strain is at or above the elastic limit at both the $x = 0$ and $x = d_l$ ends of the interlayer.
- c. The applied load is gradually increased, and at each load the shear strain as a function of location x is calculated by the equations given in figure 43.

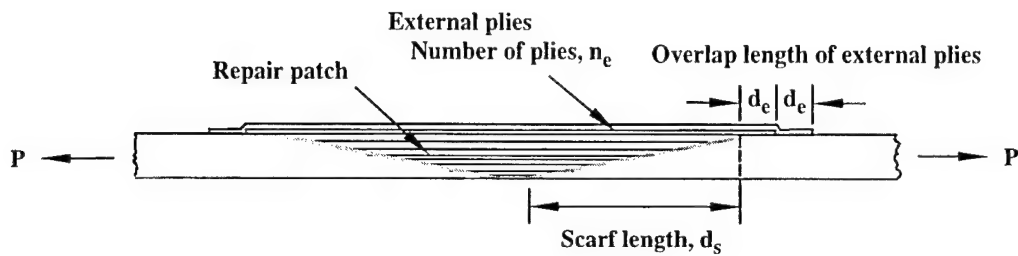
At each load in steps b. and c. the shear strain is compared to the plastic failure strain γ_{pf} . The load P at which the shear strain γ_p , at any point in the interlayer, reaches the plastic failure strain γ_{pf} , is taken to be the failure load ($P = F$).

8. MODEL OF SCARF REPAIR.

Consider a symmetric composite laminate repaired by the scarf technique (see figure 44). When such a repaired laminate is subjected to a tensile load, the laminate may fail in tension, the repair patch may fail in tension, the interlayer may fail in shear, the laminate may fail in tension while the interlayer fails in shear, and the repair patch may fail in tension while the interlayer fails in shear (see figure 45). The procedure for calculating the loads at which each of these types of failure occurs is given below.



(a) Without external ply



(b) With external plies

FIGURE 44. SCARF REPAIRS TREATED IN THE MODEL



(a) Laminate failure in tension



(d) Laminate / interlayer failure



(b) Repair patch failure in tension



(e) Repair patch / interlayer failure



(c) Interlayer failure in shear

FIGURE 45. THE TYPES OF FAILURE WHICH MAY OCCUR IN A LAMINATE REPAIRED BY THE SCARF TECHNIQUE

8.1 INTERLAYER SHEAR STRAIN.

To calculate shear strain in the interlayer, consider half of the repaired laminate, as shown in figure 46. The shear strain is calculated as follows, idealizing the taper as a series of discrete steps.

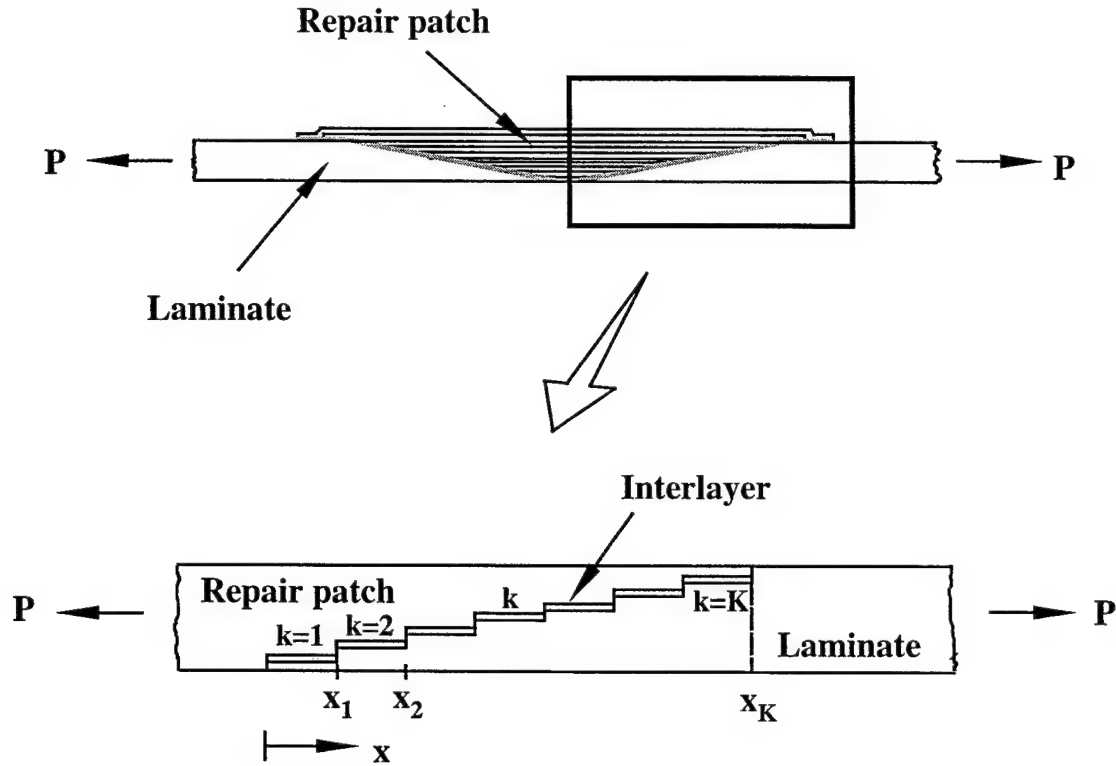


FIGURE 46. THE SCARF REPAIR TREATED IN THE MODEL

The repaired laminate is subjected to an applied in-plane load P . The superscript k refers to the k -th overlap segment. For a section dx in length (x being in the direction of the applied load, figure 46), a force balance for the laminate and the repair patch gives

$$\begin{aligned} \frac{d(^k N^L)}{dx} - ^k \tau &= 0 && \text{Laminate} \\ \frac{d(^k N^R)}{dx} + ^k \tau &= 0 && \text{Repair Patch} \end{aligned} \quad (20)$$

$^k N^L (= ^k N_x^L)$ and $^k N^R (= ^k N_x^R)$ are the in-plane loads (per unit width) inside the laminate and inside the repair patch for the k -th overlap segment, respectively. $^k \tau (= ^k \tau_{zx})$ is the shear stress in the interlayer. This is illustrated in figure 47.

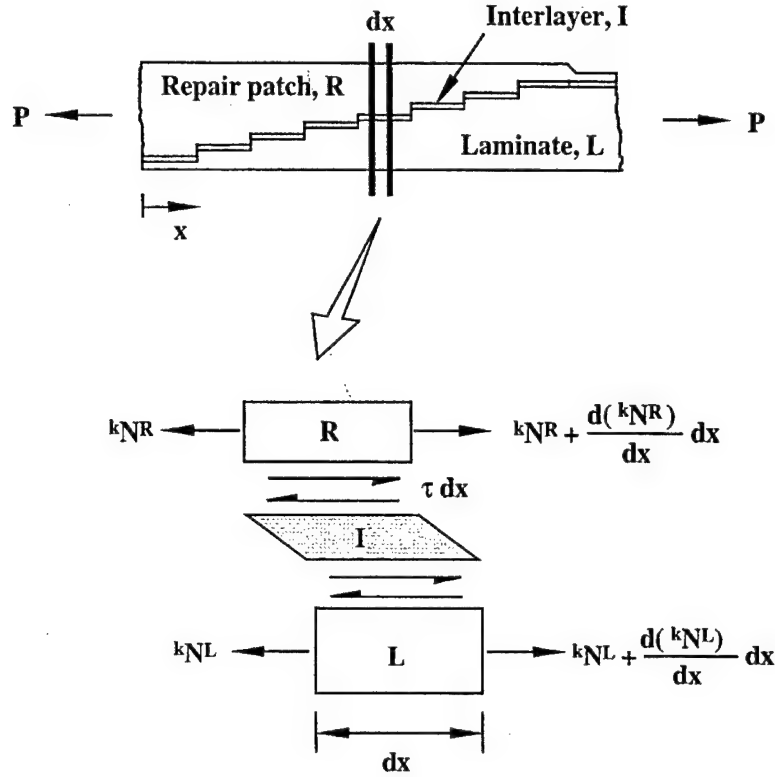


FIGURE 47. LOADS ON A SECTION dx IN LENGTH OF THE k -th SEGMENT OF THE LAMINATE REPAIRED BY THE SCARF TECHNIQUE

Neglecting shear deformations of the laminate and the repair patch, compatibility requires that the following condition be satisfied [64] (figure 48)

$$({}^k\varepsilon_x^L + 1)dx + {}^k\gamma h_i = ({}^k\varepsilon_x^R + 1)dx + \left({}^k\gamma + \frac{d({}^k\gamma)}{dx} dx \right) h_i \quad (21)$$

This can be simplified to give

$$\frac{d({}^k\gamma)}{dx} = \frac{{}^k\varepsilon_x^L - {}^k\varepsilon_x^R}{h_i} \quad (22)$$

where ${}^k\varepsilon_x^L$ and ${}^k\varepsilon_x^R$ are the off-axis in-plane strains in the laminate and in the repair patch, respectively, h_i is the thickness of the interlayer, and ${}^k\gamma (= {}^k\gamma_{zx})$ is the interlayer shear strain.

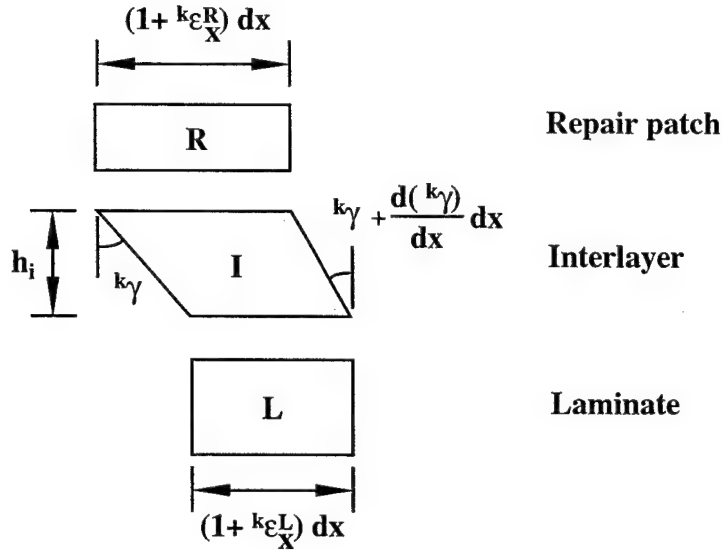


FIGURE 48. DEFORMATIONS OF THE REPAIR PATCH, THE INTERLAYER, AND THE LAMINATE IN THE k -th SEGMENT OF A LAMINATE REPAIRED BY THE SCARF TECHNIQUE

At any overlap segment the laminate and the repair patch is not necessarily symmetric. The x components of the strains in the unsymmetric laminate and in the unsymmetric repair patch are [63]

$$\begin{aligned} {}^k\varepsilon_x^L &= {}^k\alpha_{11}^L N^L && \text{Laminate} \\ {}^k\varepsilon_x^R &= {}^k\alpha_{11}^R N^R && \text{Repair Patch} \end{aligned} \quad (23)$$

where ${}^k\alpha_{11}$ is the 11 component of the laminate or repair patch compliance matrix in the k -th overlap segment (see figure 49).

Equations 22 and 23 yield

$$\frac{d({}^k\gamma)}{dx} = \frac{1}{h_i} ({}^k\alpha_{11}^L N^L - {}^k\alpha_{11}^R N^R) \quad (24)$$

By combining equations 20 and 24 one obtains

$$\frac{d^2({}^k\gamma)}{dx^2} = \frac{1}{h_i} ({}^k\alpha_{11}^L + {}^k\alpha_{11}^R) \tau \quad (25)$$

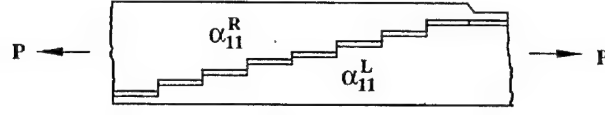


FIGURE 49. THE COMPLIANCE MATRICES IN THE LAMINATE AND THE REPAIR PATCH

There are four possible scenarios for the behavior of the interlayer (see figure 50). The entire interlayer behaves in a linearly elastic manner, there is a perfectly plastic region either near the $x = 0$ or near the $x = x_K$ end of the repair patch, or there are perfectly plastic regions near both the $x = 0$ and $x = x_K$ ends of the repair patch (x_K is defined in figure 46).

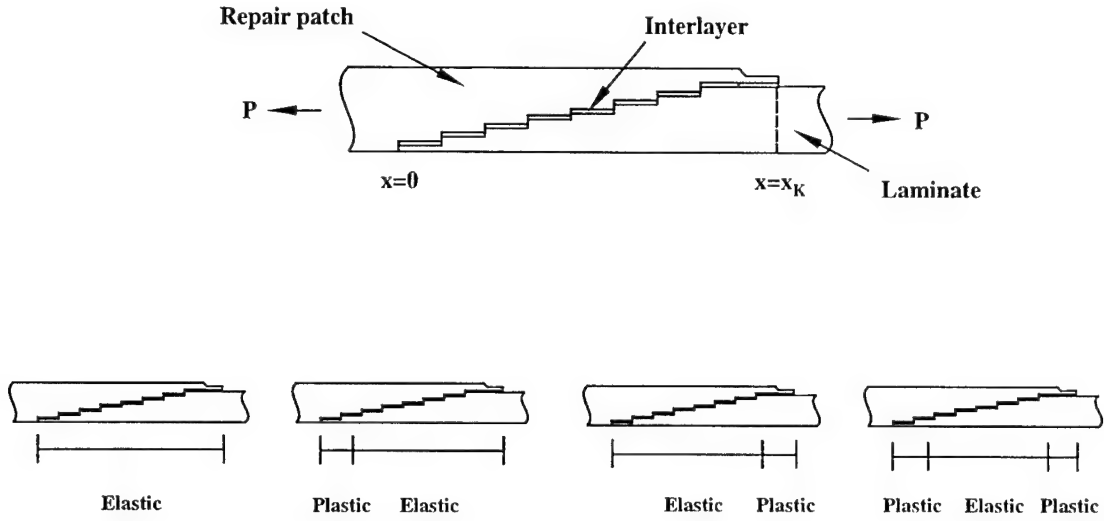


FIGURE 50. POSSIBLE REGIONS OF THE INTERLAYER UNDER AN APPLIED LOAD P
(From left to the right: interlayer is linearly elastic; interlayer is perfectly plastic near the $x = 0$ end; interlayer is perfectly plastic near the $x = x_K$ end; and interlayer is perfectly plastic near the $x = 0$ and $x = x_K$ ends. (Sarf technique))

In the elastic region, the shear strain and shear stress are

$${}^k\gamma = {}^k\gamma_e \quad \text{and} \quad {}^k\tau = G {}^k\gamma_e \quad (26)$$

where G is the shear modulus of the interlayer. From equations 25 and 26 the following expression for the shear strain is obtained

$${}^k\gamma_e = {}^k p \sinh({}^k \lambda x) + {}^k q \cosh({}^k \lambda x) \quad \text{Elastic Region} \quad (27)$$

where ${}^k \lambda$ is defined as

$$({}^k \lambda)^2 = \frac{G}{h_i} ({}^k \alpha_{11}^L + {}^k \alpha_{11}^R) \quad (28)$$

In the plastic region the shear strain and shear stress are (see figure 31)

$${}^k\gamma = {}^k\gamma_p \quad \text{and} \quad {}^k\tau = {}^k\tau_p = G\gamma_{ef} \quad (29)$$

where, as shown in figure 31, γ_{ef} is constant. Equations 25 and 29 yield

$${}^k\gamma_p = \frac{{}^k(\lambda)^2 \gamma_{ef}}{2} x^2 + {}^k r x + {}^k s \quad \text{Plastic Region} \quad (30)$$

In equations 27 and 30, ${}^k p$, ${}^k q$, ${}^k r$, and ${}^k s$ are constants which must be determined from the boundary and continuity conditions.

8.1.1 Boundary and Continuity Conditions.

The terminations of the external plies are modeled as illustrated in figure 51. Then, the boundary and continuity conditions corresponding to equations 27 and 30 are as follows.

- At the inside edge of the repair patch ($x = 0$) the axial load (per unit width) is zero in the laminate, and is equal to the applied load (per unit width) P in the repair patch (see figure 52). At the outside edge of the repair ($x = x_K$) the axial load (per unit width) is zero in the repair patch, and is equal to the applied load (per unit width) P in the laminate

$$\begin{aligned} {}^1N^L &= 0 \\ {}^1N^R &= P \end{aligned} \quad \text{at } x = 0 \quad (31)$$

$$\begin{aligned} {}^KN^L &= P \\ {}^KN^R &= 0 \end{aligned} \quad \text{at } x = x_K \quad (32)$$

By combining equations 24, 31, and 32, these boundary conditions can be expressed as

$$\frac{d({}^1\gamma)}{dx} = -\frac{P^1\alpha_{11}^R}{h_i} \quad \text{at } x=0, \quad (33)$$

and

$$\frac{d({}^K\gamma)}{dx} = \left(\frac{P^k\alpha_{11}^L}{h_i} \right) \quad \text{at } x = x_K \quad (34)$$

In equations 33 and 34 ${}^k\gamma$ is either ${}^k\gamma_e$ or ${}^k\gamma_p$ depending on whether the interlayer is in the elastic or in the perfectly plastic region at the boundary.

- At the edge of each overlap segment (at $x = x_K$, figure 53) the shear strain in the interlayer is continuous and the in-plane loads are equal and opposite on the left and right sides of the segment. It is assumed that the load is transmitted only by continuous layers

(for example in figure 53 load is transmitted by the bottom four layers in the laminate and the top three layers in the repair). Accordingly, at the edge of each segment the following continuity conditions are applied.

$${}^{k+1}\gamma = {}^k\gamma \quad (35)$$

$${}^{k+1}N^L \cong {}^kN^L \quad \text{at } x = x_k \quad (36)$$

$${}^{k+1}N^R \cong {}^kN^R \quad (37)$$

By using equations 24, 36, and 37, the above continuity conditions for the k -th segment can be expressed in terms of ${}^k\gamma$ as follows

$${}^{k+1}\gamma = {}^k\gamma \quad (38)$$

$$\frac{d({}^{k+1}\gamma)}{dx} = \frac{d({}^k\gamma)}{dx} \alpha^* + {}^kP^* \quad \text{at } x = x_k \quad (39)$$

where ${}^k\alpha^*$ and ${}^kP^*$ are defined as

$${}^k\alpha^* = \frac{{}^{k+1}\alpha_{11}^L + {}^{k+1}\alpha_{11}^R}{{}^k\alpha_{11}^L + {}^k\alpha_{11}^R} \quad (40)$$

$${}^kP^* = \frac{P}{h_i} \left(\frac{{}^k\alpha_{11}^L {}^{k+1}\alpha_{11}^R - {}^k\alpha_{11}^R {}^{k+1}\alpha_{11}^L}{{}^k\alpha_{11}^L + {}^k\alpha_{11}^R} \right) \quad (41)$$

In equations 35, 38, and 39 $\gamma = \gamma_e$ when interlayer is in the elastic region, and $\gamma = \gamma_p$ when interlayer is in the plastic region.

- At the locations where the elastic and plastic regions meet ($x = x_{p1}$ and $x = x_{p2}$ in figure 54), the shear strains in the elastic and plastic regions are equal (with the value γ_{ef}) and are continuous (see figures 54 and 56 through 58). Correspondingly,

$${}^k\gamma_e = {}^k\gamma_p = (\gamma_{ef}) \quad \text{at } x = x_{p1}, \quad x = x_{p2} \quad (42)$$

$$\frac{d({}^k\gamma_e)}{dx} = \frac{d({}^k\gamma_p)}{dx}$$

The locations x_{p1} and x_{p2} are unknown, and must be determined from the solutions of the equations summarized in figures 55 through 58.

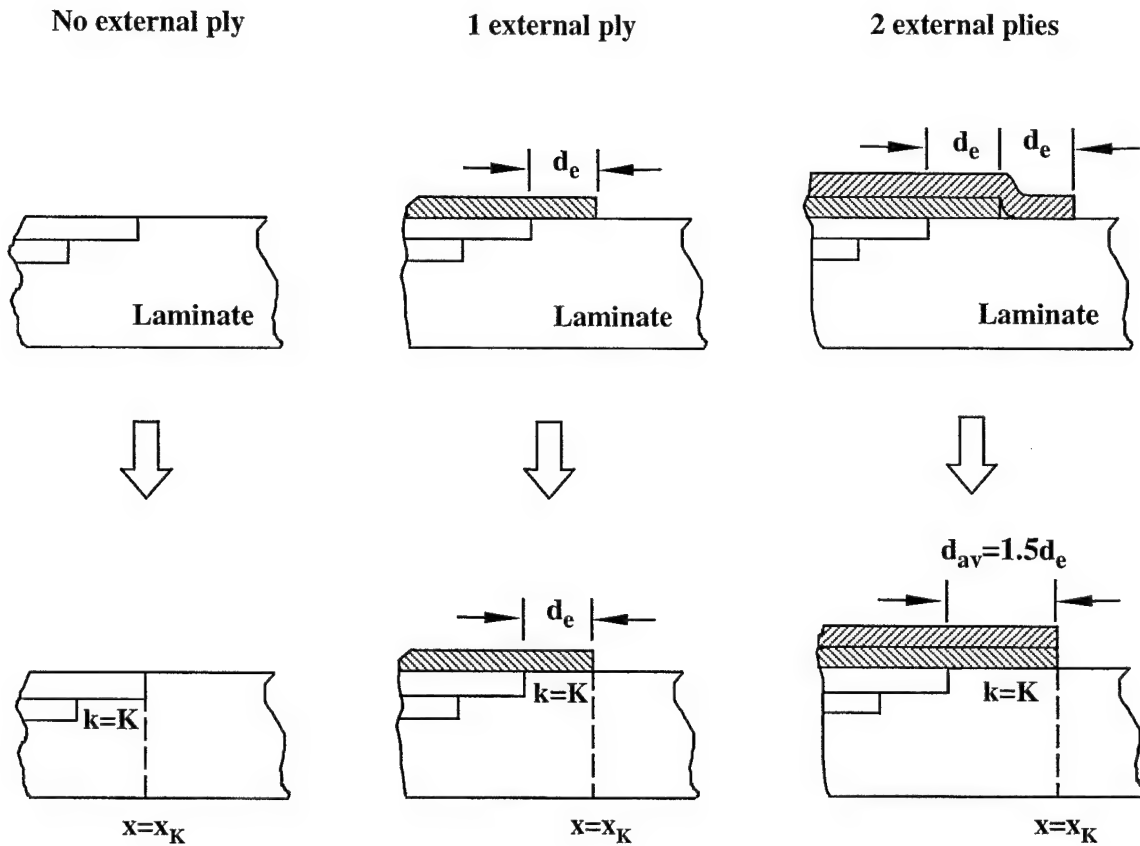


FIGURE 51. MODEL OF THE BOUNDARY AT THE OUTER EDGE ($x = x_K$) OF THE REPAIR PATCH

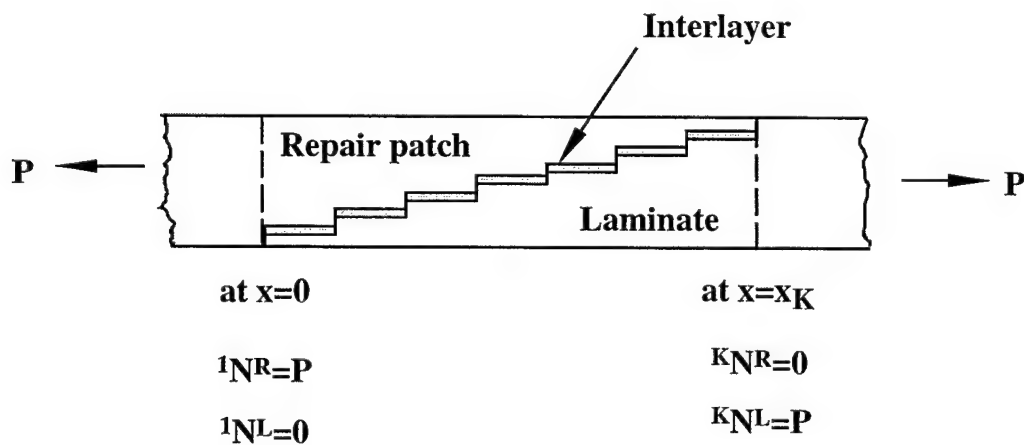
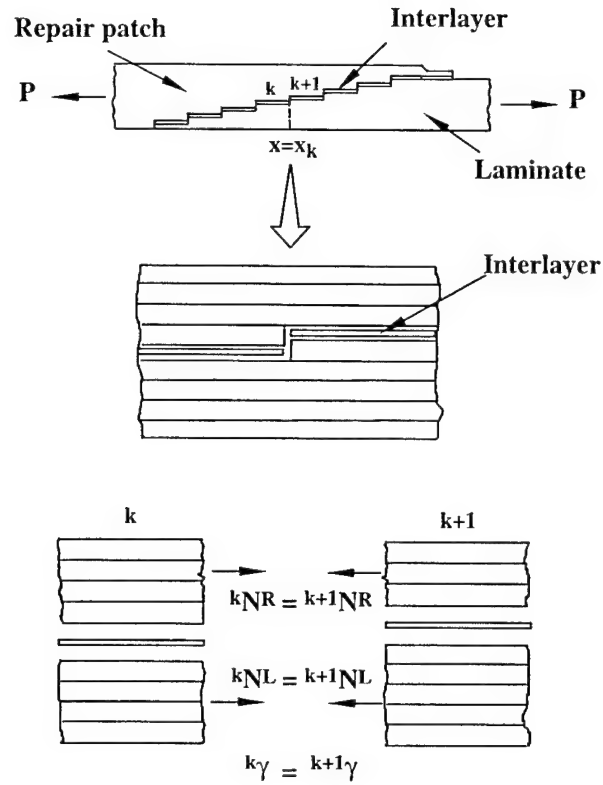


FIGURE 52. THE BOUNDARY CONDITIONS FOR THE IN-PLANE LOADS IN THE LAMINATE AND IN THE REPAIR PATCH (Scarf technique)



$\gamma = \gamma_e$ if elastic
 $\gamma = \gamma_p$ if perfect plastic

FIGURE 53. THE CONTINUITY CONDITIONS AT THE EDGE OF THE k -th SEGMENT (Scarf technique)

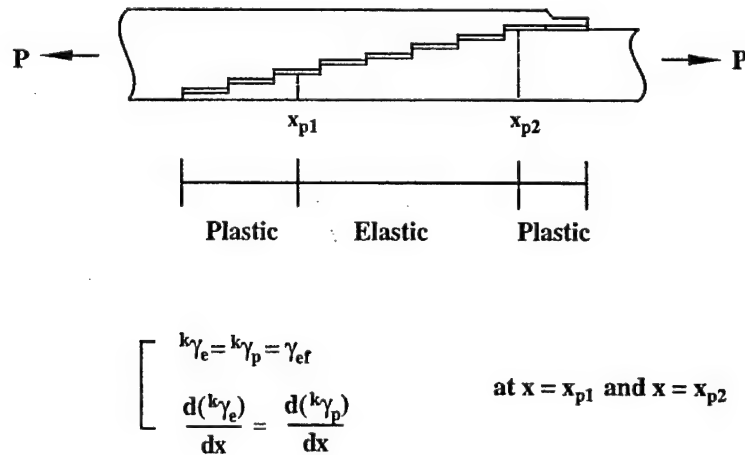
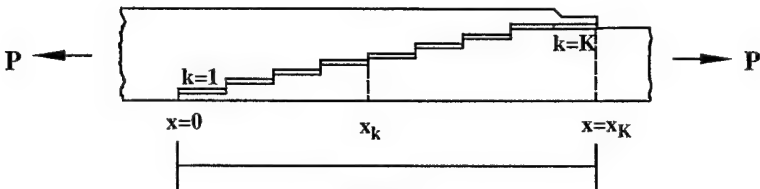


FIGURE 54. THE CONTINUITY CONDITIONS AT THE INTERLAYER BETWEEN THE ELASTIC AND PERFECTLY PLASTIC REGIONS

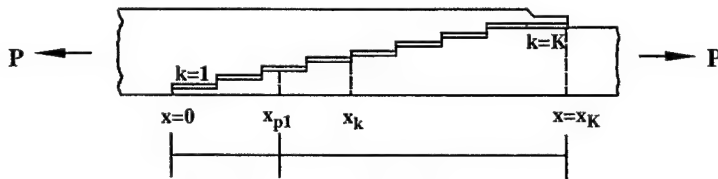


Elastic

$${}^k\gamma_e = {}^k p \sinh(k\lambda x) + {}^k q \cosh(k\lambda x)$$

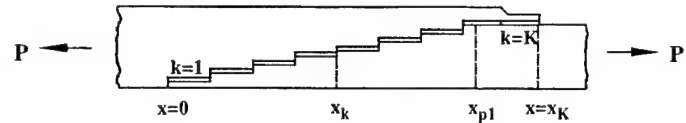
at $x = 0$	at $x = x_k$	at $x = x_K$
$\frac{d({}^1\gamma_e)}{dx} = -\frac{P({}^1\alpha_{11}^R)}{h_i}$	${}^k\gamma_e = {}^{k+1}\gamma_e$ $\frac{d({}^{k+1}\gamma_e)}{dx} = \frac{d({}^k\gamma_e)}{dx} {}^k\alpha^* + {}^k p^*$	$\frac{d({}^K\gamma_e)}{dx} = \frac{P({}^K\alpha_{11}^L)}{h_i}$

FIGURE 55. THE EQUATIONS AND BOUNDARY CONDITIONS FOR CALCULATING THE SHEAR STRAIN IN THE INTERLAYER WHEN THE ENTIRE INTERLAYER BEHAVES IN A LINEARLY ELASTIC MANNER



Plastic		Elastic	
${}^k\gamma_p = \frac{k\lambda^2 \gamma_{ef}}{2} x^2 + {}^k r x + {}^k s$		${}^k\gamma_e = {}^k p \sinh(k\lambda x) + {}^k q \cosh(k\lambda x)$	
at $x = 0$	at $x = x_{p1}$	at $x = x_k$	at $x = x_K$
$\frac{d({}^1\gamma_p)}{dx} = -\frac{P({}^1\alpha_{11}^R)}{h_i}$	${}^k\gamma_e = {}^k\gamma_p = \gamma_{ef}$ $\frac{d({}^k\gamma_e)}{dx} = \frac{d({}^k\gamma_p)}{dx}$	${}^{k+1}\gamma = {}^k\gamma$ $\frac{d({}^{k+1}\gamma)}{dx} = \frac{d({}^k\gamma)}{dx} {}^k\alpha^* + {}^k p^*$	$\frac{d({}^K\gamma_p)}{dx} = \frac{P({}^K\alpha_{11}^L)}{h_i}$
		$\gamma = \gamma_e$ if elastic $\gamma = \gamma_p$ if perfect plastic	

FIGURE 56. THE EQUATIONS AND BOUNDARY AND CONTINUITY CONDITIONS FOR CALCULATING THE SHEAR STRAIN IN THE INTERLAYER WHEN THE INTERLAYER IS PERFECTLY PLASTIC NEAR THE $x = 0$ END



Elastic Plastic

$${}^k\gamma_e = {}^k c_1 \sinh(k\lambda x) + {}^k c_2 \cosh(k\lambda x) \qquad {}^k\gamma_p = \frac{k\lambda^2 \gamma_{ef}}{2} x^2 + {}^k c_3 x + {}^k c_4$$

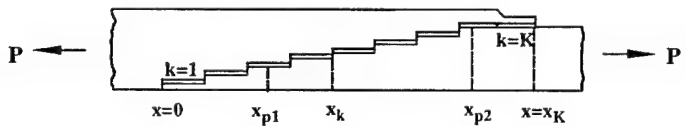
at $x = 0$ at $x = x_{p1}$ at $x = x_k$ at $x = x_K$

$$\frac{d({}^1\gamma_e)}{dx} = -\frac{P({}^1\alpha_{11}^R)}{h_i} \qquad {}^k\gamma_e = {}^k\gamma_p = \gamma_{ef} \qquad {}^{k+1}\gamma = {}^k\gamma \qquad \frac{d({}^K\gamma_p)}{dx} = \frac{P({}^K\alpha_{11}^L)}{h_i}$$

$$\frac{d({}^k\gamma_e)}{dx} = \frac{d({}^k\gamma_p)}{dx} \qquad \frac{d({}^{k+1}\gamma)}{dx} = \frac{d({}^k\gamma)}{dx} {}^k\alpha^* + {}^kP^*$$

$\gamma = \gamma_e$ if elastic
 $\gamma = \gamma_p$ if perfect plastic

FIGURE 57. THE EQUATIONS AND BOUNDARY AND CONTINUITY CONDITIONS FOR CALCULATING THE SHEAR STRAIN IN THE INTERLAYER WHEN THE INTERLAYER IS PERFECTLY PLASTIC NEAR THE $x = x_K$ END



Plastic Elastic Plastic

$${}^k\gamma_p = \frac{k\lambda^2 \gamma_{ef}}{2} x^2 + {}^k c_1 x + {}^k c_2 \qquad {}^k\gamma_e = {}^k c_3 \sinh(k\lambda x) + {}^k c_4 \cosh(k\lambda x) \qquad {}^k\gamma_p = \frac{k\lambda^2 \gamma_{ef}}{2} x^2 + {}^k c_5 x + {}^k c_6$$

at $x = 0$ at $x = x_{p1}$ and $x = x_{p2}$ at $x = x_k$ at $x = x_K$

$$\frac{d({}^1\gamma_p)}{dx} = -\frac{P({}^1\alpha_{11}^R)}{h_i} \qquad {}^k\gamma_e = {}^k\gamma_p = \gamma_{ef} \qquad {}^{k+1}\gamma = {}^k\gamma \qquad \frac{d({}^K\gamma_p)}{dx} = \frac{P({}^K\alpha_{11}^L)}{h_i}$$

$$\frac{d({}^k\gamma_e)}{dx} = \frac{d({}^k\gamma_p)}{dx} \qquad \frac{d({}^{k+1}\gamma)}{dx} = \frac{d({}^k\gamma)}{dx} {}^k\alpha^* + {}^kP^*$$

$\gamma = \gamma_e$ if elastic
 $\gamma = \gamma_p$ if perfect plastic

FIGURE 58. THE EQUATIONS AND BOUNDARY AND CONTINUITY CONDITIONS FOR CALCULATING THE SHEAR STRAIN IN THE INTERLAYER WHEN THE INTERLAYER IS PERFECTLY PLASTIC NEAR THE $x = 0$ AND $x = x_K$ ENDS

8.1.2 Calculation of the Interlayer Shear Strain.

The interlayer shear strain is calculated by the following steps using the equations and boundary and continuity conditions summarized in figures 55 through 58.

- a. Values for the applied load P and the interlayer shear strain ${}^1\gamma$ at $x = 0$ are assumed such that the shear strain both at $x = 0$ and at $x = x_K$ (i.e., ${}^1\gamma$ and ${}^K\gamma$) are in the elastic region (see figure 50, left). The shear strain as a function of location x is calculated by the equations in figure 55. At the $x = x_K$ boundary the x derivative of the shear strains is calculated and compared to the value of $\frac{P^K \alpha_{II}^L}{h_i}$

$$\frac{d({}^k\gamma)}{dx} \begin{matrix} < \\ > \end{matrix} \frac{P^K \alpha_{II}^L}{h_i} \quad \text{at } x = x_K \quad (43)$$

If the left-hand side of this equation is less or higher than the right-hand side, a new value of ${}^1\gamma$ is assigned. These calculations are repeated until the boundary condition at $x = x_K$ is satisfied, i.e., until the left-hand side of the equation becomes equal to the right-hand side. The applied load is then gradually increased, and at each load the calculation is repeated until the shear strain reaches the elastic limit γ_{ef} either near the $x = 0$ or near $x = x_K$ end of the repair patch.

- b. The applied load is gradually increased. At each load the shear strain as a function of x is calculated by the procedure in step a. using the equations given either in figure 56 (when the plastic region is near $x = 0$) or in figure 57 (when the plastic region is near $x = x_K$). The process is repeated until the shear strain is at or above the elastic limit at both the $x = 0$ and $x = x_K$ ends of the interlayer.
- c. The applied load is gradually increased in small increments, and at each load the shear strain as a function of x is calculated by the procedure in step a. using the equations given in figure 58.

8.2 FAILURE LOAD.

The applied tensile load at which the interlayer fails in shear is determined at each load step (steps b. and c. in section 8.1.2) by comparing the shear strains to the plastic failure strain γ_{pf} . The load P at which the shear strain ${}^k\gamma_p$ at any point in the interlayer reaches the plastic failure strain γ_{pf} , is taken to be the interlayer shear failure load.

To determine the applied tensile load under which either the laminate or the repair patch fails, the in-plane loads in the laminate and the repair patch are calculated as functions of axial position x

$$\begin{aligned} {}^k N^L(x) &= 0 + \int_0^x {}^k \tau dx && \text{Laminate} \\ {}^k N^R(x) &= P - \int_0^x {}^k \tau dx && \text{Repair Patch} \end{aligned} \quad (44)$$

${}^k\tau$ is the shear stress having the value of ${}^k\tau = G\gamma_e$ in the elastic region and ${}^k\tau = {}^k\tau_p = G\gamma_{ef}$ in the plastic region.

The off-axis in-plane strains as a function of x in the laminate and in the repair patch are

Laminate	Repair Patch
${}^k\varepsilon_x^L(x) = {}^k\alpha_{11}^L {}^kN^L(x)$	${}^k\varepsilon_x^R(x) = {}^k\alpha_{11}^R {}^kN^R(x)$
${}^k\varepsilon_y^L(x) = {}^k\alpha_{21}^L {}^kN^L(x)$	${}^k\varepsilon_y^R(x) = {}^k\alpha_{21}^R {}^kN^R(x)$
${}^k\varepsilon_s^L(x) = {}^k\alpha_{61}^L {}^kN^L(x)$	${}^k\varepsilon_s^R(x) = {}^k\alpha_{61}^R {}^kN^R(x)$

(45)

where the α_{ij} 's are the components of the compliance matrix [63]. The on-axis in-plane strains of each ply in the laminate or in the repair patch in k -th overlap segment are obtained by transformation

$$\begin{Bmatrix} {}^k\varepsilon_1^{L,R} \\ {}^k\varepsilon_2^{L,R} \\ {}^k\varepsilon_6^{L,R} \end{Bmatrix} = \begin{pmatrix} \cos^2 \theta^{L,R} & \sin^2 \theta^{L,R} & \cos \theta^{L,R} \sin \theta^{L,R} \\ \sin^2 \theta^{L,R} & \cos^2 \theta^{L,R} & -\cos \theta^{L,R} \sin \theta^{L,R} \\ -2 \cos \theta^{L,R} \sin \theta^{L,R} & 2 \cos \theta^{L,R} \sin \theta^{L,R} & \cos^2 \theta^{L,R} - \sin^2 \theta^{L,R} \end{pmatrix} \begin{Bmatrix} {}^k\varepsilon_x^{L,R} \\ {}^k\varepsilon_y^{L,R} \\ {}^k\varepsilon_s^{L,R} \end{Bmatrix} \quad (46)$$

Failure is calculated by the maximum strain failure criteria

Laminate	Repair Patch
$\frac{{}^kX^L}{{}^kE_1^L {}^k\varepsilon_1^L} = {}^kP^L$	$\frac{{}^kX^R}{{}^kE_1^R {}^k\varepsilon_1^R} = {}^kP^R$
$\frac{{}^kY^L}{{}^kE_2^L {}^k\varepsilon_2^L} = {}^kP^L$	$\frac{{}^kY^R}{{}^kE_2^R {}^k\varepsilon_2^R} = {}^kP^R$
$\frac{{}^kS^L}{{}^kE_6^L {}^k\varepsilon_6^L} = {}^kP^L$	$\frac{{}^kS^R}{{}^kE_6^R {}^k\varepsilon_6^R} = {}^kP^R$

(47)

${}^kP^{L,R} < 1$	Failure
${}^kP^{L,R} \geq 1$	No Failure

(48)

kX , kY , and kS are the on-axis longitudinal, transverse, and shear strengths, kE_1 , kE_2 , and kE_6 are the on-axis longitudinal, transverse, and shear moduli of the ply in k -th segment and p are loads.

The above failure criteria is evaluated in each laminate and repair ply at every overlap segment.

Failure occurs when under the applied load p is less than unity in any ply.

- If failure occurs at the $x = 0$ end of the repaired laminate, the failure is considered to have occurred in the repair patch (see figure 45, b).
- If failure occurs at the $x = x_K$ end of the repaired laminate, the failure is considered to have occurred in the laminate (see figure 45, a).
- If failure occurs in the laminate or the repair patch at one of the overlap segments, then failure is considered to have occurred due to a combination of laminate (or repair patch) failure and interlayer failure (see figure 45, d and e).

9. RESULTS.

Two computer programs were written in MATLAB to generate numerical results for the two models described in the previous two chapters. These codes are designated as "RepairL" and "RepairS" and apply, respectively, to the double-sided uniform lap repair and the scarf repair. The input parameters required by the programs are listed in tables 13 and 14. The properties of the interlayer were obtained by matching the model to one data point. The properties selected by such a "backcalculation" procedure were then used in all subsequent calculations. The programs provide the tensile failure loads in the laminate and in the repair patch and the shear failure load in the interlayer. The lowest of these three is the failure load of the repaired composite.

Failure loads generated by the model and the corresponding computer codes were compared to data generated with repaired specimens specified in figures 5 and 14. For the uniform lap repair, comparisons were made for 8- and 32-ply laminates repaired with either 1, 2, or 3 repair plies. The repair lap length varied from 0 to 3 inches. For scarf repair, comparisons were made for different scarf angles ($\beta = 1.07, 1.43, \text{ and } 2.15$ degree) and for different number of external plies ($n_e = 0, 1, \text{ and } 2$). The material properties and parameters used in the calculations are given in tables 13 and 14.

TABLE 13. THE INPUT PARAMETERS REQUIRED BY RepairL AND THE NUMERICAL VALUES USED IN THE PRESENT CALCULATIONS FOR 3k70 PLAIN WEAVE FABRIC IMPREGNATED WITH 9396 RESIN

Category	Parameter	Specimen Condition/Test Temperature	
		Dry/70°F	Moist(H ₂ O)/180°F
Laminate*	Longitudinal modulus, E_1^L (Msi) ^[a]	8.1	8.5
	Transverse modulus, E_2^L (Msi) ^[a]	8.1	8.5
	Shear modulus, E_6^L (Msi) ^[b]	0.48	0.45
	Longitudinal Poisson's ratio, $\nu_1^{L[b]}$	0.045	0.045
	Transverse Poisson's ratio, $\nu_2^{L[b]}$	0.045	0.045
	Longitudinal tensile strength, X^L (ksi) ^[a]	101	93
	Transverse tensile strength, Y^L (ksi) ^[a]	101	93
	Shear strength, S^L (ksi) ^[b]	5.0	4.5
	Ply thickness, h^L (in) ^[a]	0.0094	0.0094
	Orientation of each ply, θ^L (degree)	0	0
	Number of plies, n_l^L	8, 32	8, 32
Repair Patch*	Longitudinal modulus, E_1^R (Msi) ^[a]	7.2	7.5
	Transverse modulus, E_2^R (Msi) ^[a]	7.2	7.5
	Shear modulus, E_6^R (Msi) ^[b]	0.48	0.45
	Longitudinal Poisson's ratio, $\nu_1^{R[b]}$	0.045	0.045
	Transverse Poisson's ratio, $\nu_2^{R[b]}$	0.045	0.045
	Longitudinal tensile strength, X^R (ksi) ^[a]	75	68
	Transverse tensile strength, Y^R (ksi) ^[a]	75	68
	Shear strength, S^R (ksi) ^[b]	5.0	4.5
	Ply thickness, h^R (in)	0.0094	0.0094
	Orientation of each ply, θ^R (degree)	0	0
	Number of plies per side, n_l^R	1,2,3	1,2,3
	Maximum lap length, d_l (in)	0 to 3.0	0 to 3.0
Interlayer	Shear modulus, G (ksi)] ^[c]	200	100
	Shear strength, τ_p (ksi)] ^[c]	2.0	1.6
	Maximum shear strain, γ_{pf} ^[c]	0.28	0.30
	Thickness, h_i (in) ^[c]	0.008	0.008

* Parameters listed are for each ply.

[a] from tables 2 and 3.

[b] from Naik [65]

[c] by backcalculation.

TABLE 14. THE INPUT PARAMETERS REQUIRED BY RepairS AND THE NUMERICAL VALUES USED IN THE PRESENT CALCULATIONS FOR 3k70 PLAIN WEAVE FABRIC IMPREGNATED WITH 9396 RESIN

Category	Parameter	Specimen Condition/Test Temperature	
		Dry/70°F	Moist(H ₂ O)/180°F
Laminate*	Longitudinal modulus, E_1^L (Msi) ^[a]	8.1	8.5
	Transverse modulus, E_2^L (Msi) ^[a]	8.1	8.5
	Shear modulus, E_6^L (Msi) ^[b]	0.48	0.45
	Longitudinal Poisson's ratio, $\nu_1^{L[b]}$	0.045	0.045
	Transverse Poisson's ratio, $\nu_2^{L[b]}$	0.045	0.045
	Longitudinal tensile strength, X^L (ksi) ^[a]	101	93
	Transverse tensile strength, Y^L (ksi) ^[a]	101	93
	Shear strength, S^L (ksi) ^[b]	5.0	4.5
	Ply thickness, h^L (in)	0.0094	0.0094
	Orientation of each θ^L (degree)	[(0/45) ₂] _s	[(0/45) ₂] _s
	Number of plies, n_s^L	8	8
	Scarf angle, β (degree)	1 to 2.5	1 to 2.5
Repair Patch*	Longitudinal modulus, E_1^R (Msi) ^[a]	7.2	7.5
	Transverse modulus, E_2^R (Msi) ^[a]	7.2	7.5
	Shear modulus, E_6^R (Msi) ^[b]	0.48	0.45
	Longitudinal Poisson's ratio, $\nu_1^{R[b]}$	0.045	0.045
	Transverse Poisson's ratio, $\nu_2^{R[b]}$	0.045	0.045
	Longitudinal tensile strength, X^R (ksi) ^[a]	75	68
	Transverse tensile strength, Y^R (ksi) ^[a]	75	68
	Shear strength, S^R (ksi) ^[b]	5.0	4.5
	Ply thickness, h^R (in)	0.0094	0.0094
	Orientation of each ply, θ^R (degree)	[(0/45) ₂] _s	[(0/45) ₂] _s
	Orientation of external ply, θ_e (degree)	0	0
	Number of plies, n_s^R	8	8
	Number of external plies, n_e	0,1,2	0,1,2
	Overlap length of external ply, d_e (in)	0.25 to 0.375	0.25 to 0.375
Interlayer	Shear modulus, G (ksi) ^[c]	200	100
	Shear strength, τ_p (ksi) ^[c]	2.0	1.6
	Maximum shear strain, γ_{pf} ^[c]	0.28	0.30
	Thickness, h_i (in) ^[c]	0.008	0.008

* Parameters listed are for each ply.

[a] from tables 2 and 3.

[b] from Naik [65].

[c] by backcalculation.

The failure loads calculated by the model are compared to the data in figures 59 through 62. The calculated and measured failure loads agree well, both for dry specimens tested at 70°F and for moisturized specimens tested at 180°F. These agreements lend support to the validities of the models, keeping in mind that the first failure prediction at each environment was used to obtain interlayer properties which were subsequently used for all other predictions. Thus, one can conclude that the trends are very well predicted by the model but not necessarily the absolute values of the failure load.

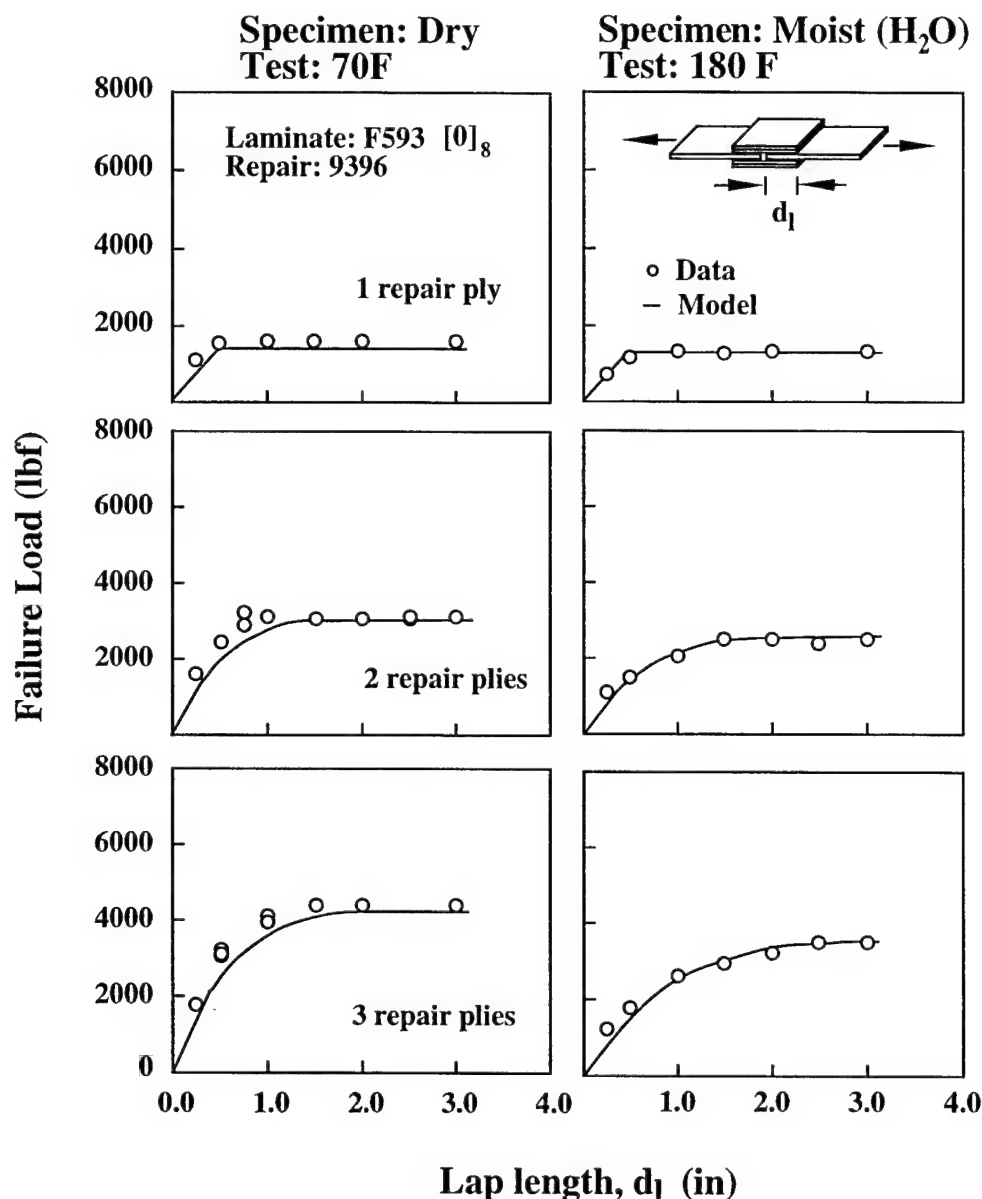


FIGURE 59. COMPARISONS OF THE CALCULATED (MODEL) AND THE MEASURED (DATA) FAILURE LOADS AS A FUNCTION OF LAP LENGTH FOR 8-PLY LAMINATE

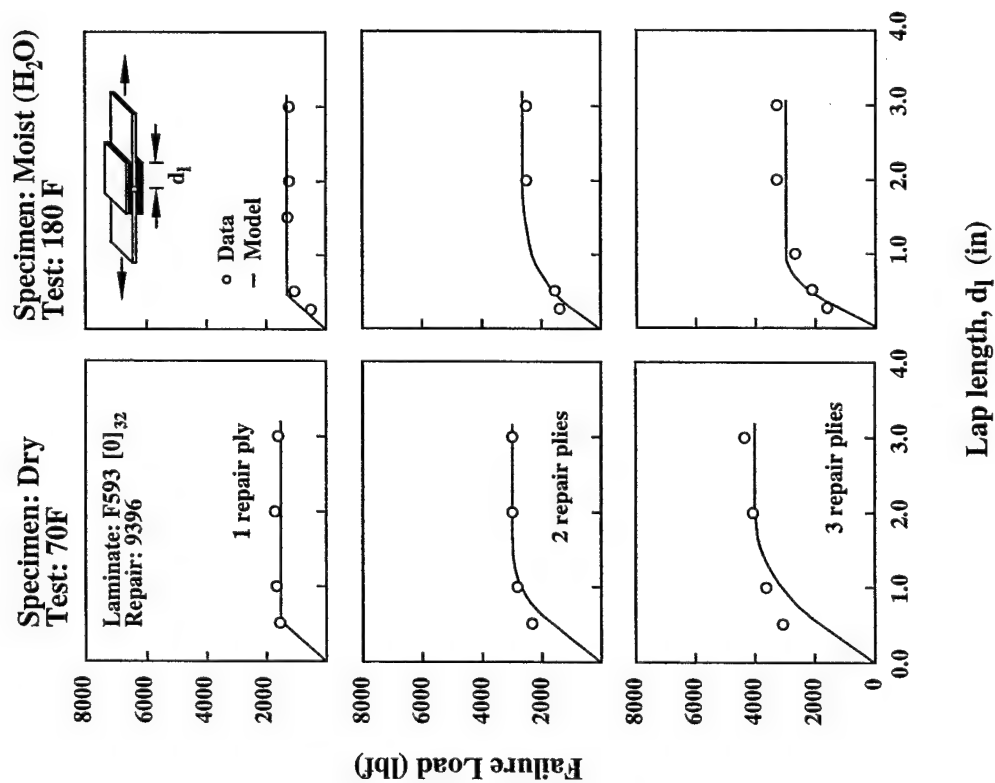


FIGURE 60. COMPARISON OF THE CALCULATED (MODEL) AND THE MEASURED (DATA) FAILURE LOADS AS A FUNCTION OF LAP LENGTH FOR 32-PLY LAMINATE

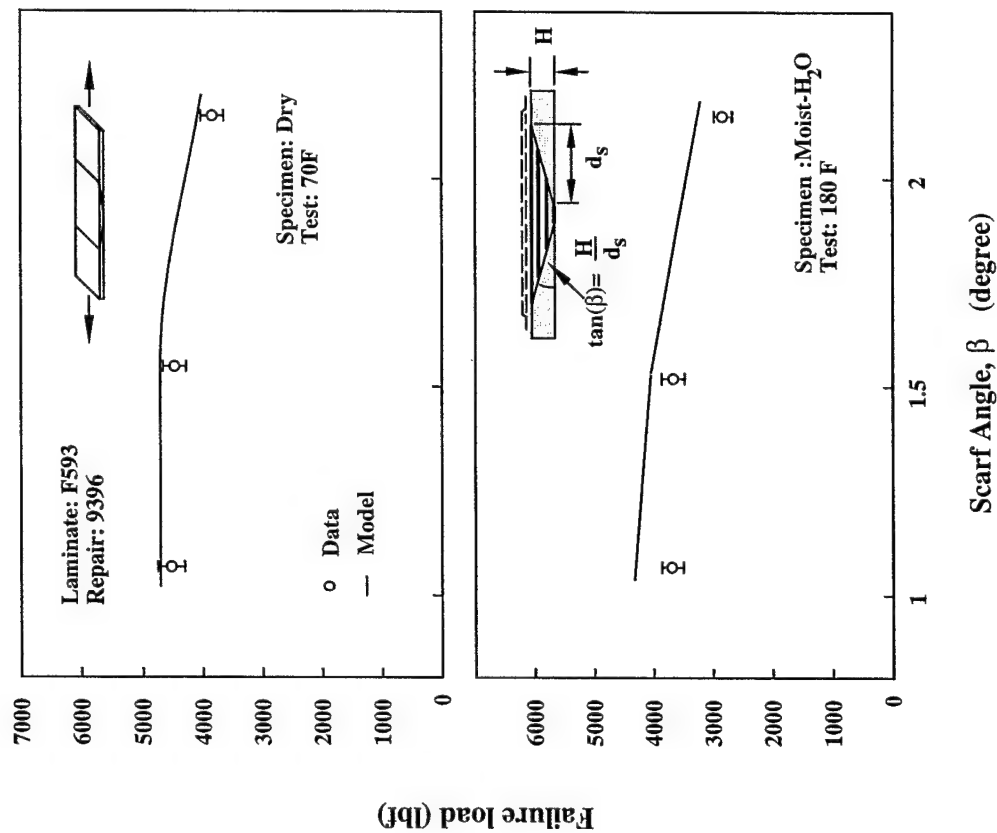


FIGURE 61. COMPARISONS OF THE CALCULATED (MODEL) AND THE MEASURED (DATA) FAILURE LOADS AS A FUNCTION OF SCARF ANGLE

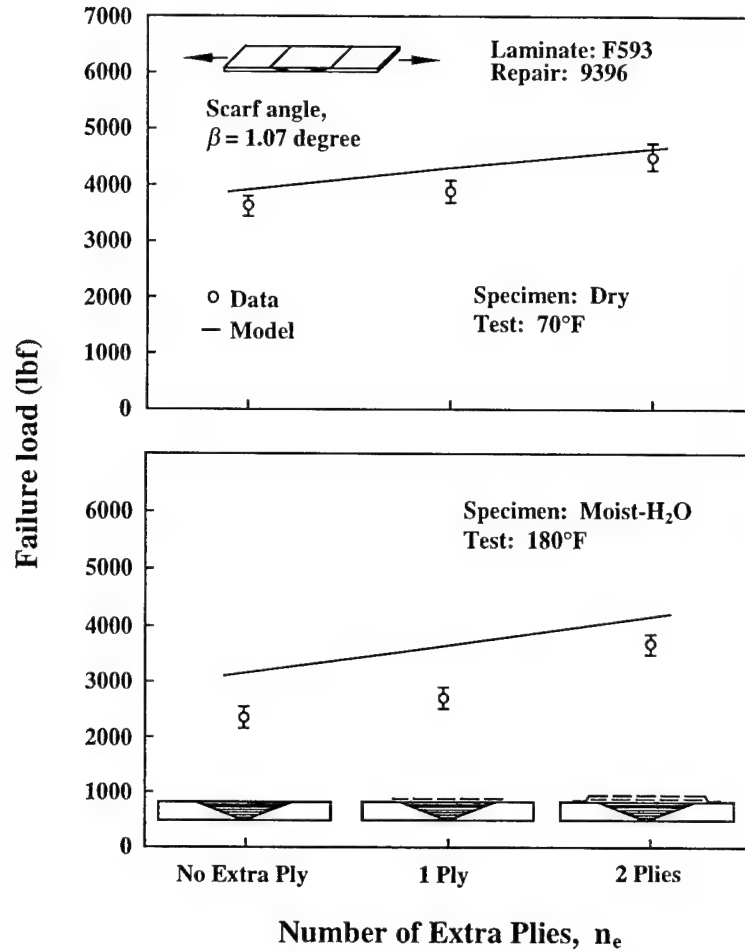


FIGURE 62. COMPARISON OF THE CALCULATED (MODEL) AND THE MEASURED (DATA) FAILURE LOADS AS A FUNCTION OF EXTRA PLIES

10. CONCLUDING REMARKS.

The models and the corresponding computer codes described in the previous chapters are applicable to one-dimensional specimens. Nonetheless, the results of these models serve as useful guides in the design of actual repairs by providing information on the various parameters affecting the failure load. In the present forms the models are for composite laminates. However, the models may be applied to the repair of isotropic plates by replacing the properties of the composite with the corresponding properties of an isotropic material.

11. REFERENCES.

1. *Boeing 777 Structural Repair Manual*. Boeing Commercial Aircraft Co., 1995.
2. *Boeing 737 Structural Repair Manual*. Boeing Commercial Aircraft Co., 1991.
3. *Repair Procedures for Composite Structures, D-53900*. Boeing Commercial Aircraft Co., 1993.
4. E. F. Chesmar, "Metal Bond and Composite Repairs: Similarities and Differences," *Composites '96 Manufacturing and Tooling Conference, Society of Manufacturing Engineers*, pp. 281-290, 1996.
5. R. F. Wegman and T. R. Tullos, "Adhesive Bonded Structural Repair, Part III-Repair of Composite, Honeycomb Cored, and Solid Cored Structures," *SAMPE Journal*, Vol. 29, No. 6, pp. 8-12, 1993.
6. F. Lee, S. Brinkerhoff, and S. McKinney, "Low Energy Cured Composite Repair System," *Composite Repairs, SAMPE Monograph No. 2 (C. L. Hamermesh, ed.)*, pp. 24-35, 1991.
7. M. J. Cichon, "Repair Adhesives: Development Criteria for Field Level Conditions," *Composite Repairs, SAMPE Monograph No.2 (C. L. Hamermesh, ed.)*, pp. 36-50, 1991.
8. R. S. Riefier and W. D. Steinmetz, "Development of Rapid Cure Adhesive for Naval Aircraft Field Repair Applications," *Composite Repairs, SAMPE Monograph No. 2 (C. L. Hamermesh, ed.)*, pp. 51-62, 1991.
9. E. C. Clark and K. D. Cressy, "Field Repair Compounds for Thermoset and Thermoplastic Composites," *Composite Repairs, SAMPE Monograph No. 2 (C. Hamermesh, ed.)*, pp. 63-70, 1991.
10. C. L. Ong and S. B. Shen, "Repair of F-104 Aircraft Nosedome by Composite Patching," *Theoretical and Applied Fracture Mechanics*, Vol. 15, pp. 75-83, 1991.
11. S. R. Hall, M. D. Raizenne, and D. L. Simpson, "A Proposed Composite Repair Methodology for Primary Structure," *Composites*, Vol. 20, pp. 479-483, 1988.
12. J. W. Deaton, "Repair of Advanced Composites Commercial Aircraft Structures," *Engineered Materials Handbook, ASM International*, Vol. 3, pp. 829-839, 1987.
13. S. H. Myhre, "Advanced Composite Repair-Recent Development and Some Problems," *Composite Repairs, SAMPE Monograph No. 1 (H. Brown, ed.)*, pp. 14-25, 1985.

14. R. H. Stone, "Development of Repair Procedures for Graphite/Epoxy Structures on Commercial Transports," *Composite Repairs, SAMPE Monograph No. 1* (H. Brown, ed.), pp. 26-39, 1985.
15. J. F. Knauss and R. H. Stone, "Demonstration of Repairability and Repair Quality on Graphite/Epoxy Structural Supplements," *Composite Repairs, SAMPE Monograph No. 1* (H. Brown, ed.), pp. 40-51, 1985.
16. R. H. Stone, "Field-Level Repair Materials and Processes," *Composite Repairs, SAMPE Monograph No. 1* (H. Brown, ed.), pp. 87-99, 1985.
17. A. S. Falcone, "Field Repairs for the AH-1 Composite Main Rotor Blade," *Composite Repairs, SAMPE Monograph No. 1* (H. Brown, ed.), pp. 100-109, 1985.
18. J. R. Scott and C. K. Mashiba, "Improved Resins for Wet Layup Repair of Advanced Composite Structure," *Composite Repairs, SAMPE Monograph No. 1* (H. Brown, ed.), pp. 110-116, 1985.
19. J. Mahon and J. Candella, "Development of Large-Area Damage Repair Procedures for the F-14A Horizontal Stabilizer, Phase I-Repair Development," *Composite Repairs, SAMPE Monograph No. 1* (H. Brown, ed.), pp. 184-194, 1985.
20. R. H. Stone, *Repair Techniques for Graphite/Epoxy Structures for Commercial Transport Applications*. NASA Contractor Report, CR 159056, 1983.
21. *Advanced Composite Repair Guide, Nor 82-60*, Northrop Corporation, 1982.
22. S. H. Myhre and J. D. Labor, "Repair of Advanced Composite Structures," *Journal of Aircraft*, Vol. 18, pp. 546-552, 1980.
23. S. H. Myhre and R. W. Kiger, "Problems and Options in Advanced Composite Repair," *Fibrous Composites in Structural Design, Plenum Press*, pp. 359-380, 1981.
24. L. O. Bardygula, "CACRC: Progress and Plans," *Composites '96 Manufacturing and Tooling Conference, Society of Manufacturing Engineers*, pp. 229-239, 1996.
25. P. Shyprykevich, C. S. Springer, and S. H. Ahn, "Standardization of Composite Repairs for Commercial Transport Aircraft," *Composite Repair of Aircraft Structures Symposium*, pp. 1-24, 1995.
26. S. H. Ahn, G. S. Springer, and P. Shyprykevich, "Composite Repair with Wet Lay-up and Prepreg," *Composites '96 Manufacturing and Tooling Conference, Society of Manufacturing Engineers*, pp. 211-226, 1996.

27. L. J. Hart-Smith, R. W. Ochsner, and R. L. Radecky, "Surface Preparation of Composites for Adhesive-Bonded Repair," *Engineered Materials Handbook, ASM International*, Vol. 3, pp. 840-844, 1987.
28. H. S. Kim, S. J. Lee, and D. G. Lee, "Development of a Strength Model for the Cocured Stepped Lap Joints Under Tensile Loading," *Composite Structures*, Vol. 32, pp. 593-600, 1995.
29. S. H. Myhre and C. E. Beck, "Repair Concepts for Advanced Composite Structures," *Journal of Aircraft*, Vol. 16, pp. 720-728, 1979.
30. W. S. Chan and C. T. Sun, "Interfacial Stresses and Strength of Lap Joints," *21st Conference of Structures, Structural Dynamics, and Materials, AIAA/ASME/ASCE/AHS*, pp. 656-663, 1980.
31. S. J. John, A. J. Kinloch, and F. L. Matthews, "Measuring and Predicting the Durability of Bonded Carbon Fiber/Epoxy Composite Joints," *Composites*, Vol. 22, pp. 121-126, 1991.
32. J. E. Robson, F. L. Matthews, and A. J. Kinloch, "The Bonded Repair of Fibre Composite: Effect of Composite Moisture Content," *Composite Science and Technology*, Vol. 52, pp. 235-246, 1994.
33. B. M. Parker, "The Effect of Composite Prebond Moisture on Adhesive-Bonded CFRP-CFRP Joints," *Composites*, Vol. 14, pp. 226-232, 1983.
34. S. H. Mylire, J. D. Labor, and S. C. Aker, "Moisture Problems in Advanced Composite Structural Repair," *Composites*, Vol. 13, pp. 289-299, 1982.
35. O. Volkersen, "Die Nietkraftverteilung in Zugbeanspruchten Nietverbindungen mit Konstanten Laschenquerschnitten," *Luftfahrtforschung*, Vol. 15, pp. 41-47, 1938.
36. M. Goland and E. Reissner, "The Stresses in Cemented Joints," *Journal of Applied Mechanics*, Vol. 11, pp. A17-A27, 1944.
37. J. Pirvics, "Two Dimensional Displacement-Stress Distributions in Adhesive Bonded Composite Structures," *Journal of Adhesion*, Vol. 6, pp. 207-228, 1974.
38. D. J. Aliman, "A Theory for Elastic Stresses in Adhesive Bonded Lap Joints," *Quarterly Journal of Applied Mathematics*, Vol. XXX, Pt. 4, pp. 415-436, 1977.
39. I. U. Ojalvo and H. L. Eidinoff, "Bond Thickness Effects Upon Stresses in Single-Lap Adhesive Joints," *AIAA Journal*, Vol. 16, pp. 204-211, 1978.
40. W. J. Renton and J. R. Vinson, "The Efficient Design of Adhesive Bonded Joints," *Journal of Adhesion*, Vol. 7, pp. 175-193, 1975.

41. F. Thamm, "Stress Distribution in Lap Joints With Partially Thinned Adherends," *Journal of Adhesion*, Vol. 7, pp. 301-309, 1976.
42. G. R. Wooley and D. R. Carver, "Stress Concentration Factors for Bonded Lap Joints," *Journal of Aircraft*, Vol. 8, pp. 817-820, 1971.
43. R. D. Adams and N. A. Peppiatt, "Stress Analysis of Adhesive-Bonded Lap Joints," *Journal of Strain Analysis*, Vol. 9, pp. 185-196, 1974.
44. D. A. Bigwood and A. D. Crocombe, "Elastic Analysis and Engineering Design Formulae for Bonded Joints," *International Journal of Adhesion and Adhesives*, Vol. 9, pp. 229-242, 1989.
45. D. A. Bigwood and A. D. Crocombe, "Nonlinear Adhesive Bonded Joints Design Analyses," *International Journal of Adhesion and Adhesives*, Vol. 10, pp. 31-41, 1990.
46. A. D. Crocombe, "Global Yielding as a Failure Criterion for Bonded Joints," *International Journal of Adhesion and Adhesives*, Vol. 9, pp. 145-153, 1989.
47. F. Szépe, "Strength of Adhesive-Bonded Lap Joints With Respect to Change of Temperature and Fatigue," *Experimental Mechanics*, Vol. 6, pp. 280-286, 1966.
48. R. D. Adams, J. Coppendale, and N. A. Peppiatt, "Failure Analysis of Aluminium-Aluminium Bonded Joints," *Adhesion 2* (K. W. Allen, ed.), Applied Science Publisher, pp. 105-120, 1978.
49. J. L. Lubkin, "A Theory of Adhesive Scarf Joints," *Journal of Applied Mechanics*, Vol. 24, pp. 255-260, 1957.
50. W. J. Renton and J. R. Vinson, "On The Behavior of Bonded Joints in Composite Material Structures," *Engineering Fracture Mechanics*, Vol. 7, pp. 41-60, 1975.
51. W. J. Renton and J. R. Vinson, "Analysis of Adhesively Bonded Joints Between Panels of Composite Materials," *Journal of Applied Mechanics*, Vol. 44, pp. 101-106, 1977.
52. R. M. Baker and F. Hatt, "Analysis of Bonded Joints in Vehicular Structures," *AIAA Journal*, Vol. 11, pp. 1650-1654, 1973.
53. G. C. Grimes, "Stress Distribution in Adhesive Bonded Lap Joints," *SAE Trans. 710107*, pp. 370-378, 1971.
54. F. Erdogan and M. Ratwani, "Stress Distribution in Bonded Joints," *Journal of Composite Materials*, Vol. 5, pp. 379-393, 1971.
55. C. L. Johnson, "Effect of Ply Staking Sequence on Stress in a Scarf Joint," *AIAA Journal*, Vol. 27, pp. 79-86, 1989.

56. L. J. Hart-Smith, *Adhesive-Bonded Single-Lap Joints*. NASA Contract Report, CR 112236, 1973.
57. L. J. Hart-Smith, *Adhesive-Bonded Double-Lap Joints*. NASA Contract Report, CR 112235, 1973.
58. L. J. Hart-Smith, *Non-Classical Adhesive-Bonded Joints in Practical Aerospace Construction*, NASA Contract Report, CR 112238, 1973.
59. L. J. Hart-Smith, "Further Developments in the Design and Analysis of Adhesive-Bonded Structural Joints," *Joining of Composite Materials*, ASTM STP 749 (K. T. Kedward, ed.), American Society for Testing and Materials, pp. 3-31, 1981.
60. R. D. Adams, R. W. Atkins, J. A. Harris, and A. J. Kinloch, "Stress Analysis and Failure Properties of Carbon-Fiber-Reinforced-Plastic/Steel Double-Lap Joints," *Journal of Adhesion*, Vol. 20, pp. 29-53, 1986.
61. R. D. Adams, "Theoretical Stress Analysis of Adhesively Bonded Joints," *Joining Fibre-Reinforced Plastics*, (F. L. Matthews, ed.), Elsevier Applied Science Publisher, pp. 185-226, 1987.
62. L. J. Hart-Smith, *Adhesive-Bonded Scarf and Stepped-Lap Joints*, NASA Contract Report, CR 112237, 1973.
63. S. W. Tsai and H. T. Hahn, *Introduction to Composite Materials*, Technomic Publishing Company, 1980.
64. T. H. G. Megson, *Aircraft Structures for Engineering Students*, 2nd ed., Halsted Press, pp. 405-406, 1990.
65. N. J. Naik, *Woven Fabric Composites*, Technomic Publishing Co., 1994.

APPENDIX A—MOISTURE LOSS OF SPECIMEN DURING TEST

In this appendix, the percent change of the moisture content of the specimen, tested at 180°F, is given. The measured moisture content as a function of time is shown in figure A-1 for laminates moisturized at 180°F. The diffusivity D is obtained from the expression [A-1]

$$D = \pi \left(\frac{h}{4M_m} \right)^2 \left(\frac{M_2 - M_1}{\sqrt{t_2} - \sqrt{t_1}} \right)^2 \quad (\text{A-1})$$

$$= 6 \times 10^{-10} \text{ in}^2/\text{sec}$$

where M_m is the maximum moisture content (% weight gain) ($M_m = 1.8$ percent) and h is the specimen thickness ($h = 0.075$ in). M_1 and M_2 are the moisture contents at time t_1 and t_2 , respectively. The change in the moisture content as a function of time is [A-1]

$$M = G_M(M_m - M_i) + M_i \quad (\text{A-2})$$

where M is the moisture content, M_i is the initial moisture content, and G_M is

$$G_M = 1 - \exp \left(-7.3 \left(\frac{Dt}{h^2} \right)^{0.75} \right) \quad (\text{A-3})$$

The initial moisture content was $M_i = 1.1$ percent, and $M_m = 0.0$ percent for drying. The duration of the test was 600 seconds. With these values, equations A-2 and A-3 give

$$M = 1.093 \text{ percent} \quad (\text{A-4})$$

The change in moisture content is

$$M_i - M = 1.1 \text{ percent} - 1.093 \text{ percent} \quad (\text{A-5})$$

$$= 0.007 \text{ percent} \quad (\text{A-6})$$

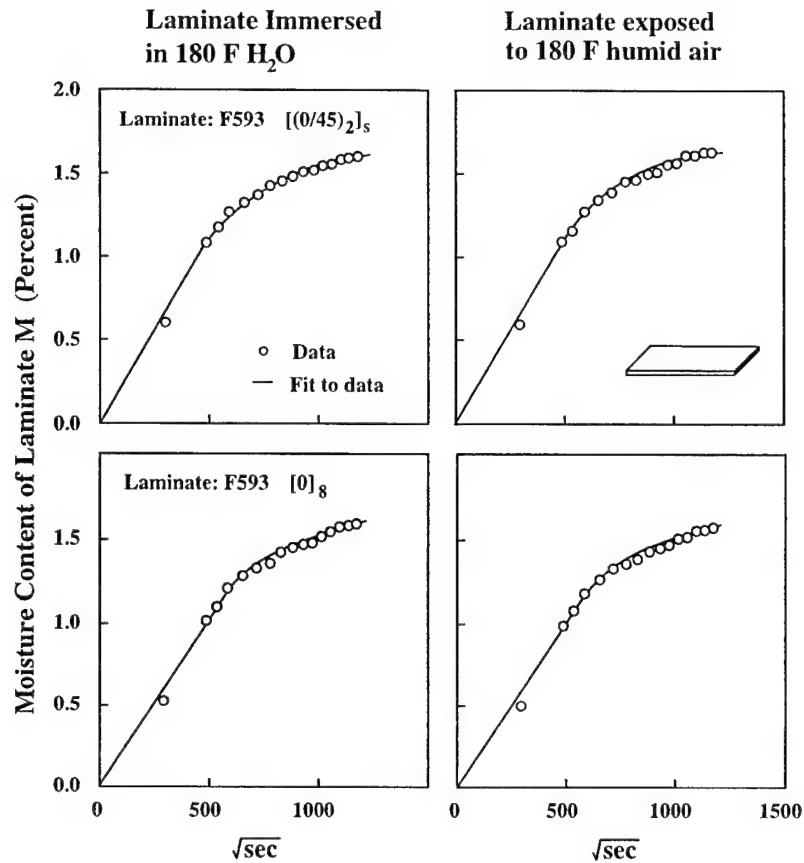


FIGURE A-1. MOISTURE CONTENTS OF THE BASE LAMINATES IMMERSED IN WATER AT 180°F (LEFT), OR EXPOSED TO 100 PERCENT HUMID AIR AT 180°F (RIGHT)

REFERENCE.

- A-1. H. Shen and G. S. Springer, "Moisture Absorption and Desorption of Composite Materials," *Journal of Composite Materials*, Vol. 10, pp. 2-20, 1976.

APPENDIX B—FAILURE LOADS OF SPECIMENS EXPOSED TO HUMID AIR

The failure loads of the specimens repaired by the scarf (figure B-1) and stepped lap (figure B-2) techniques are included in this appendix.

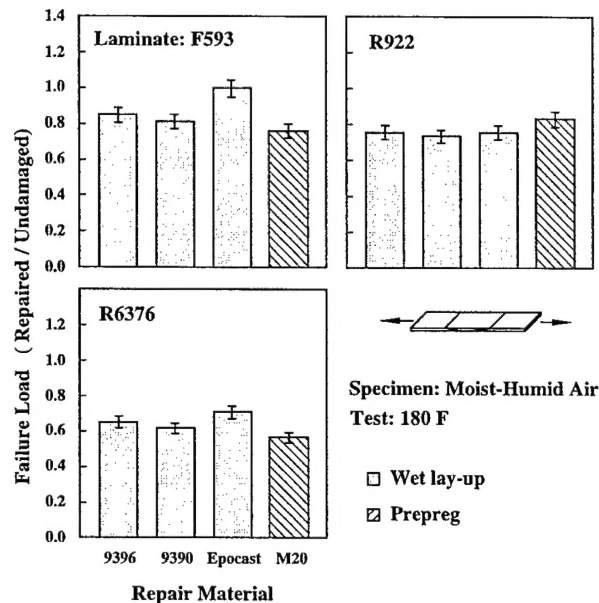


FIGURE B-1. FAILURE LOADS OF DIFFERENT BASE LAMINATES REPAIRED WITH DIFFERENT REPAIR MATERIALS (SCARF REPAIR)

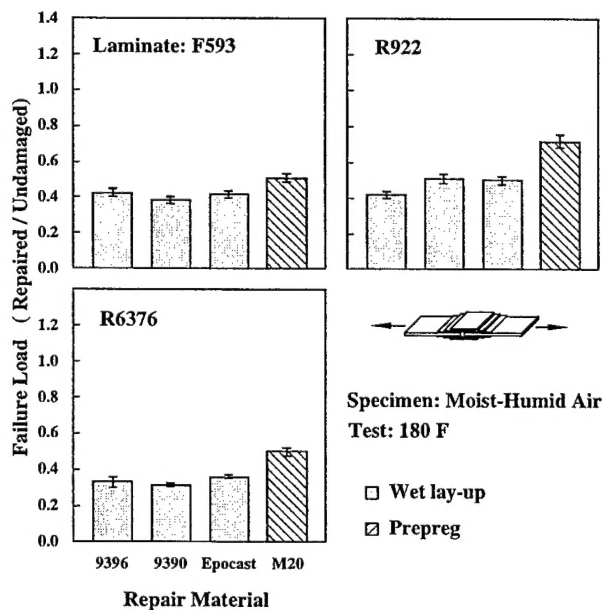


FIGURE B-2. FAILURE LOADS OF DIFFERENT BASE LAMINATES REPAIRED WITH DIFFERENT REPAIR MATERIALS (STEPPED LAP REPAIR)

APPENDIX C—TEST RESULTS

The failure loads used in normalizing the data are summarized in tables C-1 through C-5.

TABLE C-1. THE FAILURE LOADS (in lbf) USED IN NORMALIZING THE DATA IN FIGURES 17, 18, AND 21

Repair Type	Parameter	Specimen Condition/ Test Temperature	
		Dry/70°F	Moist(H ₂ O)/180°F
Stepped lap	1 repair ply ($d_l = 3$ in)	1583	1295
	2 repair ply ($d_l = 3$ in)	3893	2394
	3 repair ply ($d_l = 3$ in)	4289	3224
Uniform lap	8 laminate, 1 repair plies ($d_l = 3$ in)	1601	1290
	8 laminate, 2 repair plies $d_l = 3$ in)	3134	2521
	8 laminate, 3 repair plies ($d_l = 3$ in)	4368	3168
	8 laminate, 4 repair plies ($d_l = 3$ in)	5646	3858
	32 laminate, 1 repair plies ($d_l = 3$ in)	1710	1238
	32 laminate, 2 repair plies ($d_l = 3$ in)	2997	2502
	32 laminate, 3 repair plies ($d_l = 3$ in)	4055	3256

TABLE C-2. THE FAILURE LOADS (in lbf) USED IN NORMALIZING THE DATA IN FIGURES 22, 23, AND D-1

Repair Type	Specimen Condition/ Test Temperature	Failure Load (lbs)
Scarf	Dry/70°F	4526
Stepped lap	Dry/70°F	3360

TABLE C-3. THE FAILURE LOADS (in lbf) OF SPECIMENS WITH GRIT NUMBER $g = 60$ USED IN NORMALIZING THE DATA IN FIGURE 24

Repair Type	Specimen Condition/ Test Temperature	Failure Load (lbs)
Scarf	Dry/70°F	4475
Stepped lap	Dry/70°F	3278
Scarf	Moist (H ₂ O)/180°F	3536
Stepped lap	Moist (H ₂ O)/180°F	3012

TABLE C-4. THE FAILURE LOADS (in lbf) OF SPECIMENS WITH CURE TEMPERATURE $T_c = 150^\circ\text{F}$ USED IN NORMALIZING THE DATA IN FIGURE 28

Repair Type	Specimen Condition/ Test Temperature	Failure Load (lbs)
Scarf	Dry/70°F	4553
Stepped lap	Dry/70°F	3365

TABLE C-5. THE FAILURE LOADS (in lbf) USED IN NORMALIZING THE DATA IN FIGURE D-2

Repair Type	Specimen Condition/ Test Temperature	Failure Load (lbs)
Scarf	Dry/70°F	4541
Stepped lap	Dry/70°F	4516

APPENDIX D—FAILURE LOADS OF SPECIMENS UNDER MOISTURE AND TEMPERATURE

The failure loads of the specimens repaired with wet lay-up (figure D-1) and with prepreg (figure D-2) materials are included in this appendix.

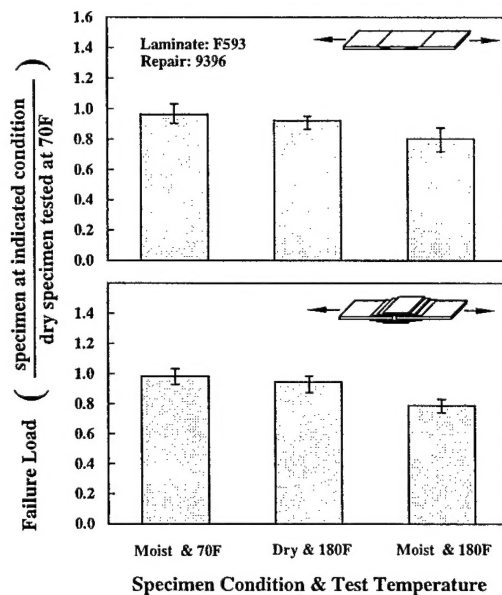


FIGURE D-1. THE EFFECTS OF SPECIMEN MOISTURE CONTENT AND TEST TEMPERATURE ON THE FAILURE LOAD

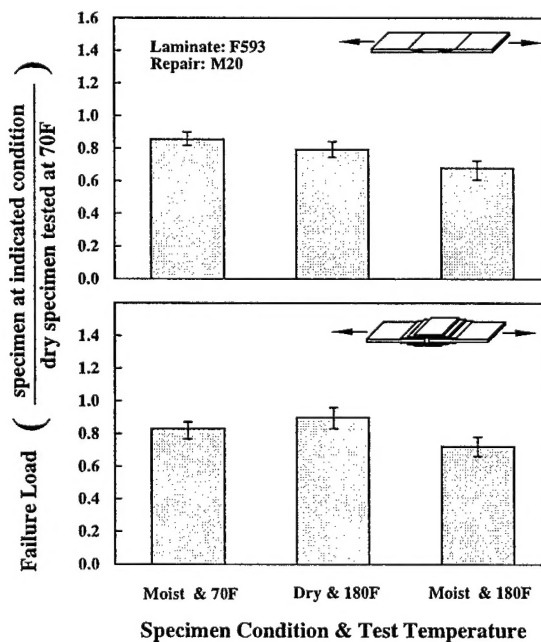


FIGURE D-2. THE EFFECTS OF SPECIMEN MOISTURE CONTENT AND TEST TEMPERATURE ON THE FAILURE LOAD. REPAIR MATERIAL M20 (PREPREG).